5-2009

Chloride Characterization from Pavement Runoff Using Automated Samplers and Specific Conductivity Sensors at Three Eastern Massachusetts Locations

Paul G. Chang
University of Massachusetts - Amherst

Chloride Characterization from Pavement Runoff Using Automated Samplers and Specific Conductivity Sensors at Three Eastern Massachusetts Locations

A Masters Project Presented

By

Paul G. Chang

Submitted to the Department of Civil and Environmental Engineering of the University of Massachusetts Amherst in partial fulfillment of the requirements for the degree of

MASTER OF SCIENCE IN ENVIRONMENTAL ENGINEERING

May 2009

Chloride Characterization from Pavement Runoff Using Automated Samplers and Specific Conductivity Sensors at Three Eastern Massachusetts Locations

A Masters Project Presented

by

Paul G. Chang

Approved as to style and content by:

_____
David W. Ostendorf, Chair

_____
Mi-Hyun Park, Committee Member

_____
John E. Tobiason,
Graduate Program Director
M.S. in Environmental Engineering

DEDICATION

This work is dedicated to my entire family
and especially my grandfather,

Kwong Hwa Chang

ACKNOWLEDGMENTS

I would like to thank the Massachusetts Highway Department for funding for this research project and all the help in acquiring the necessary data needed to complete this project. The grant provided by the University of Massachusetts on ISA No. 38721 “Salt Remediation Program” supervised under the direction of Mr. David White of the Environmental Division of MHD. The views, opinions and findings presented in this manuscript are those of the author and do not necessarily reflect the official view of the Massachusetts Highway Department. This study does not constitute a standard, specification or regulation.

I would like to thank Dr. Ostendorf for his guidance and support in deriving solutions to the modeling involved and his valuable input during this research project. I would also like to extend thanks my committee member, Dr. Mi-Hyun Park for taking the time to reside on my thesis committee.

I also would like to thank the assistance provided by all my peers and fellow field trip personnel as well as the whole lab crew. I would like thank the past students, Cora and Marina, the present students, Cat, Marie, and Dan, all the staff, Erica SK, Erich and Aaron and I am especially thankful to Camelia for her patience in explaining some puzzling aspects of laboratory procedure and the concepts I had difficulty in grasping.

I would like to end with thanking all the staff and faculty of the Civil and Environmental Engineering Departments.

ABSTRACT

The objective of this research is to relate the chloride concentration of highway runoff through specific conductivity measurements and to characterize the role that the pavement surface texture has in the dissolution kinetics of the chloride residing in this layer. The quantity of deicing agents applied throughout the winter season is correlated to the concentration of chloride in highway runoff and linked to the length of time since application. A unit hydrograph was developed from precipitation measurements and the resulting hydraulic parameters were calibrated for use in a specific conductivity flux model. From this model a pollutograph was developed characterizing a specific conductivity flux source term and a first flush value. These two terms are optimized to characterize the dissolution kinetics and predict chloride runoff concentrations.

The runoff decay constants optimized for all three sites reduced to very similar averages of 3.02×10^{-4}, 4.21×10^{-4}, and 3.6×10^{-4} s^{-1} respectively for Andover, Cohasset and Plymouth from ranges of three orders of magnitude for each site between individual events over the five year period. The depression storage layers were 0.9, 1.3, and 3.0 mm respectively for Andover, Cohasset and Plymouth indicating a connection between pavement age and texture as Andover is the new of all pavements. Along with the similar calibrated hydraulic parameters, the three sites had very similar optimized chloride source parameters of 5.64×10^{-4}, 1.30×10^{-4}, and 2.16×10^{-4} mg/m^2-s for Andover, Cohasset and Plymouth respectively. The 177 storms modeled between all three sites had source terms ranging from 10^{-3} to 10^{-8} and averaged to the above optimized values. A clear indication the lumped parameter linear reservoir approach is applicable to storage facilities and active highway routes.

This research provides support understanding the role impervious surface texture has in the chloride dissolution kinetics controlling stormwater runoff quality. A common model has been shown to be able to characterize stormwater runoff hydraulics and chloride flux from both salt storage facilities and heavily traveled highway lanes. Seasonal stormwater quality trends as well as event first flush concentrations have been identified and characterized with calibrated watershed parameters. Automated samplers coupled with continuous monitoring equipment have shown per storm or seasonal correlation between pavement texture, meteorological data, distributed deicing agent data, and water quality information at different Eastern Massachusetts locations.

TABLE OF CONTENTS

Page

LIST OF TABLES

Table Page

LIST OF FIGURES

Figure Page

LIST OF SYMBOLS

a = free surface width of flow through weir (m)

A = cross sectional area of flow thorough weir (m^2)

A_{Eff} = effective runoff area (m^2)

A = ionic activity

C = conductivity (μS/cm)

C_D = discharge coefficient

c = runoff concentration (kg/m^3)

c_i = concentration of ith ion

$C_{measured}$ = conductivity measured in the field, automated sampler (μS/cm)

$C_{predicted}$ = conductivity predicted by model (μS/cm)

Š = calculated error (μS/cm or mg/L)

δ_{mean} = mean error (μS/cm or mg/L)

g = gravity (m^2/s)

h = depth of water before weir at water level meter (m)

H = hydraulic head (m)

i = ion charge

I = ion strength (moles)

γ = Davies activity coefficient

κ^o = conductivity at infinite dilution (μmho/cm)

κ_{calc} = calculated conductivity (μS/cm)

K = constant for 90^o V-notch

λ = decay rate constant (d^{-1})

λ = mass based ionic conductance ($mS\text{-}m^3/cm\text{-}kg$)

λ_{max} = minimum value for λ in model search (d^{-1})

λ_{min} = minimum value for λ in model search (d^{-1})

λ^o_i = equivalent conductance of the ith ion (cation or anion)

m = ion molar mass (kg/mole)

n = porosity

nn = total number of measurements of parameters during storm event

σ = surface tension (N-m)

p = precipitation intensity (m/s)

Q = flow rate (gpm)

r = temperature coefficient correction for Arrhenius equation

Re = Reynolds Number

S = storage in linear reservoir (m^3)

T = temperature (^oC)

τ_G = Fibonocci Golden Ration (1.6180339887….)

ν = viscocity (m^2/s)

V = velocity (m/s)

We = Weber number

y_c = water level above V-notch weir (m)

z_i = charge on ith ion

$z_{1,2}$ = water depth from datum in weir (m)

LIST OF ABBREVIATIONS

ASCE	American Society of Civil Engineers
ASTM	American Society for Testing and Materials
CMA	Calcium Magnesium Acetate
$CaCl_2$	Calcium Chloride
DEP	Department of Environmental Protection
FHWA	Federal Highway Administration
ISA	Inter Agency Service Agreement
ISO	International Organization for Standardization
MHD	Massachusetts Highway Administration
NaCl	Sodium Chloride
NCDC	National Climatic Data Center
SC	Specific Conductivity
SR25	State Route 25
TRB	Transportation Research Board
USEPA	United States Environmental Protection Agency
USGS	United State Geological Survey

CHAPTER 1

INTRODUCTION

1.1 Deicing Agents

Deicing agents are the primary chemicals distributed by highway departments to prevent hazardous driving conditions on slippery roadways during the winter months. Road salt was first introduced for snow melting operations in New Hampshire in the winter of 1941- 42 (Transportation Research Board, 1991a). Through the next two decades the use expanded every year leveling off in the 1970's to the extent of use seen today.

The most common and economical substance is sodium chloride (NaCl) or better known as rock salt. This is a granular product that has been mined, crushed, screened, and treated with an anti-caking agent. NaCl is stored and distributed in this granular form. General practice is to distribute straight onto the pavement or with sand to increase traction. Another commonly used agent is calcium chloride ($CaCl_2$). Calcium chloride comes from natural brines and comes in dry form in pellets or flakes and in solution. The Massachusetts Highway Department (MHD) stores and uses $CaCl_2$ in liquid form and in the solid form in premix. Premix is a deicing agent mixture used by MHD and most highway departments which consists of 20% $CaCl_2$ and 80% NaCl part by mass (Ostendorf *et al*., 2006). This combination maximizes the strength of NaCl and the thermal diversity of $CaCl_2$. Ratios of sand, NaCl, and $CaCl_2$ all depend on road temperature, duration and quantity of precipitation and other factors. Further discussion

of this and other agents will be discussed below. The term 'salt' will be used throughout this thesis to refer to either $CaCl_2$ or NaCl.

While the roadways are made safer by reducing icy condition to wet roadways, the brine produced from the salt treatment has impacts on the road itself, adjacent infrastructure and the surrounding ecology. In 1974 the Federal Highway Administration (FHWA) initiated the first research program to evaluate the overall cost of deicing agents and develop chemical alternatives (Transportation Research Board, 1991b). Widespread documentation of the negative environmental effects of deicing agents and this initiative led to the development of alternative deicing agents such as calcium magnesium acetate (CMA) ($Ca_{0.3}Mg_{0.7}(CH_3COO^-)_2$). CMA is a more expensive substitute that has been used in the past but has less of an impact on the environment. The only site of the three studied here that applied CMA is Plymouth. Its use has been discontinued due the degradation of surface and groundwater dissolved oxygen levels.

The crystalline form of rock salt, the primary agent examined in this research, allows the residual effects of its deicing capabilities to persist as the solid dissolves. This residual effect directly related to the pavement texture is the key characteristic that allows NaCl to be highly effective as a deicing chemical. The ability of the salt granule to reside in the surface of the pavement and dissolve as the melting snow and ice runoff in the form of water, the relative abundance of the chemical and the ease of distribution and handling has made this deicing agent the most popular and widely used. It is estimated that Massachusetts applies 223 million kg of road salt each year to maintain its public roads (Granato, 1996).

1.2 Deicing Agent Impact

It is estimated that the United States applies approximately 15 million tons of salts each year and spends roughly $2.3 billion annually to keep roads clear of snow and ice (Shi, 2005). The environmental impact of deicing agents, particularly NaCl, has been the center of many studies. Long term use of NaCl damages roadside vegetation and the soil matrix, vehicles, roadway infrastructure such as bridges, drainage structures and pipelines, and to deteriorate the road asphalt itself. Highway runoff resulting from the melted precipitation contaminates the surrounding soils, groundwater, and surface water bodies which can lead to salt accumulation in sediments. Although NaCl is fairly inexpensive to de-ice roadways, the related costs to public and private infrastructure and damage to water quality have brought about some serious concerns about the use of alternatives. Corrosion on vehicles and structures is estimated to be the largest cost impact of chloride based chemicals. Efficient use is the most immediate means to facilitate control of infrastructure and environmental damages. Even relatively small amounts of chloride will significantly accelerate existing corrosion (Wisconsin T.C., 1996).

The development of deicing chemicals more forgiving to the environment has led to the application of potassium chloride (KCl), magnesium chloride ($MgCl_2$) and the CMA mentioned previously. Each agent has positive and negative aspects to its use with cost being the foremost determinant considered in application each season. Considerations include roadside ecology and economic impact, especially in aquifer recharge areas. Under special circumstances, alternatives have been used with the impact closely monitored. $CaCl_2$ and MgCl are more effective at lower temperature than

NaCl is. Experiments have shown that $CaCl_2$ has a better deicing capability than NaCl at -10° C and that premix had superior performance at temperatures ranging from -10° C to 10° C than either material alone. At lower temperatures NaCl takes longer to melt the same quantity of ice than $CaCl_2$ does. Comparison of the three most popular deicing agents are in Figure 1.1 below. The first graph shows the relationship of NaCl efficiency and temperature. The second graph in Figure 1.1 below is a comparison for different compounds to melt 1/8" of glare ice.

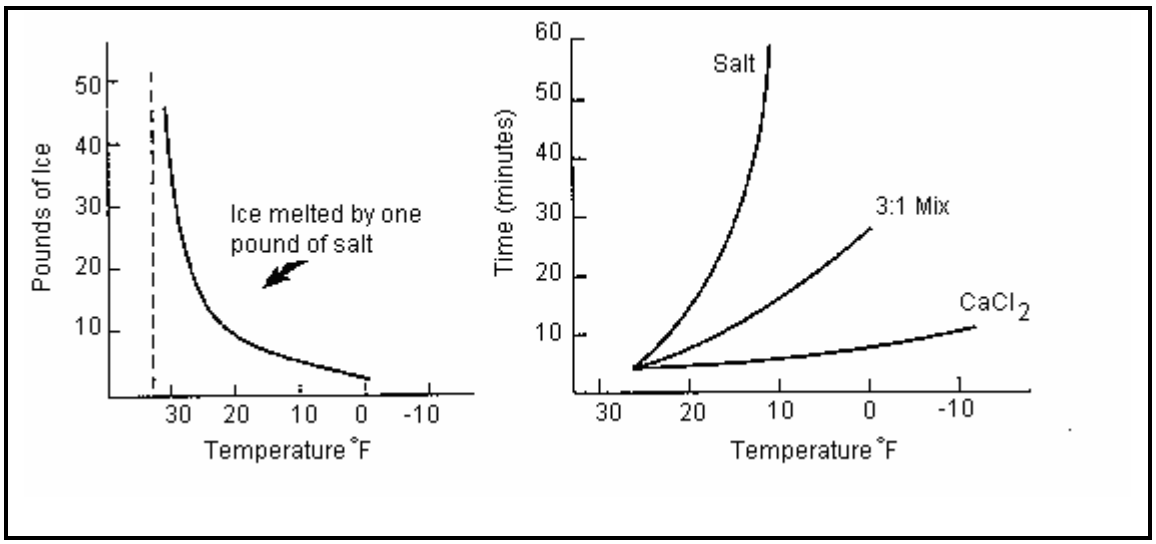

Figure 1.1: Comparison of Deicing Agent Efficiencies (Wisconsin T. C., 1996)

1.3 Research Objectives

The University of Massachusetts Amherst in cooperation with the (MHD) has been studying the water quality issues related to applications and storage of deicing agents for a number of years at various locations in Eastern Massachusetts. Auto sampling devices have been installed in conjunction with weirs and precipitation gauges to continuously collect storm runoff data at the two salt storage facilities and at the infiltration basin.

The objective of this research is to analyze the latest five years of data from each of the sites and characterize the watershed hydraulic parameters whether it is a salt storage facility or highway lane miles. The distinct calibrated parameters of each watershed will then be utilized to develop the mass flux of specific conductivity discharged over the weir during each storm for the entire period. The linear relationship between specific conductivity and chloride concentration will be utilized in estimating measured flux of dissolved chloride. This will be done with theory analyzing the dissolution kinetics of the pavement texture. Finally the seasonal variations in the chloride flux model calibrated with the hydrologic parameters of each watershed will be compared with seasonal deicing agent distribution.

Records of deicing agent materials applied to lane miles or stored at the storage facilities studied will be a reference of actual solids applied and provide a scale to compare first flush characterized runoff on a per event and seasonal basis. The result will provide insight into the relationship of the depression storage layer in the pavement surface and its connection to chloride persistence in deicing agent runoff.

1.4 Scope of Work

This research project implemented a large database of runoff information for three sites in southeastern Massachusetts. Hyetographs derived from the precipitation data provided the first step in the dissolution investigation leading towards site characterization with a specific conductivity flux model. Hydrographs of the runoff from storms using data measured by the rain gauges and weir discharge were developed through classic linear reservoir theory and a lumped parameter search characterizing each specific watershed. A watershed in this research refers to the paved area of each

salt storage facility that contributes to the runoff measured at each respective weir or to the lane miles, shoulder area, and grassy swales contributing to the weir in the Plymouth infiltration basin. Calibrated hydraulic parameters characterized each individual storm at each watershed from the analysis of 47 storms over four years in Andover, 71 storms over five years in Cohasset, and 69 storms over 5 years in Plymouth have been applied to develop a model of specific conductivity leaving the depression storage layer. Automated sampler ion analysis of a storm within the same month provided a conversion factor of specific conductivity to chloride relying on the linear relationship between the two. This model was compared to solids applied from material expenditures records and mass transport hydraulics of the weirs relevant to each research site. At this point the depression storage layer has been characterized as well as its role is dissolution kinetics of chloride on the pavement surface and its persistence throughout the year. Each storm's calibrated parameters were evaluated and compared to the site's average values and previous calibrated values from prior research where applicable. Thus with the link between specific conductivity and chloride, contaminant loading in highway runoff can be accurately measured and utilized in best management practices of highway runoff.

The approach of this research assumed the majority of the deicing agents used, NaCl and $CaCl_2$, account for the majority of the mass of deicing agents applied. While it is mathematically possible to deduce from laboratory ion analysis how much of each agent contributes to the runoff, our interest is in the common element of chloride and its unique characteristics. The ubiquitous nature of road salt allows specific conductivity to be a surrogate for chloride (Cl^-) concentration in watershed runoff. This is the main

theoretical connection between dissolution of the salt in the depression storage layer and the sodium and chloride concentrations analyzed in a laboratory sample. The autosampler results will calibrate the flux model of specific conductivity and chloride concentration to a specific field sample taken at a specific moment of each measured storm.

Chapter 2 reviews previous works relevant to concepts used during this research. Chapter 3 presents background and site description for each of the three research sites which includes any updates from previous works and details on the deicing agents application rates. Chapter 4 describes the equipment and methods used for field data collection and laboratory analysis. Chapter 5 presents the model development with parameter explanation and theoretical discussion. Chapter 6 presents results and Chapter 7 closes with a discussion.

CHAPTER 2

LITERATURE REVIEW

2.1 Deicing Agent Impact on Water Quality

The environmental impact of deicing agents, particularly NaCl, has been the focus of many studies. Highway runoff from deicing operation has had a deteriorating effect on soil and water quality. This review of previous work will address the deicing agent environmental impact on water quality via salt accumulation and the impact on roadside soil structure caused through cation exchange.

Previous theoretical developments characterizing watershed hydraulics utilizing approaches with linear reservoirs and lumped parameter solutions similar to the methods used in this research are described here as well a automated sampling procedures and sampling strategies.

2.1.1 Increased Salt Concentration

The growth of the use of deicing agents developed as the network of highways grew throughout the United States. This growth of infrastructure reached deeper into more rural areas as the demand for commerce expanded the reach of transportation of manufactured goods and agricultural products. Over time the dissolved salt accumulated in water resources and roadside environments and infrastructure damage became more prominent. Not only roadside areas have been affected by the distribution, but also the storage practices became causes for concern.

Urbanized areas have had the most impact due to the larger area of paved surfaces to deice. Ramakrishna (2005) reviewed the relationship between the chloride

contamination level in surface and groundwater and climatic factors. Impacts were grouped into general categories of degradating effects: change in density gradient, increased chloride concentrations, salt-induced stratification, and salt stimulation of algal growth. Scott (1981) identified the correlation between the salt inputs into the streams to the length and type of road draining into the streams and the amount of salt applied prior to thaw periods. It was determined that the level and duration of deicing salt concentration in the roadside stream was affected by the road drainage system, the topography, the discharge of the receiving stream, temperature and precipitation, and the degree of urbanization of the watershed. Jones and Jeffery (1992) noted the significant impact occurring to smaller bodies of water compared to larger ones and the effect of the change in density gradient of the water layers has on the normal cycle of eco-system mixing of layers with the water body. Salt induced stratification was seen in First Sister Lake, Ann Arbor Michigan (Judd and Stegall, 1982) and Irondequoit Bay, Rochester, New York (Diment *et al.*, 1973). It was found in First Sister Lake that the entire lake below ten feet deep was virtually devoid of dissolved oxygen (DO) for about eight months and that some deeper zone were anoxic for ten months. It was reported that First Sister Lake did not undergo complete mixing of layers following the winters of 1964–1965 and 1966–1967. Chloride levels reached as high as 177 mg/L in the lower three feet of the lake. Briggins and Walsh (1989) described the link between the increases in sodium concentration and the increase the growth of blue-green algae. Although sodium concentrations greater than 40 mg/L may be necessary for triggering undue growth of blue-greens, the EPA (1971) indicated that only 5 mg/L of sodium is required to provide an optimum growth of *Anabaena cylindria*. The algal growth is

essential to the suspected relationship between eutrophication and sodium build up from deicing salts.

Clearly the accumulation of sodium and chloride is inevitable as in the study by Goodwin *et al.* (2003). It was shown that in Mohawk River basin in upstate New York, the concentration of Na^+ and Cl^- had increased by 130% and 243%, respectively from 1950's to 1990's while other constituents have decreased or remained the same. This was despite a decrease in population, an increase in environmental stewardship, and enactment of The Clean Water Act.

Persistence in roadside soils was observed by the Scott (1980) study of road salt movement into two streams on the northern boundary of metropolitan Toronto. Increased levels of deicing salts in the runoff water generally coincided with thaw periods but significantly higher levels than base values were observed during snow storms and during summer months as the salts stored in the roadside soils leached into the stream and caused elevated salt levels. Although the levels were not as high as observed during the winter months, the increased levels continued for most of the spring and summer. Crowther and Hynes (1977) reported on their study on Laurel Creek in Vermont, that the summer discharge, steadily decreasing lower due to regular evaporation, high temperatures and low rainfall, had fairly high salt levels that were found many months after the last treatment of roads. Ostendorf *et al.* (2001) modeled this persistence in the salt storage facility surface runoff system and Ostendorf *et al.* (2006) for the same 11 lane mile section of State Route (SR) 25 highway runoff system in Eastern Massachusetts. The work at the Cohasset salt storage facility used data

collected before a drainage and storage system overhaul and the SR25 data used was also earlier but without any major roadway or drainage changes.

Although it is that clear that in flux modeling of highway runoff there is mass lost to infiltration, Blomqvist and Johansson (1999) concluded that between 20 and 63% of de-icing salt applied on the roads on a site 50 km south of Stockholm was transport by the air and deposited on the ground 2 – 40 m away. McBean and Al-Nassri (1987) concluded that 90% of road spray loss was deposited within 13m assuming that the maximum distance could be 30 m. Pederson and Fostad (1996) showed that 10-25% of the salt applied was deposited within 8 m of the roadway.

A study from Bowser and Hesterberg (1992) on lakes in Northern Wisconsin showed some links for the transport of chloride between road salting and lakes via groundwater systems indicating ground water as a potential pathway for the road salt contaminants into the surface waters.

2.1.2 Cation Exchange

Direct runoff is the most commonly investigated method of transport of contaminants but the reactions taking place within the roadside soils can have an impact on not just the chloride levels in surrounding water but other constituents from the highway runoff. Sodium has been shown to increase the mobilization of organic matter and elevate concentrations of metal such as chromium, nickel, lead, iron, and copper Amrhein *et al.*(1992). Most studies have focused on direct runoff rather than subsurface transport mechanisms. Amrhein *et al.* (1992) suggested through laboratory study of roadside soil samples from Donner Pass, CA, Albany and Buffalo, NY, and Cape Cod, MA, that ligand complexation and competitive exchange affected mobilization. It was

concluded that the dominant mechanism controlling metal mobilization was dispersion of organic matter under conditions of high exchangeable Na and low electrolyte concentration.

Mobilization of released ions such as calcium, magnesium, potassium and ammonium substituted by sodium uptake through cation exchange, Mason *et al*. (1999) and Shanley (1994) and other trace constituents seemed to be substantially higher downgradient than upgradient from the highway as shown through work by Granato *et al.* (1995). This mobilization of major and trace constituents due to road salt and CMA was indicated by analyses of groundwater (Granato *et al.* 1995), from groundwater wells at sites near the Plymouth infiltration basin site in this research project. The generally homogenous, fairly quick groundwater flow of the Plymouth-Carver aquifer has made it an ideal site for many of USGS studies (Granato, 1996 and Granato and Smith, 1999). The inclusion of these works highlights the general concern that if groundwaters are significant pathways to surface water systems it would lead to believe that all the other contaminants share the same pathway and equal concern should be given to other soluble contaminants released due to deicing agent application. While these other constituents are not the subject of this study, inclusion in the subsurface transport model of deicing agents from impervious surface runoff, cation exchange and ligand complexation has been studied. (Kallergis, 2007).

Not only does the cation exchange mobilize metal, but organic and inorganic particles are also flushed through the soil column, thus the soil structure is changed. This results in decreased soil permeability, aeration and increased overland flow, surface runoff and erosion. The increased erosion eventually results in nutrient removal

and heavy metal transport from the roadside to surface waters (Defourny, 2000) (Fritzsche, 1992).

2.2 Watershed Hydraulics

Hydrologic modeling used to produce simplified conceptual representations of a part of the hydrologic cycle of single to multiple watersheds has grown in use since the 1960's. The most prominent works of the time are the basis for most applied variations used today. Dooge (1959) began with defining general unit hydrograph development procedure based on two fundamental principles of invariance and superposition. Nash (1960) models the surface watershed as a linear reservoir routing runoff with a defined convolution integral of the precipitation hyetograph and an instantaneous unit hydrograph. The initial onset of runoff is delayed by a pavement storage layer due to texture (Black, 1991).

A general lumped parameter approach using two and three component hydrograph separations have been utilized Hinton and Schiff (1994) to characterize surface as well as subsurface storm event runoff through identification of impervious area hydrologic parameters (Alley, 1981). This is a popular method utilized in software development. The use of a lumped parameter gamma distribution characterizing a source term Alley (1981) has been incorporated with linear reservoir theory to produce storm pollutograph models (Ostendorf, 2001). This application to three component separation of interflow, baseflow and surface flow of an access road at a salt storage facility formed the basis of the model developed in this research. Three impermeable watersheds in Eastern Massachusetts will be characterized using the conservative properties of chloride as a tracer and the dissolution kinetics occurring in the depression

storage layer. This will illustrate the need in understanding these runoff mechanisms to efficiently apply best management practices to all types of watersheds.

'First flush' of contaminants from watershed surfaces, primarily impervious pavement, has drawn more attention as highway storm water runoff is being addressed as a non-point source pollutant influencing aquifers, surface waters and the roadside environment. The concept of the first flush phenomenon was developed in the 1970's and is based on concentration or mass. Deletic (1997) used cumulative load curves constructed to monitor water quality characteristics and regression analysis to characterize the pollutant load in the first 20% of runoff. It was found that characteristics were site specific and complicated therefore could not be described with universal runoff or rainfall characteristics or even complex multiple regression curves. Han and Stenstrom *et al.* (2006) observed a strong first flush for chemical oxygen demand and organic pollutants with 40% of the pollutant mass being discharged in the first 20% of the event while calculating event mean concentration, partial event mean concentration, and first flush concentration factors for 20 watershed parameters. Mass surges in the beginning of each individual event, an important factor in developing BMP's, is usually ranging multiple orders of magnitude. Kim and Sansalone (2008) proposed a model based on predicted stormwater runoff volume not dependent on continuous flow measurements. Additional input model variables contributing to pollutant load were found to be antecedent dry periods and traffic volume as well as typical runoff volume and precipitation intensity. The washoff model is capable of predicting runoff concentration based on linear, exponential, and gamma functions using defined parameters. Due to the fact that exponential based models do not predict

dilution and the fact that seasonal load considerations are evident at the three research sites, the dissolution mechanism operating in the depression storage layer will be the center of the model development for this research.

2.3 Prior Research with Automated Samplers

Since the enforcement of the Clean Water Act, non-point sources such as stormwater runoff have become the leading source of water pollution in the United States. It is only recently that stormwater monitoring programs have been developed. As a result, regulatory agencies are requiring stormwater monitoring programs implemented through the National Pollutant Discharge Elimination System (NPDES) to quantify and eventually reduce stormwater pollution (Lee *et al.,* 2007).

Total Maximum Daily Loads (TMDL) are based on mass and discharge permits are generally based on concentration. Sansalone and Cristina (2004) examined the significance in sampling strategy to properly characterize suspended and dissolved solids in highway runoff. It was found that the concentration based sampling strategy is needed when the control of high concentration is needed. This strategy would sample frequently to totally characterize the duration of the initial high concentration surge. Mass based sampling strategy would entail regular measurements following the hydrograph throughout the duration of the storm to appropriately characterize the event.

Urban area runoff data has been evaluated by many: Makepeace *et al*. (1995), Robinson, *et al*. (1996), and Wu *et al*. (1996) to name a few but considerably less have concentrated on highway runoff until recently Irish *et al*. (1995), Barrett *et al*. (1998), and Han *et al*., (2006). Sampling strategies utilized are important to achieve an appropriate balance between accurate characterization of storm water quality and runoff

quantities. Harmel *et al*. (2002) examined the important sampling strategy components such as minimum flow threshold, sampling interval, and discrete versus composite sampling. These procedural choices depend upon project specific considerations like sampling goal, sampling and analysis resources, and watershed characteristics. Most sampling strategies usually use either discrete sampling, composite sampling, flow weighted or time weighted intervals. In earlier work, Clark *et al.* (1981) explores inaccuracies of storm representation in discrete sampling as runoff characteristics may change as the storm progresses. Depending on sampling protocol, small storms may pass unsampled, peaks in concentration may occur between samples or large storms may only be partially represented. Volume weighted composite samples can be used to represent large runoff events.

Khan *et al*. (2006) showed that oil and grease concentrations in samples from highways in the first 15 minutes of runoff were several times higher than the event mean concentrations (EMC). Best management practices (BMP) are vital in any application improving the quality of highway runoff. First flush phenomenon is a characteristic of impervious runoff that needs to be integrated in BMPs. Kang *et al.* (2008) predicted first flush indices such as mass first flush ratio and partial event mean concentration to an event mean concentration ratio from rainfall intensities and watershed parameters. These results correlated to time of concentration as calculated using the ASCE kinematic wave equation.

The programmed procedures of the continuous monitoring equipment at the three locations subject to this study have been established over many years as this Salt Project for the MHD expanded. The automated sampling strategy had been established

through prior research done by Stygar (2005) based on historical data. Optimization of four parameters comprising the final sampling rule established the strategy currently used for the data collected during this study. These four parameters were the length of interval one, the length of interval two, the number of sample for interval one and the number of samples for interval two. The goal has been to capture samples that will characterize the hydraulics of the watershed and provide enough sampling constituent information to establish weir loading characteristics. Storm sampling begins at specific depth of flow over the weir and continues through at preset sampling times. This is a typical strategy popular for small watershed projects with the objective of comparing BMP's on water quality and characterizing pollutant fluxes.

CHAPTER 3

SITE DESCRIPTIONS AND BACKROUND

The MHD has utilized the research capabilities of the Civil and Environmental Engineering Department at University of Massachusetts, Amherst by funding various projects like the Salt Remediation Program and Highway Deicing Agent Impacts on Soil and Groundwater. Research sites have been analyzed for many different aspects related to water quality revealing many interesting results. The underlying goal is to determine the impact of foul weather roadway deicing agent application by the MHD to provide safe travel on many hundreds of miles of public highways.

The focus of the approach to the underlying issue will be on two of the older sites involved in the MHD salt program; the Plymouth infiltration basin and the Cohasset salt storage facility, and a five year old salt storage facility in Andover, Massachusetts. For all of these research sites, the term 'watershed' refers to the effective area the runoff is collected from. At the storage facilities it is the paved areas contributing to the runoff and at the Plymouth site it includes the grass swales between the directions of travel, the shoulders, and the travel lanes of SR25 that contribute runoff to the storm drains.

3.1 Plymouth Infiltration Basin

The research site is located along SR25 which extends Interstate 495 to the Bourne Bridge over the Cape Cod Canal. The geographic coordinates of the site are $41^{o}46'53"$ North and $70^{o}36'50"$ East approximately 5500 m north of the canal. Figure 3.1 shows the location of the site in the south eastern section of Massachusetts. The surrounding area is

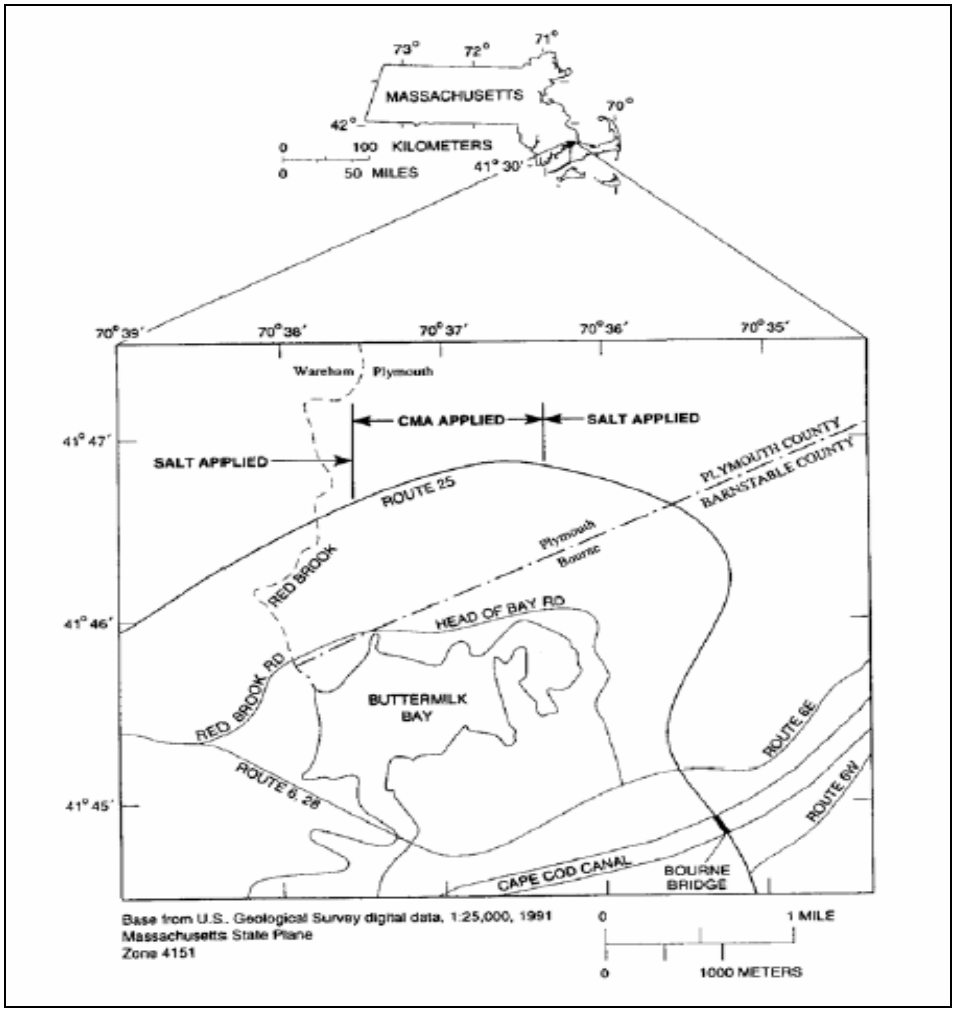

Figure 3.1: Location of Plymouth Infiltration Basin

an environmentally sensitive area due to the location of actively harvested cranberry bogs to the west, a surface water source to the south, and a replacement wetland to the north as well as the basin being on top of the Plymouth-Carver Aquifer.

The Plymouth-Carver aquifer is a regional aquifer that underlies the infiltration basin and covers an area of 360 km^2 with an estimated storage capacity of approximately 500–540 billion gallons of water USGS (1996). The aquifer along with a surface water source provides the water supply to the adjacent bogs during the growing season and throughout the harvest. The aquifer is comprised of flat-lying to gently dipping beds of sand and gravel deposited by glacial meltwater streams, Ostendorf *et al*. (2007). The

proximity of the salt source is of concern as well as the fact that infiltration is relatively quick and the groundwater flows approximately from the northeast to the southwest with a velocity roughly 0.3 to 0.9 m/day, Kelley (2003). This orientation is directly towards the bogs and the surface water source. Due to the sensitivity of this stretch of SR25, CMA was applied for the 1.2 mile (1930 m) stretch as seen in Figure 3.1 from 1987 until 2006. Use was discontinued due to documented degradation of dissolved oxygen in the groundwater immediately adjacent to the bogs and surface water source.

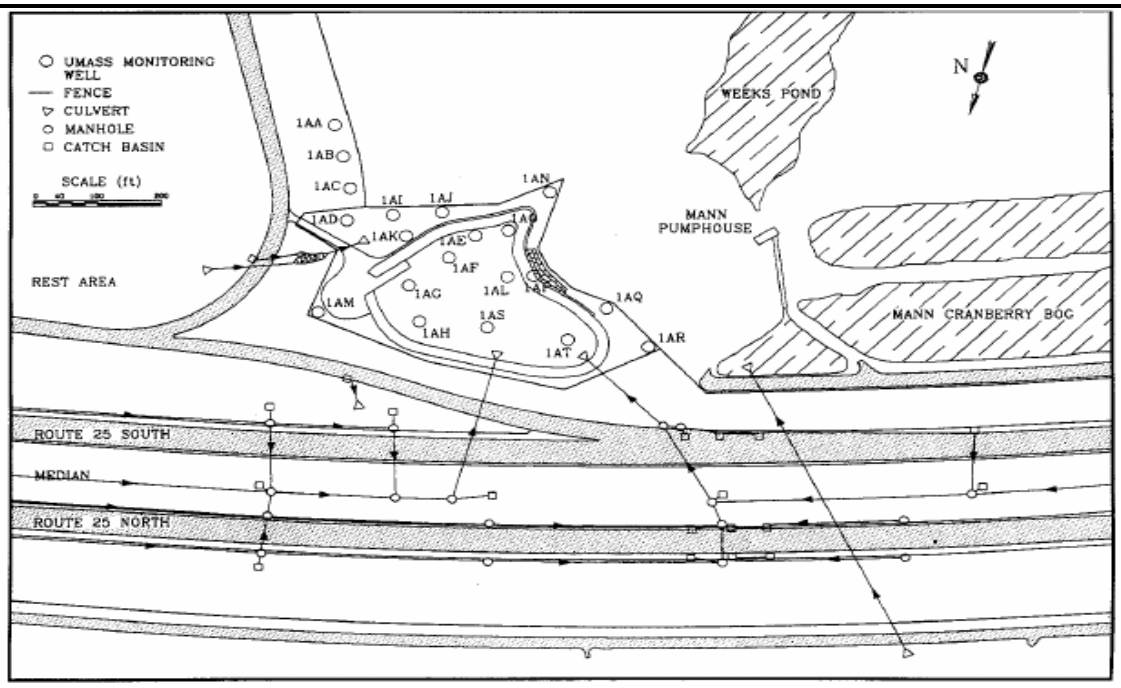

Figure 3.2: Drainage Area of SR25 Collected in Infiltration Basin

(Note the northerly direction is opposite of previous Figure 3.1)

The drainage system of the section of SR25 for approximately 2.95 km (11 lane mile) that contributes the runoff contained by the infiltration basin can be seen in Figure 3.2.

The expansion of SR25 completed in August 1987 is comprised of six 3.66 m (12 ft) wide travel lanes, a 3.04 m (10ft) wide breakdown lane, a 1.22 m. wide inner shoulder,

Ostendorf *et al*. (2006) and a 30 m (100ft) wide grass median swale Kelley (2003) between the two travel directions. The catch basins in the median are 90 m (300ft) apart and located down the center of the grass swale. The roadway catchbasins are along both shoulders in the east direction and along the inner shoulder in the west direction. The drainage of this section of SR25 is divided into eight catchments, each with the length of 103 meters. The storm drains route the eight catchments, as seen with arrows in Figure 3.2, in series to an east and west weir as discharge to the infiltration basin. The west weir receives the majority of the runoff with the east weir receiving runoff only during major storm events. This investigation used data from an autosampler installed in the west weir located on the right side of Figure 3.2. The contributions that the drainage system routes through this weir was calculated through the utilization of effective runoff area incorporated in the Visual Basic program used to analyze each storm event.

Monitoring wells are located throughout the infiltration basin, on the perimeter of the surrounding berm, at locations closer to SR25, distributed on the private cranberry farm, throughout the replacement wetlands and at USGS cluster locations surrounding this section of highway to characterize the subsurface transport of the road salt. Monthly records for over ten years have provided data analyzed to reveal CMA effects on dissolved oxygen levels in groundwater, the NaCl plume development, the flux of deicing agents through one of the weirs contributing to the infiltration in this basin, and for half of these ten years of this study duration, soil characterization.

3.1.1 Wareham Deicing Agent Application Data

The Wareham Salt Shed is one of the storage facilities in District 5B of the MHD. The Wareham Salt Shed provides material to deice 147 lane miles along Interstates 195 (I195), Interstate 495 (I495), and State Route 25 (SR25). A total 2.95 km (11 lane miles)

along SR25 was the section involved in this study of the total 147 lane miles maintained by this facility. Materials expenditure reports for the MHD District 5B - Wareham Salt Shed were provided by the Massachusetts Highway Department summarizing the usage per week and on a seasonal basis, both in hard copy and electronic versions. All quantities are in tonnage. The total material distributed annually stretches from the fall to the spring. Five seasons were analyzed from this site with the storms being analyzed beginning in January 2004 through September 2008 as part of the research.

To estimate the amount of deicing material expenditures for the area of study as shown in Table 3.1, the total annual usage of the storage facility is multiplied by 11/147 for salt and premix quantities. This fraction represents the section of highway that the study comprises. The CMA quantities were specifically distributed in the section of study to lower the impact of salt on the bogs. This material use has since been discontinued and the 2005-2006 season was the last distribution of CMA at the Plymouth site. Liquid calcium chloride (LCC) was used as a deicing agent to prepare roadways prior to a storm and prevent adherence of snow and ice upon the roadways.

Table 3.1: Wareham/Plymouth Deicing Agent Applications

Season	*Salt(tons)*	*Pre-Mix(tons)*	*CMA(tons)*	*LCC(ft^3)*
03-04	281	23	0	0
04-05	470	0	0	0
05-06	214	6	0	2351
06-07	85	14	0	78
07-08	167	16	0	97

3.2 Andover Salt Storage Facility

The Andover Salt Storage Facility is in Andover, MA and located at the intersection of I495 and I93. The research site is a state highway salt depot abutting the northbound connector between I93 and I495 and has been in operation since 1998. The regional location is depicted in Figure 3.3. The southern side of the site borders the northeastern edge of the Fish Brook watershed and lies directly north of the Haggets Pond aquifer. The Fish Brook watershed feeds the Fish Brook aquifer, the primary drinking water source for Dedham, MA. Haggets Pond lies approximately 0.67 miles to the southwest of the research site. Both aquifers have been the subject of recent environmental concern.

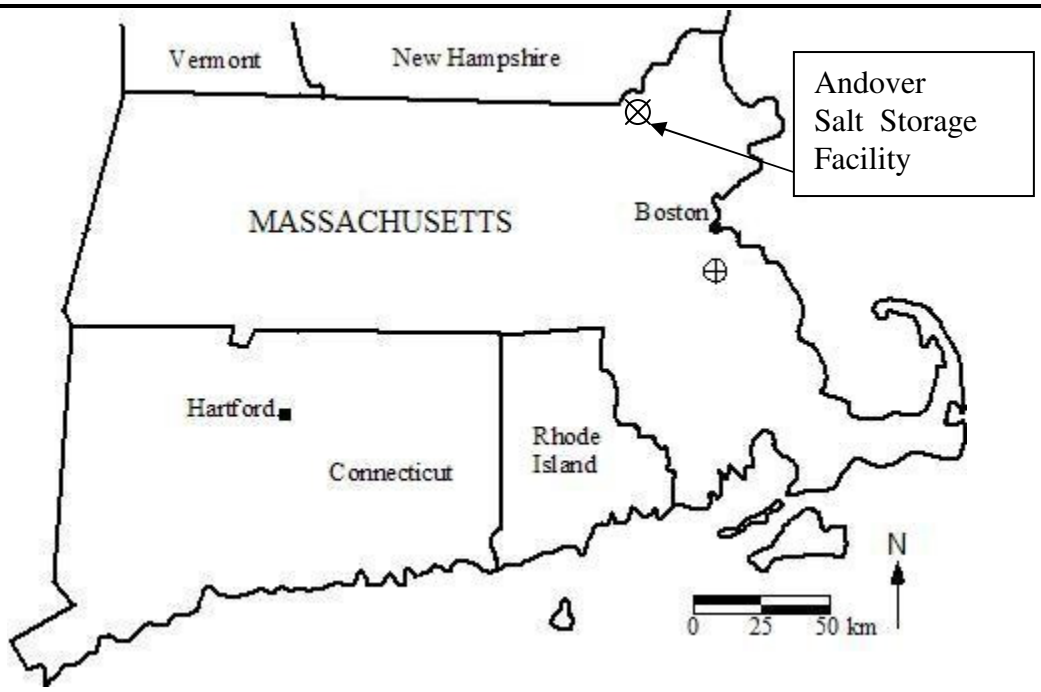

Figure 3.3: **Andover Salt Storage Facility**

A study was performed to evaluate the influence of the salt facility and other possible pollution contributors adjacent to the 5.25 mile stretch of Fish Brook. It was determined that during the years between 1998 and 2003 the sodium level in Andover's finished drinking water increased from 0.032 mg/L to 0.070 mg/L (Town of Andover, 2006). Measures have been taken to control site runoff and one aspect of this research can be used to evaluate the effectiveness of these measures taken. Since the concerns with salt contamination, the surrounding I93 & I495 roadways have had zones marked as "Reduced Salt Areas" to decrease the impact of roadway deicing agents. This area includes 9.7 linear or 38.8 lanes miles on I93 and 4.9 linear or 19.6 lanes miles on I495.

The following Figure 3.4 is a result of the most recent site survey of the paved area at the Andover facility contributing to the surface runoff. The area in front of the storage shed to the weir is contained with curbing to control the surface runoff. The contours were constructed using QuickSurf 5.1 (PetroByte, Englewood, CO). The figure denotes the location of the covered salt storage facility, the LCC storage tanks, the weir and the continuous monitoring equipment. The area estimated to contribute to the flow over the weir is approximately 25 m (82 ft) by 45 m (147ft) on average or $100m^2$.

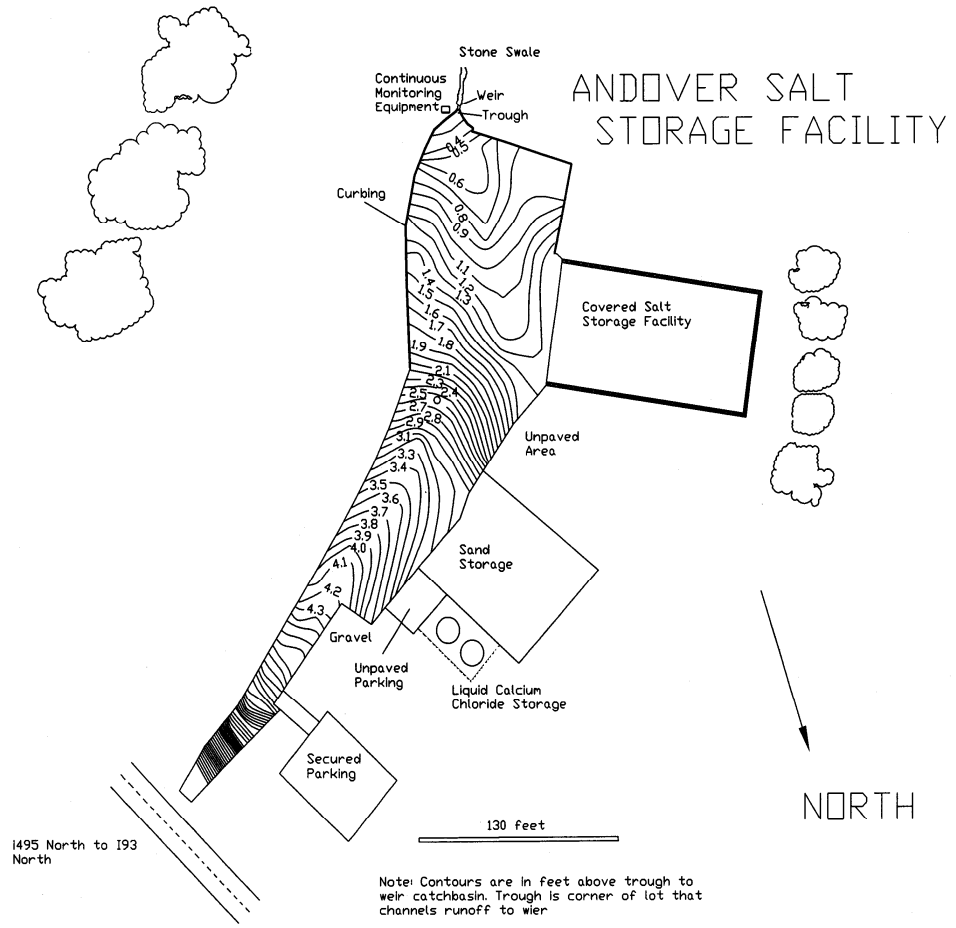

Figure 3.4: Paved Runoff Area of Andover Salt Storage Facility

Figure 3.5 displays the housing for the data collection equipment and weir arrangement located in the south corner of the Andover site. The amount of deicing material expenditures for the Andover facility is shown in Table 3.2. The facility stores deicing agents for approximately 130 lane miles of I93 and I495. The total annual usage of the storage facility is in tons and LLC is liquid calcium chloride in cubic feet. CMA is not an agent used at this site.

Figure 3.5: Data Collection Equipment at the Andover Salt Storage Facility

Table 3.2: Andover Deicing Agent Applications

Season	*Salt (tons)*	*Pre-Mix (tons)*	*CM A(tons)*	*LCC (ft^3)*
03-04	281	23	0	0
04-05	470	0	0	0
05-06	214	0	0	0
06-07	85	14	0	78
07-08	167	16	0	97

3.3 Cohasset Salt Storage Facility

The Cohasset Salt storage facility is located on top of Situate Hill in Cohasset, MA, approximately 30 miles south of Boston and ½ mile west of Route 3A as seen if Figure 3.6. The hill is a glacial drumlin and a predominant natural feature in the

surrounding landscape directly adjacent to a closed private landfill to the southwest. The entire facility encompasses approximately 13 acres (35,000 m^2), which includes a large salt shed reconstructed before the 2001-2002 deicing season and several smaller storage sheds around the perimeter.

The property was formerly a Nike missile base during the Cold War and was converted to a salt storage facility when ownership was turned over to the Commonwealth of Massachusetts in the 1950s. Practice in the beginning was not concerned with protecting the salt and sand from the elements but has since changed upon growing concerns of environmental damage from salt in the facility storm runoff.

The adjacent landfill's leachate is subject to environmental monitoring and in 1986 elevated levels of sodium and chloride were detected. A study, beginning in 1988 and performed by SAIC Engineering Inc in 1993 and 1995 (Peeling, 1999) was focused on the salt facility. In 1992 the State of Massachusetts was ruled to be responsible for the elevated levels and held responsible to compensate the additional expense in treatment of the landfill leachate already being performed. At this point the University of Massachusetts was appointed to investigate the extent and potential contamination sources from the storage facility.

The first sheds were constructed in the 1970's and the adjacent material handling area was paved. In the fall of 2002 the facility was overhauled with an upgraded drainage system and the replacement of the two smaller storage sheds with a much larger shed (Ostendorf *et al.* 2001). All material handling and storage is now conducted under cover.

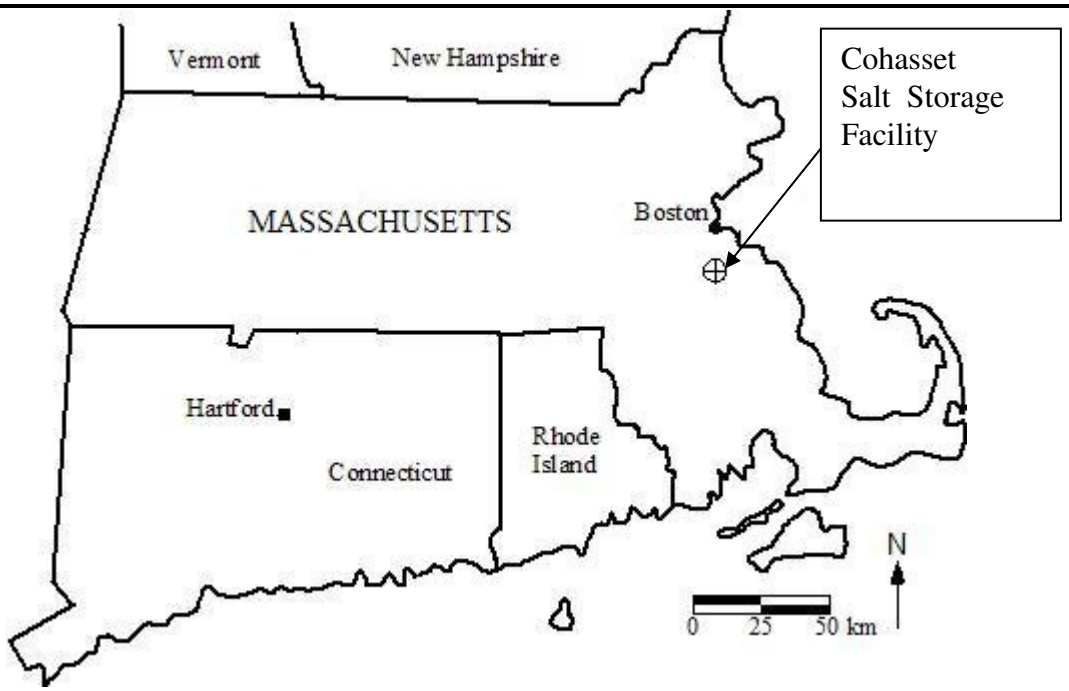

Figure 3.6: **Cohasset Salt Storage Facility (Rotaru, 2005)**

The rebuilt drainage system channels the storm drains of the paved area to an infiltration wetlands area below the western slope of the drumlin, between the MHD property and the private landfill. The drainage area encompassed approximately 10,680 m^2 (115,000 ft^2) pre-reconstruction and approximately 11,560 m^2 after the new shed and drainage system was constructed as seen in Figure 3.7. The heavy dashed line encloses the pavement comprising the watershed area of the drainage system directed to the weir in the southwestern corner of the drawing used in this study.

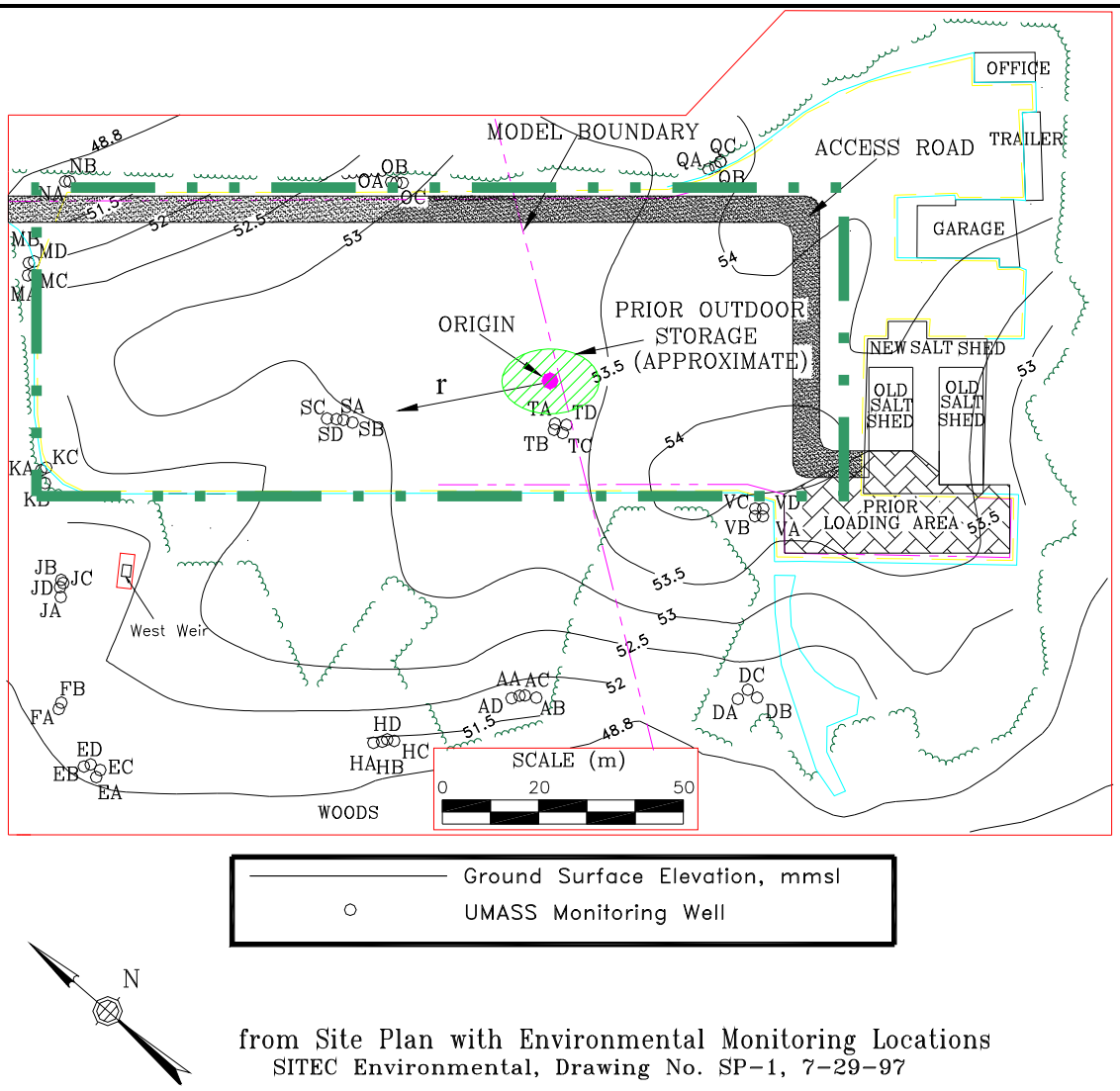

Figure 3.7: **Cohasset Storage FacilityWatershed Runoff Area**

A comprehensive distribution of 42 monitoring wells were installed from 1998 to 2004 to characterize the subsurface chloride contamination resulting mostly from the uncovered salt left to the elements in the past but also from the leaking original drainage system and cracked pavement and continuing use of the facility. Surface runoff data has been compiled of the drainage system pre and post reconstruction of the channeled storm drains through a series of weirs since 1998. A three component flow model of surface runoff, groundwater base flow, and interflow was analyzed by Peeling (1999) to reveal the effects of insufficient drainage system and catch basin/curbing system through hydraulic and flux models. Rotaru (2005) developed a two dimensional steady state analytic model of the aquifer hydraulics and used it to simulate the groundwater age distribution by tracking chloride ions as they migrate via advection. Kallergis (2007) analyzed cation exchange capacity of the subsurface and the distribution of dissolved and sorbed sodium frames as they are transported in the aquifer.

3.3.1 Cohasset Deicing Agent Application Data

The facility services approximately 90 miles (145 km) of local roads. The deicing agents used at this site are rock salt and premix and the approximate average rate of distribution is 240 lbs/lane mile. This of course varies with the temperature of the surface, the type of precipitation, and the intensity of the precipitation. The route the distribution trucks take in and off the property can be seen in Figure 3.6 from in front of the newer large storage shed, up to the northeast, and along the northeastern curbed border of the paved area before the trucks descend down the rest of the driveway off the property and the immediate drainage area. Ostendorf *et al*. (2001) established the fraction of chloride applied to this 100 m (0.062 lane mile) access road compared to the whole 90 miles

(145km) serviced by this facility for a percentage factor for comparison of modeled mass flux of chloride through the drainage system. The total material distributed by the facility is in Table 3.3 below with estimated contribution to the access road. All values are tonnage. Figure 3.8 displays the equipment storage booth, access and the automated sampler and weir at the Cohasset site.

Figure 3.8: Data Collection Equipment at the Cohasset Salt Storage Facility

Table 3.3: Cohasset Deicing Agent Applications

Season	***Salt (tons for 90 miles)***	***Salt (tons for access road)***
03-04	3454	2.4
04-05	3956	2.7
05-06	2621	1.8
06-07	Not available	Not available
07-08	Not available	Not available

CHAPTER 4

METHODS OF INVESTIGATION

This section describes the field methods used to monitor and measure the hydraulic and transport parameters of storm event runoff and ionic composition of the runoff at the three research sites and a brief description of the laboratory analysis utilized to evaluate water quality for this investigation.

4.1 Field Measurements

Each of the research sites has an arrangement of equipment designed to monitor and record all storm runoff and precipitation occurrences and sample some significant runoff events. Remote sensing equipment continuously records precipitation and water quality data and an automated sampler obtains a number samples from the beginning and periodically throughout a significant runoff event.

Remote sensing continuous monitoring equipment associated with each site includes rain gauges, specific conductivity meters, pH meters, a water level meter and data loggers. The automated sampler and remote sensing equipment is housed in a phone booth type structure with battery power in Andover and positioned adjacent to the weir. A direct power source is provided for the Plymouth data logger, meters and gauges and is located the same type of structure adjacent to the east weir. In Plymouth the automated sampler is housed in an insulated lockbox mounted next to the west weir with battery power. In Cohasset, there is a direct power source and the equipment is in a similar but larger booth structure sized to accommodate a ladder because the drainage channel is approximately 12 ft below the surface of the pavement. The automated sampler and remote sensing equipment are in this one booth with a direct power source. All the booth structures are

enclosed, locked, insulated and secured to a concrete foundation to protect data loggers, automated samplers, and backup battery power sources.

Highway runoff sampling and water quality data is collected and analyzed on a per storm basis from the automated samplers associated with each v-notch weir. The goal is to introduce two storms analyzed on a water quality basis (ion analysis) per month into the database with proper field equipment function and precipitation quantification.

The automated samplers used at each site are an ISCO 6712 (ISCO; Lincoln, NE). The samplers were programmed to begin collection after a certain water level is reached in the weir and to continue for 24 sampling periods at preset time increments. Each site has a 15 minute increment for the first 5 samples taken and a 25 minute increment for the remaining 6 thru 24 samples taken of the stormwater. Stygar (2005) optimized the Plymouth sampling rules and this procedure has been adapted to the Andover and Cohasset sites. The 25 min increment most efficiently captures representative storm samples at each respective watershed although 35 and one hour increments have been experimented with after the vital first five representative samples have been collected. Before each sample is taken, a 20 seconds air purge is exited from the automated sampler to clean the line of stagnant water. This draw line is also wrapped in a heating coil to prevent freezing. The Cohasset site does not need the heating coil due to the depth below the ground surface the equipment is located. The pH, specific conductivity and water level data was recorded and downloaded to a laptop computer loaded with Flowlink® support software (ISCO) utilizing ISCO cabling during twice-a-month field trips. The trips were designed to provide equipment maintenance and calibration, sampling bottle exchange, and overall site maintenance and monitoring.

4.1.1 Water Quality Monitoring

Continuous monitoring equipment recorded precipitation, water level in the weir, specific conductivity, pH, and temperature different increments at all sites. The Plymouth site records data every five minutes, the Andover logger is set to record data every fifteen minutes and the Cohasset sampler began at five minute increments, increased to ten and is now set to fifteen minute increments since December 2005.This equipment is housed on site in the previously mentioned protective structures.

The specific conductivity and pH was measured with an YSI model 600 (YSI; Yellow Springs, OH) Multi-Parameter Water Quality Monitor. The probes for this system were secured to posts with plastic ties within the weir and are removed, cleaned, and calibrated each sampling trip. The specific conductivity meter has an accuracy of ±0.5% for a measurement between 0 – 100 mS/cm. The pH accuracy is ±0.2. The data is recorded with the same time interval as the water level meter and rain gauge. A 1500W Floating Stock Tank Deicer (McMaster Carr, New Brunswick, NJ) heating element is submerged within the weir in Andover to prevent the surface of the standing water from freezing. Plymouth and Cohasset does not normally have standing water. The probe arrangement at the Plymouth site can be seen in Figure 4.1. Similar arrangements are at the Andover and Cohasset sites.

4.1.2 Precipitation Monitoring

The precipitation was measured with rain gauges at all three sites that are ISCO model 674L with tipping bucket style collection devices. The tipping buckets have a sensitivity of 0.25 mm (0.01 in) and a capacity of 760 mm/hr. Each gauge is 20 cm in diameter and is 33 cm high. The precision of the rain gauge is ±1.0 % of the bucket volume for precipitation rates up to 560 mm/hr. The rain gauges are constructed of steel,

stainless steel, aluminum, and plastic with all the appropriate platings and coatings to provide weather resistance. The rain gauges were leveled with an installed bubble level and secured to the roof of the remote sensing equipment shed at each site. The top of the rain gauges were covered with a fine screen to prevent debris from collecting and interference from insects. The location of all storage sheds are within

Figure 4.1: Rain Gauge, Weir, Automated Sampler, and Water Quality Probes in Plymouth Infiltration Basin

the manufacturer's recommended distance from surrounding overhead objects. The Cohasset site has two rain gauges with one being heated which are approximately 100 yards apart, Plymouth has a heated rain gauge, and the Andover site's rain gauge is not heated. The heat is provided by three 10" long by 3" wide 150 watt silicon heating mats (Cole-Parmer Instrument Company, Vernon Hills, IL.) bonded to the outside of the housing. The mat temperatures are regulated using a transformer located inside the storage

shed. The data loggers were programmed to record precipitation measurements every fifteen minutes with the capacity to store 33 days of data on a rollover basis. Data is downloaded to a laptop computer using the ISCO 674L support software. A schematic of the ISCO 674 rain gauge is Figure 4.2.

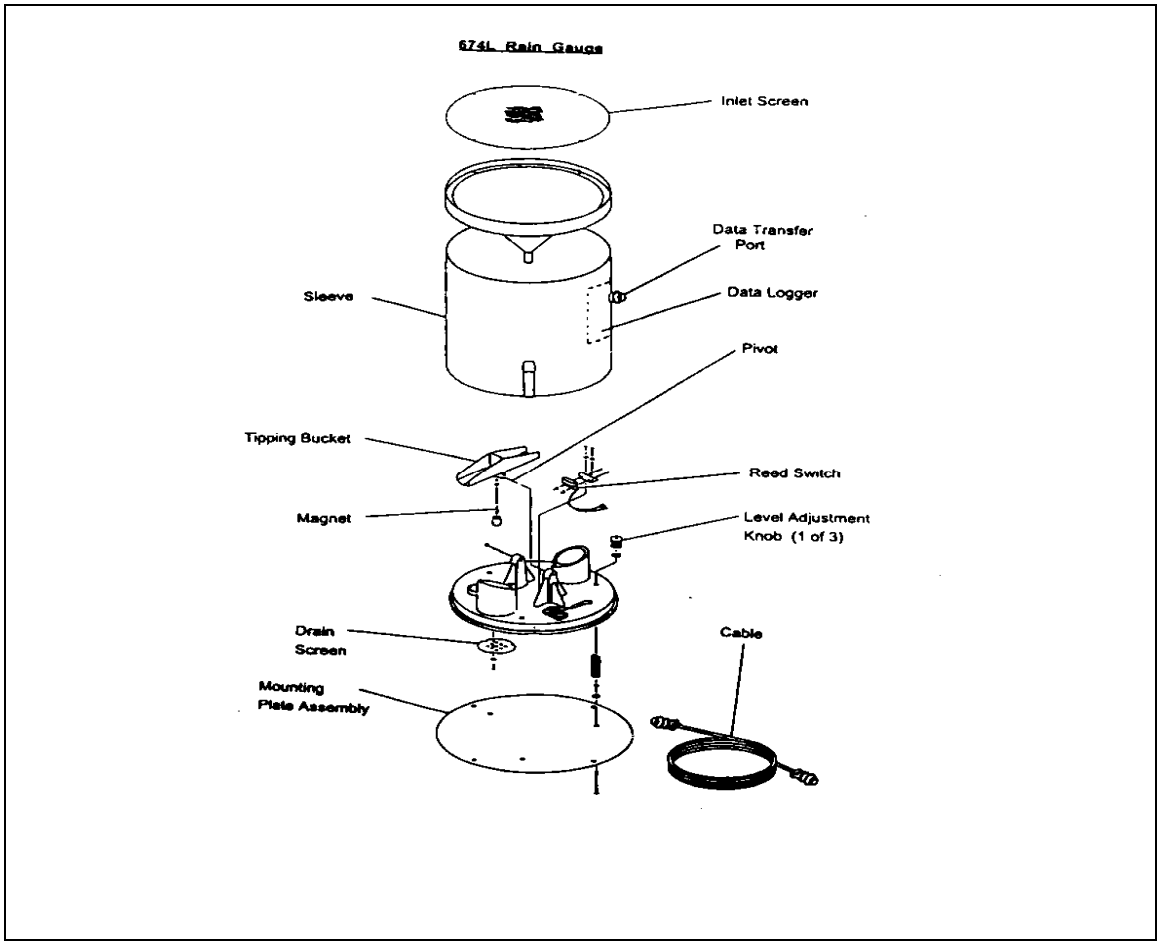

Figure 4.2: ISCO 674L Rain Gauge

Precipitation data is reinforced with local national weather service precipitation data from surrounding sites. The Blue Hill Observatory in Milton, MA is used for Cohasset, the East Wareham monitoring station for Plymouth, and another MHD/UMass rain gauge nearby

adjacent to Interstate 495 in Andover, MA and the Lawrence Municipal Airport Rain Gauge.

4.1.3 Watershed Runoff Monitoring

Watershed runoff is consolidated with a system of storm drains and subsurface pipeline at the section of SR25 that feeds the infiltration basin in Plymouth and at the salt storage facility in Cohasset. The pipeline leads to channels feeding each weir at the respective sites. At the Andover salt storage facility the runoff is contained with curbing and runs directly off the paved area to the weir. At all of the research sites the amount of water leaving the watershed is controlled with V notch weirs. The weirs obstruct the flow of water and release the flow through the V notch of standard measurements.

The 90^{o} V notch weirs are constructed with 1/8" aluminum in accordance to USGS specifications and measure 0.91 m high, 1.52 m long, and 1.22 m wide. The base of the notch is 0.458 m above the base of the weir. As seen in Figure 4.1 above, the weir in Plymouth covers the end of the culvert so dimensions are slightly adjusted.

The weirs are equipped with an ISCO model 4230 Bubbler Flow Meter (New England Environmental Equipment, Bedford, MA) and the previously mentioned specific conductivity and pH meters. The water level meter operates by releasing a bubble of air from a known distance above the bottom of the weir with a measured amount of pressure. The amount of pressure to release the bubble is directly related to the amount of head above the release point and hence the water level is acquired. The flow meter has a resolution of 3.05 mm (0.01 ft) with an error of ±1.52 mm (0.005 ft). The weir is equipped with low flow and high flow baffles to ensure uniform hydraulics approaching the notch. Figure 4.3 is the typical layout of the weir and data acquisition equipment.

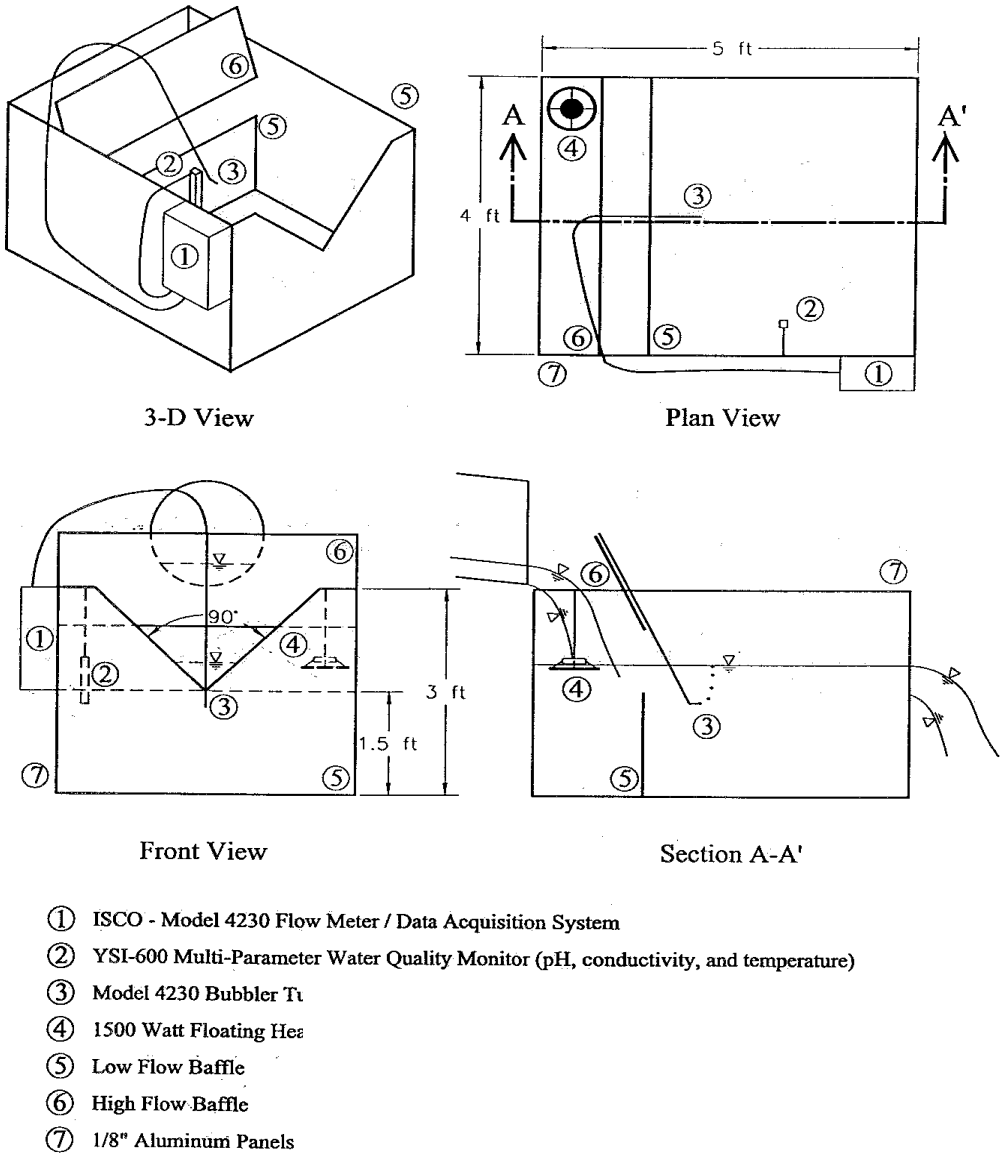

Figure 4.3: Weir Construction Details (Ostendorf, 1998)

The bubble meter must operate at a distance of at least 4*H before the notch of the weir to avoid the slope of the water flowing over the V notch. 4.2 The measured height of water above the weir is H as in the example of flow over a V notch weir in Figure 4.4.The

dotted line represents the datum reference line with y_C the height of runoff Q flowing through the weir. The flow is from right to left in the figure.

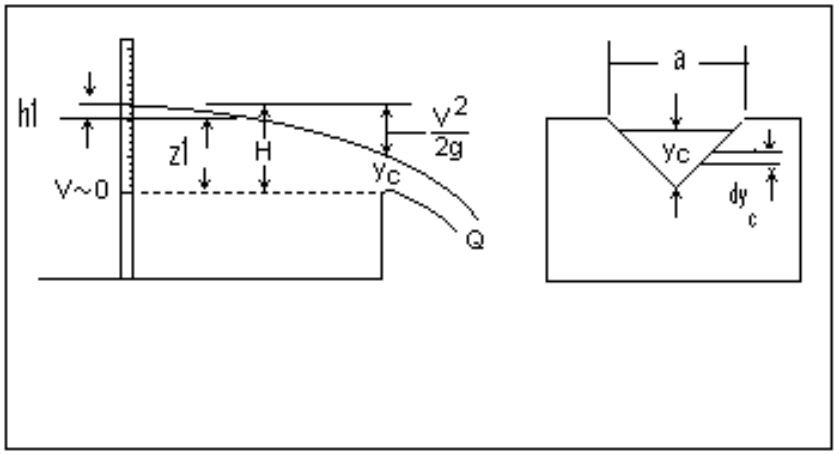

Figure 4.4: Typical V-Notch Weir with Flow

A theoretical presentation follows starting with the use of the conservation of mass and conservation of energy equations resulting in the Bernoulli equation as seen in Equation 2.1 with the kinetic energy represented by $V^2/2g$. This equation states that the static pressure in the flow + the dynamic pressure + the height above a datum will be equal to the second locations head + dynamic + static pressure in the same flow, assuming there is no loss in head. The assumption is fine given the short distance between the two measurement positions.

$$\frac{P_1}{\rho g}+\frac{V_1^2}{2g}+z_1=\frac{P_2}{\rho g}+\frac{V_2^2}{2g}+z_2 \qquad \textbf{4.1}$$

The measured gauge pressure at the two positions, P_1 and P_2 are equal, given the channel is a free surface, y_C is the height of water through the weir, v is velocity at respective points, ρ is density of water, z_1 is the water level at the location before the weir, z_2 is the water level at the weir, and g is gravity. The system pressure is atmospheric at the point

before the weir (position of bubble meter) and at the point the flow crosses the plane of the weir at the V notch, therefore both pressures at depth y_C allows elimination from both sides of the equation. If the water on the top of the free surface is the observed 'plug' of water being tracked from a position with water level z_1, and then at the plane of the V notch with the velocity at the first point negligible compared to the velocity over the weir, Equation 4.1 reduces to Equation 4.2 and then Equation 4.3 defines the velocity over the weir to be used to calculate flow.

$$H = h_1 + z_1 = \frac{V_2^2}{2g} + y_C \qquad \textbf{4.2}$$

$$V_2 = \sqrt{2gy_C} \qquad \textbf{4.3}$$

In Figure 4.4, *a* represents the width of the free surface flowing over the weir and *da* would be the change in that distance as depth through the weir, dy_C changes with change in flow, Q over the weir. Integrating Equation 4.3 over the area A of the cross sectional plane of flow over the weir opening represented by Equations 4.4 and 4.5,

$$dA = a dy_C \qquad \textbf{4.4}$$

$$a = 2(H - y_C)\tan\frac{\theta}{2} \qquad \textbf{4.5}$$

produces Equation 4.6,

$$Q = \int_A VA = \int_0^H \left[(\sqrt{2gh}) 2(h - y_C)\tan\frac{\theta}{2} \right] dh \qquad \textbf{4.6}$$

with θ equal to the angle of the V notch in the weir of 90^o. The more commonly known form is Equation 4.7 with weir coefficient C_D,

$$Q = C_D \frac{8}{15}\sqrt{2g}\tan\frac{\theta}{2}H^{\frac{5}{2}} \qquad \textbf{4.7a}$$

$$C_D = 0.56 + \frac{0.70}{(R_e W_e)^{0.165}} \qquad \text{[Ostendorf (2006)]} \qquad \textbf{4.7b}$$

Applying the characteristics of the flow from the Reynolds number Re and Weber number We adjusts C_D in Equation 4.8

$$R_e = \frac{H\sqrt{gH}}{\upsilon} \qquad (\upsilon = 10^{-6}\ m^2/s) \qquad \textbf{4.8a}$$

$$W_e = \frac{\rho g H^2}{\sigma} \qquad (\sigma = 0.074\ \text{N-m}) \qquad \textbf{4.8b}$$

$$C_D = 0.56 + 0.00803H^{\frac{-7}{12}} \qquad (\text{H in m}) \qquad \textbf{4.8c}$$

The weir discharge coefficient, C_D is 1122 for flow in gpm and head in feet and C_D is 1.38 $m^{1/2}/s$ for head in meters and flow in m^3/s with υ as viscosity of the water and σ as surface tension. The discharge coefficient compensates for viscous effects, contraction and the upstream kinetic energy fluid effects in this estimate. The discharge calculated with Equation 4.7 was checked against actual measured flow at Cohasset and the match is excellent as seen in Figure 4.5.

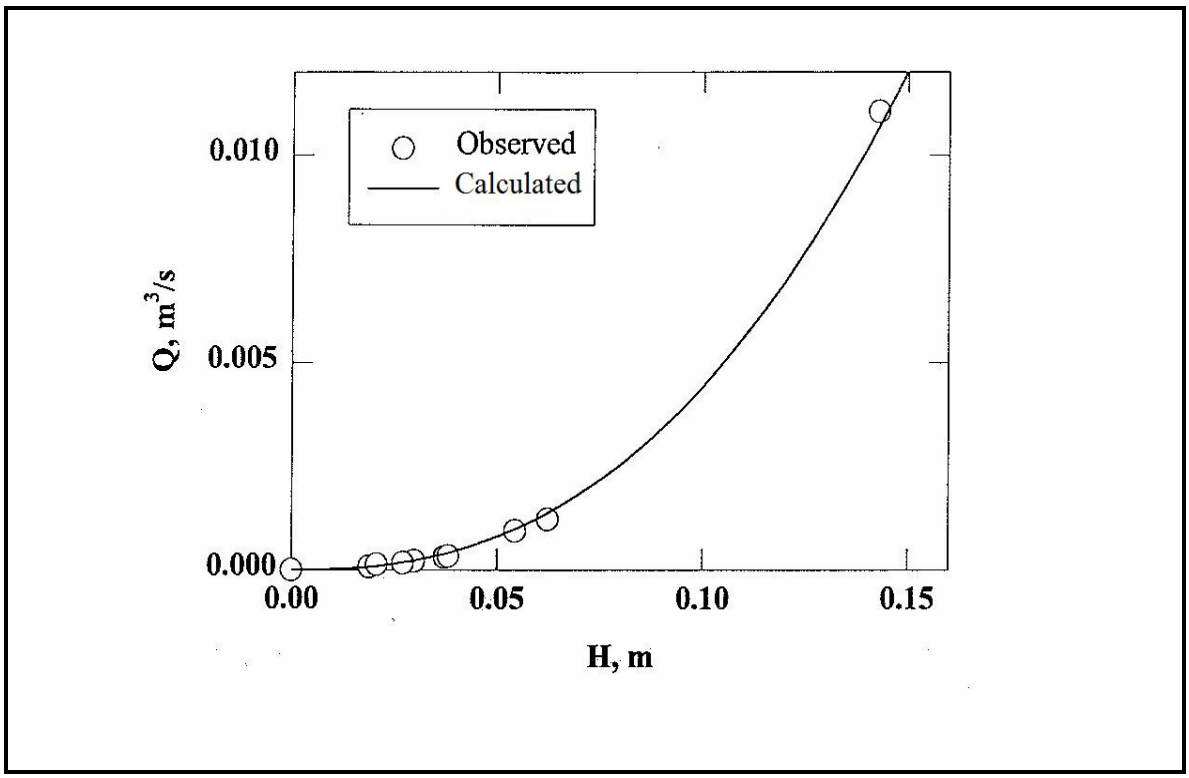

Figure 4.5: Calibration of Predicted with Observed Weir Discharge, Ostendorf(1998)

4.2 Laboratory Analysis

The 24 ≈ 0.75 L stormwater samples collected by the automated sampler were collected as soon as possible after detection of a sampling cycle run. Detection of a sample run was done through a phone line connection that indicated sufficient runoff triggered a sampling procedure. Upon return to the laboratory the samples were stored at 4^{o}C until the subsampling procedure began. During the subsampling the pH and specific conductivity (SC) values were recorded. The SC value was compared to a table developed from previous known values of ion content and SC values. This comparison will determine the dilution factor to be applied to the field sample. Table 4.1 contains the dilution information used for determining cation and anion dilution factors for the automated samples collected based on specific conductivity.

Samples must be diluted for high concentrations of ions above certain values to prevent damage to the ion analysis equipment and to adhere to the sensitivity range and detection limit of the instrument. The dilution factor depended upon if the sample was being prepared for cation or anion analysis. Before dilution, a small representative sample was drawn with a polypropylene 20 ml syringe (Becton Dickinson and Company; Franklin Lakes, NJ) and filtered with a 25 mm, 0.45 μm pore size (Millipore Corp, Bedford, MA) filter and set aside in a clean, acid washed glass vial. Total organic carbon (TOC) subsamples do not get filtered.

Table 4.1: Dilutions Based on Specific Conductivity

Cation Dilutions for 6712 Automated Sampler					
Dilution	SC (μS)	HNO_3 14%	Sample (mL)	RO water (mL)	Total Volume (mL)
1:1	<500	1.0	1.4	11.6	14.0
1:10	500 – 4,500	1.0	0.52	12.0	13.52
1:25	4,500 – 11,000	1.0	0.26	12.0	13.26
1:50	11,000 – 22,000	1.0	0.16	12.0	13.16
1:75	22,000 – 30,000	1.0	0.13	12.0	13.13
1:100	30,000 – 37,000	1.0	0.065	12.0	13.065
Anion dilution for 6712 Automated sampler					
Dilution	SC (μS)	HNO_3 14%	Sample (μL)	RO water (mL)	Total Volume (mL)
1:1	<3000	--	1,500	0	1.5
1:10	3,000 – 25,000	--	150	1.35	1.5
1:20	25,000 – 50, 000	--	80	1.52	1.6

The cation subsamples were prepared by adding into a polypropylene vial (120 X 17 ml, Sarstedt; Newton, NC) the tabulated quantity of filtered sample, 1 ml of nitric acid to preserve the metal in solution, and dilution water. The anion subsamples were prepared by dilution if necessary, into sterile 1.5 ml glass vials. The water for dilution is laboratory stock reverse osmosis (RO) water. The RO water was allowed to run for a period of time prior to dilution use and during programmed instrument runs to ensure the highest quality RO water was available.

For quality assurance and quality control, various measures were taken during the subsampling and analytical steps of the examination to verify precautions taken were effective. The quality assurance measures are:

1.) Field blanks were integrated into the array of samples which are samples of water purified by reverse osmosis (RO) treatment. They were preserved and analyzed the same way storm water samples are as described in the ICP, IC and TOC analysis procedure that follows. This quality assurance step was utilized to detect cross contamination during sampling procedures.

2.) Field spikes are a predetermined volume of an ionic concentration added to the surface water sample. Analysis revealed recovered ion concentration in comparison to the added quantity and the unaltered sample. Typical spike recoveries were aimed at being between 90% and 110% recovery. If analysis was not within this range of accuracy the samples were rerun to obtain a result within this range. If the result was not within the range an explanation was sought and mentioned in monthly reports. This spike procedure was implemented for the automated samplers at the initial set up of the weirs in Cohasset

and Plymouth through June 2005. This quality control measure is no longer practiced on the automated collection samples.

3.) Duplicate samples are prepared for the analysis equipment every ninth or eleventh sample. For a typical 24 array of automated samples, two time period samples would be duplicated. The operational procedure of the IC, ICP, and TOC machines duplicated every tenth sample for each programmed analysis set. Each duplicate result was compared to ensure reproducibility, precision, and quality of sample collection and preparation.

Standard stock solutions of known concentrations of ions were prepared for the calibration of cation, anion and TOC analysis equipment. Standard laboratory procedures were followed to safely store and prevent contamination. The standards (Absolute Standards, Inc) are a set of standards used for two purposes. One is to produce a calibration curve for determination of ion concentrations in the samples and the second is as a check of operational errors during the analysis of the set of samples. Intermittent standards were run with the surface runoff samples throughout the programmed set of samples analyzed to check operational errors. Table 4.2 is an example of anion and cation stock solution dilutions used to produce the calibration curve used for the analysis of chloride as displayed in Figure 4.6. These calibration curves are produced before each programmed run of samples analyzed by both the IC and ICP instruments. A typical chloride calibration curve usually consists of five to eight chloride standards. Each ion has a calibration curve produced prior to field sample analysis for each different run. A run would be an entire set of field samples from a particular storm. For higher concentrations of sodium and calcium there is a separate stock solution (Baker Chemical; Mumbia, India) of 1,000 mg/L that may be used during the winter and spring months. An acetate standard

was also used when CMA investigation was still being untaken. This study was discontinued after 2006 at the only site subject to CMA deicing, Plymouth.

Table 4.2: Anion & Cation Stock Solution and Dilutions

	Stock (mg/L)	1:2 (mg/L)	1:5 (mg/L)	1:10 (mg/L)	1:100 (mg/L)
Anions					
Cl^-	200	100	40	20	2
SO_4^{-2}	100	50	20	10	1
NO_3^-	5	2.5	1	0.5	0.05
PO_4^-	5	2.5	1	0.5	0.05
Cations					
Na^+	100	50	--	10	1
K^+	100	5	--	1	0.1
Mg^{+2}	20	10	--	2	0.2
Ca^{+2}	25	12.5	--	2.5	0.25

Analytic chemistry utilizes a method detection limit (MDL) to determine the lowest quantity of a substance that can be distinguished from the absence of that substance. The U.S. Environmental Protection Agency (EPA) defines the MDL as the lowest amount that differentiates a sample that contains the substance from one that does not, and the quantification limit as the lowest amount of a substance that an be measured with a stated level of confidence (EPA, 1983). The confidence interval for this research is 99% leaving 1% error. Standards are made according to Standard Methods Section 3111 (Standard methods, 1995). The MDL levels for the anions and cations identified is this research are shown in Table 4.3.

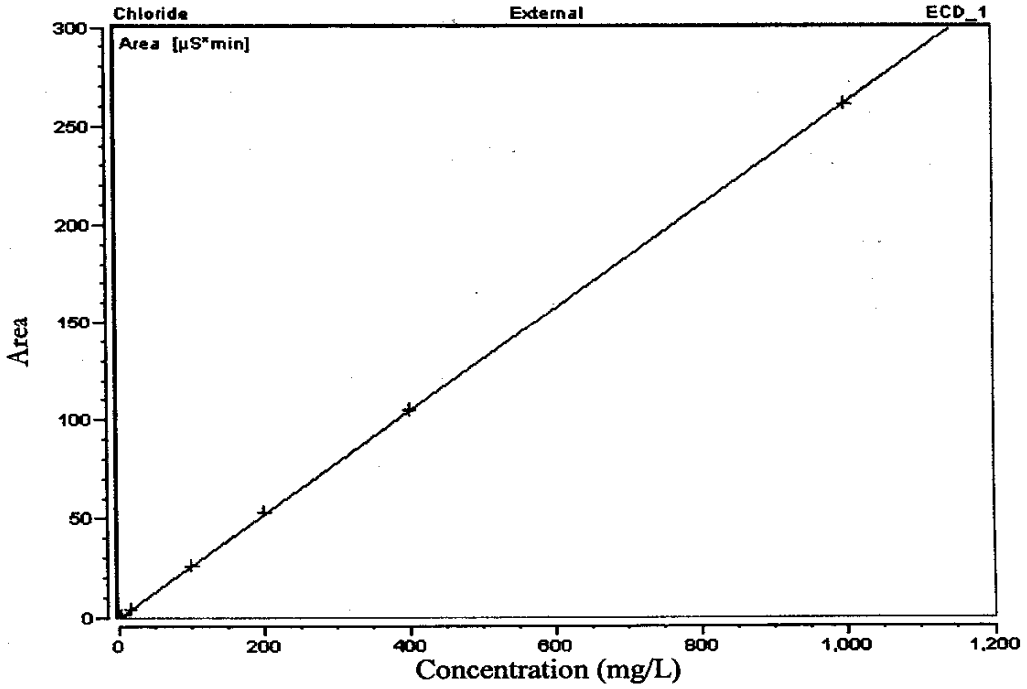

Figure 4.6: Chloride Standardized Calibration Curve

Table 4.3: Anion & Cation MDL Limits

	Cl^-	SO_4^{-2}	NO_3^-	PO_4^-	Na^+	K^+	Mg^{+2}	Ca^{+2}
mg/L	**0.03/1000**	**0.09/250**	**0.05/25**	**0.10/25**	**0.06/100**	**0.04/20**	**0.01/75**	**0.01/75**

4.2.1 ICP Cation Analysis

The inductively coupled plasma spectrometer (ICP) used to analyze the cations, sodium (Na^+), potassium (K^+), magnesium (Mg^{2+}), and calcium (Ca^{2+}) was a (Perkin Elmer; Shelton, CT) Optima model 5300 DV. The plasma source has a vertical torch configuration with a glass cyclonic spray chamber and a low-flow GemCone nebulizer coupled with a

peristaltic pump. It has 1.2 and 2.0 mm Alumina injector. It is accompanied with a fully automated AS93 plus autosampler. Optical Emission Spectroscopy (ICP-OES) was used to measure the light wavelength emitted from each element in the sample as it was energized. Ultra high purity liquid argon (Merriam Graves, Springfield, MA) is the noble gas used to build the plasma and as the carrier gas.

The plasma gas flow is 15 L/min, auxiliary gas flow is 0.2 L/min, the nebulizer gas flows at 0.8 L/min, with the radio-frequency (RF) power of 1500 watts. A sample was injected into the plasma through the nebulizer within the spray chamber at a rate of 1.5 m/min. Each sample was flushed and vaporized into the separate cations and analyzed in triplicate during the sample introduction time of 40 seconds. The reading time is 1 to 10 seconds with 15 second delay. The 30 second rinsing time used 1% nitric acid to cleanse the auto-sampler probe and peristaltic pump introduction system which was flushed for 40 seconds. Signals emitted from the elements analyzed were focused by desired wavelength and captured by a segmented-array charge coupled device (OES). WinLab32™ ICP software provided seamless data transfer.

A laboratory technician ensured proper maintenance of the equipment and accuracy of results. Calibration was done before each programmed procedure of each sample set with the addition of replicate samples for accuracy comparison and reproducibility. An output was generated for each run of the chromatograph with a typical sample shown in Figure 4.7. The area under the curve is representative of the concentration of the ions present in the sample. Utilization of the calibration curve and multiplication by the dilution factor from sample preparation revealed the true concentration of each ion.

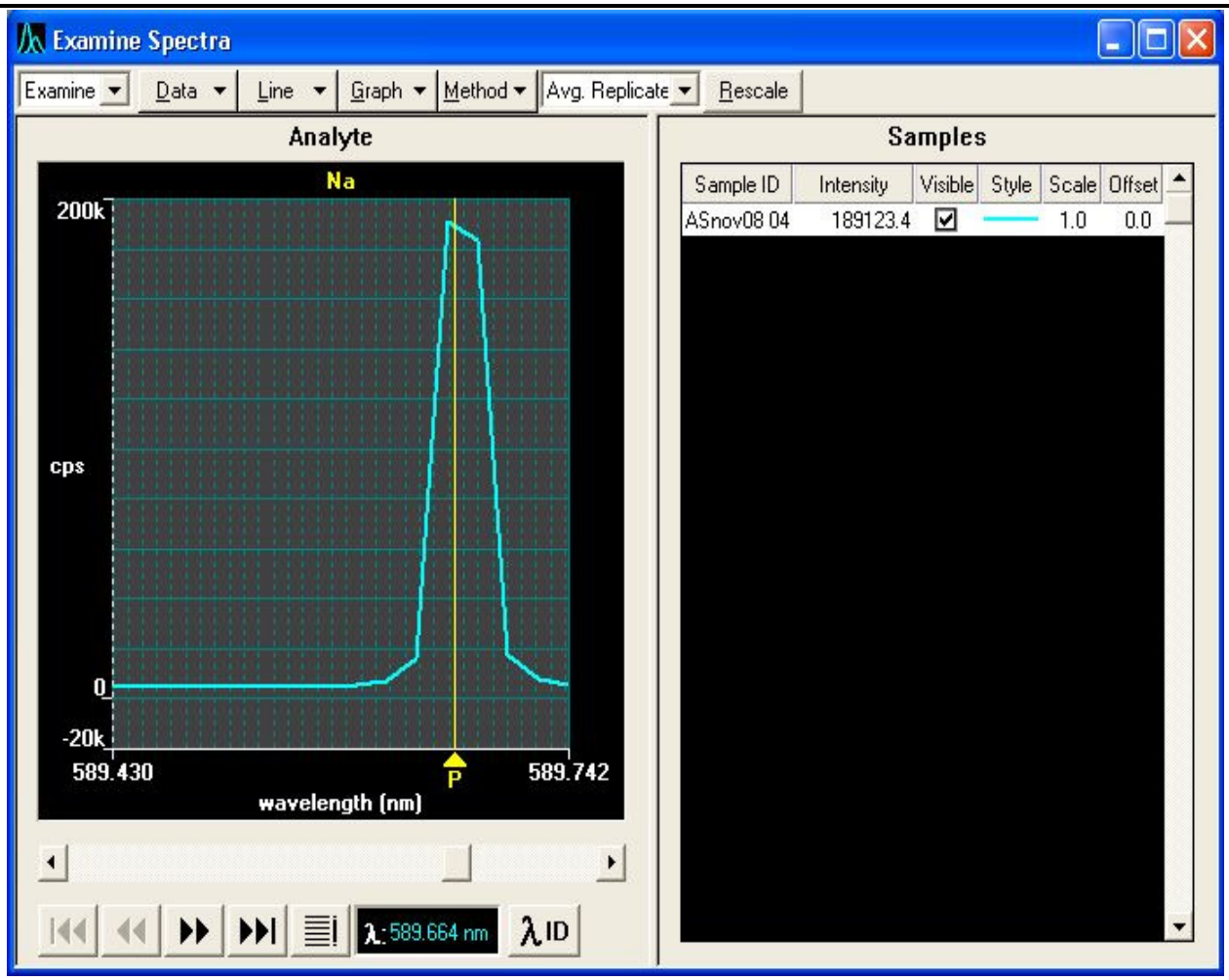

Figure 4.7: Typical ICP Cation Chromatogram

4.2.2 IC Anion Analysis

The Ion chromatograph used is a Dionex 2500 Ion Chromatograph (Dionex Corporation; Marlton, NJ). The components comprising the system are an AS50 autosampler, a AS50 Chromatograph, a EG50 eluent generate, a GP50 gradient pump, a 4 mm ASRS-ULTRAII suppressor, a anion trap column (CR-ATC), a 4 x 50 mm guard column (AG-15), a 4 x 250 mm analytic column (AS-15)and a CD25 conductivity detector. The data acquisition system is the Dionex Chromeleon 6.6.

Potassium hydroxide is the eluent with Helium (Merriam Graves; West Springfield, MA) as the carrier gas to prevent carbonate formation. As a 25µL portion of sample was injected, travel proceeded through a sample loop and into the trap column filled with high capacity anion exchange resin. The sample then went onto the guard and analytic column which are both filled with 13 µm diameter stationary packing material that are especially selective with hydroxide eluents. Both columns were specifically designed for inorganic anion and organic acid ion detection. Travel through the system is propagated by the eluent flow of 2.0 mL/min. The sample was then distinguished with the conductivity detector by time of detection. The anions analyzed for were sulfate (SO_4^{2-}), phosphate (PO_4^{3-}), nitrate (NO_3^-), and chloride Cl^-. Figure 4.8 displays a typical sample represented on an anion chromatograph showing peak magnitude time of detection. Figure 4.9 is a magnified view of the peaks inside the rectangle selected in Figure 4.8. Similar to the cation analysis, the peak time is calibrated with previous developed calibration curves to obtain the actual concentration of each element. A calibration curve was generated for each ion for each programmed series of samples analyzed.

Operator:IC Timebase:Anions_Analysis Sequence:11B

Page 1-1
1/12/2009 2:22 PM

183 ASnov08 04

Sample Name:	**ASnov08 04**	*Injection Volume:*	**25.0**
Vial Number:	**34**	*Channel:*	**ECD_1**
Sample Type:	**unknown**	*Wavelength:*	**n.a.**
Control Program:	**Anions(SK)**	*Bandwidth:*	**n.a.**
Quantif. Method:	**Anions(SK)**	*Dilution Factor:*	**1.0000**
Recording Time:	**11/18/2008 7:26**	*Sample Weight:*	**1.0000**
Run Time (min):	**30.00**	*Sample Amount:*	**1.0000**

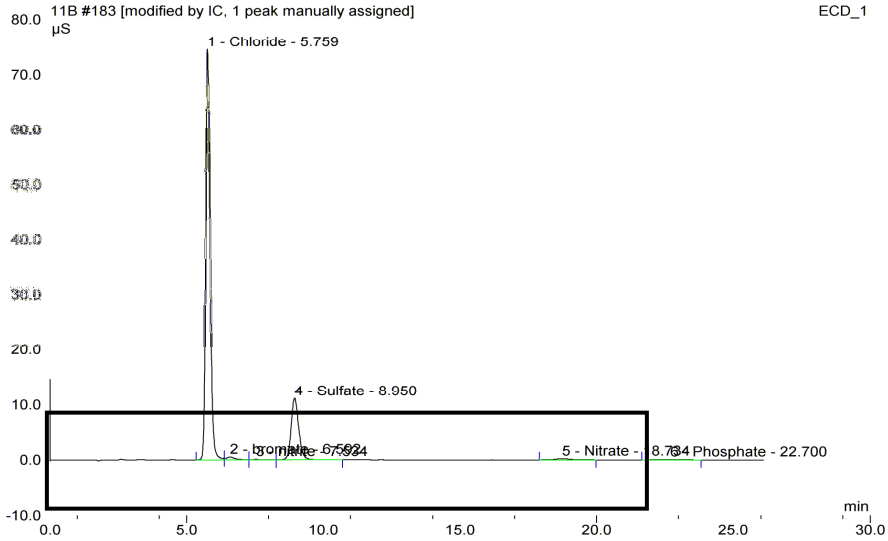

No.	Ret.Time min	Peak Name	Height µS	Area µS*min	Rel.Area %	Amount	Type
1	5.76	Chloride	74.560	14.208	78.12	61.539	BM *
2	6.59	bromate	0.488	0.193	1.06	n.a.	M *^
3	7.53	nitrite	0.088	0.034	0.19	n.a.	M *
4	8.95	Sulfate	11.101	3.592	19.75	21.127	MB*
5	18.73	Nitrate	0.212	0.133	0.73	1.239	BMB
6	22.70	Phosphate	0.027	0.025	0.14	0.458	BMB
Total:			86.477	18.186	100.00	84.363	

Acetate/Integration

Chromeleon (c) Dionex 1996-2001
Version 6.60 Build 1428

Figure 4.8: Typical Anion Chromatogram

Operator:IC Timebase:Anions_Analysis Sequence:11B

Page 1-1
1/12/2009 2:32 PM

183 ASnov08 04

Sample Name:	**ASnov08 04**	*Injection Volume:*	**25.0**
Vial Number:	**34**	*Channel:*	**ECD_1**
Sample Type:	**unknown**	*Wavelength:*	**n.a.**
Control Program:	**Anions(SK)**	*Bandwidth:*	**n.a.**
Quantif. Method:	**Anions(SK)**	*Dilution Factor:*	**1.0000**
Recording Time:	**11/18/2008 7:26**	*Sample Weight:*	**1.0000**
Run Time (min):	**30.00**	*Sample Amount:*	**1.0000**

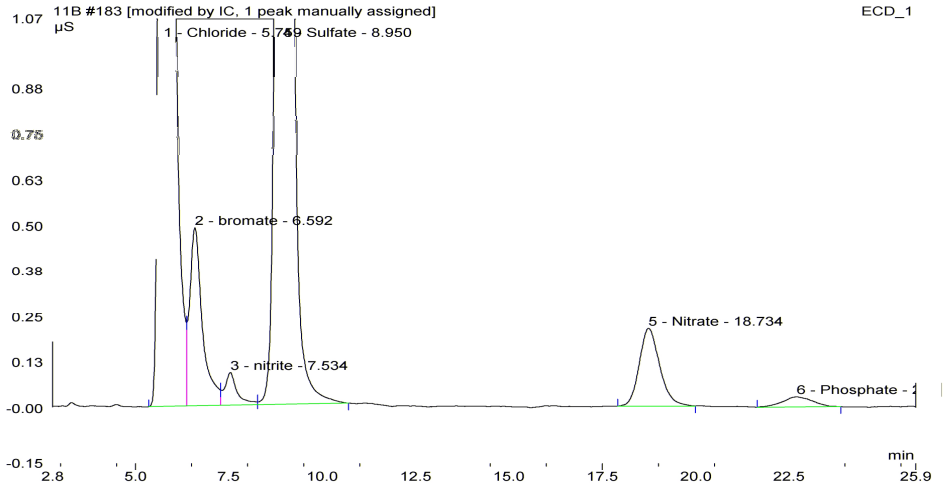

No.	Ret.Time min	Peak Name	Height µS	Area µS*min	Rel.Area %	Amount	Type
1	5.76	Chloride	74.560	14.208	78.12	61.539	BM *
2	6.59	bromate	0.488	0.193	1.06	n.a.	M *^
3	7.53	nitrite	0.088	0.034	0.19	n.a.	M *
4	8.95	Sulfate	11.101	3.592	19.75	21.127	MB*
5	18.73	Nitrate	0.212	0.133	0.73	1.239	BMB
6	22.70	Phosphate	0.027	0.026	0.14	0.470	BMB*
Total:			86.477	18.187	100.00	84.375	

Acetate/Integration

Chromeleon (c) Dionex 1996-2001
Version 6.60 Build 1428

Figure 4.9: Magnification of Smaller Peaks of Anion Chromatogram

4.2.3 TOC Analysis

A Shimadzu TOC-5050A (Shimadzu Corporation; Kyoto Japan) total organic carbon (TOC) analyzer was used to analyze bicarbonate concentrations. The feed was with a ASI-5000A autosampler and the reagent is phosphoric acid (25%, Shimadzu Corporation; Kyoto Japan) which coverts the inorganic carbon components of the sample to carbon dioxide (CO_2) gas. Less than 2 ml of sample was automatically injected into the phosphoric acid reagent. The zero-grade carrier gas was bubbled through the reagent to force the generated CO_2 into a non-dispersive infrared gas analyzer (NDIR). The NDIR outputs an analog detection signal which generates a peak whose area was determined by the data processor. The peak area as seen in Figure 4.10 was correlated to an inorganic carbon calibration curve based on standards by the data processor. The same standard preparation and calibration curve is produced as described previously. Samples were injected for at least three but no more than six times until the standard deviation between the injections is less than 200 unit areas. This ensured the maximum accuracy of the analysis. Standards were run throughout the process to evaluate accuracy.

The inorganic carbon concentration was converted to total bicarbonate concentration by multiplication with the molecular weight of bicarbonate to carbon. The speciation of the total bicarbonate concentration was adjusted according to the pH of the field sample representative of an open carbonate system.

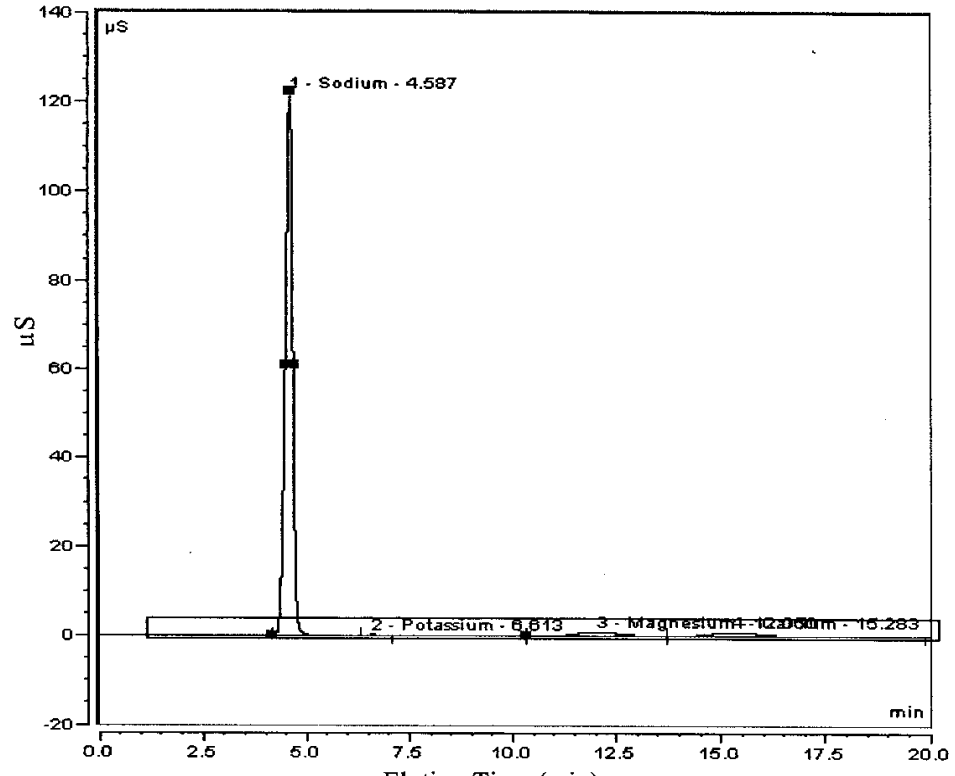

No.	Peakname	Ret.Time min	Area µS*min	Amount mg/L	Type	Height µS	Rel.Area %	Resolution
1	Sodium	4.587	25.0315	122.7487	BM *	122.004	91.24	6.53
2	Potassium	6.613	0.0596	0.4361	Rd*	0.253	0.22	n.a.
3	Magnesium	12.050	1.0736	2.7789	M *	0.870	3.91	1.52
4	Calcium	15.283	1.2699	5.0725	MB*	0.879	4.63	n.a.

Figure 4.10: Typical Carbon Analysis Diagram

4.2.4 Charge Balance

Analytic results are reported in concentration units, mass per volume of mg/L. Each individual analysis for the ICP cations, IC anions, and TOC carbonate concentrations have quality assurance measures within there respective procedures as described above. Overall analysis accuracy is assured by comparing total charge of the identified cations to total charge of identified anions. This was done with cation and anion concentrations determined in the analysis with a cumulative charge balance calculated with Equation 4.1.

$$\sum_{CATIONS}\left(\frac{mg/L}{molar\cdot mass}\bullet ch\arg e\right)=\kappa_{CATIONS} \qquad 4.1a$$

$$\sum_{ANIONS}\left(\frac{mg/L}{molar\cdot mass}\bullet ch\arg e\right)=\kappa_{ANIONS} \qquad 4.1b$$

$$\delta_{CHARGE}=\frac{2\left(\kappa_{CATIONS}+\kappa_{ANIONS}\right)}{\kappa_{CATIIONS}-\kappa_{ANIONS}} \qquad 4.1c$$

The charge balance is a useful check on the inclusion of all major ions in the water quality analysis. A good balance suggests that all major cations and anions in the weir samples have been identified. Practice is to have the charge balance be within ±10%. The accuracy record is very good. For example, the 216 samples collected through the first 9 collected events of 2008 in Andover through May have an average departure from exact cation to anion charge balance of 4.4%.

Another evaluation of accuracy based on the ionic charges of the samples is by comparison of the field specific conductivity and the calculated specific conductivity. The calculated conductivity uses the concentration resulting from the analytic process. The theoretical conductivity was calculated according to Standard Method 2510A (1995) procedure. Calculations follow in step as described by the parts of Equation 4.2 which compute the infinite dilution, the ionic strength, the ionic activity coefficient using the Davies Equation (Benjamin, 2002), and finally the theoretical conductivity, K_{calc}.

$$K^{o}=\sum_{CATIONS}\left|z_{I}\right|\lambda^{0}_{+i}c_{i}+\sum_{ANIONS}\left|z_{i}\right|\lambda^{o}_{-i}c_{i} \qquad 4.2a$$

Where K^o is the conductivity at infinite dilution (μohm/cm), c_i is the concentration of the i-th ion, z_i is the charge of the i-th ion, and λ^o_{+i} , λ^o_{-i} are equivalent conductance of the i-th ion.

$$I = \frac{1}{2}\sum z_i^2 c_i \qquad 4.2b$$

$$\log \gamma = -Az^2\left(\frac{\sqrt{I}}{1+\sqrt{I}} - 0.2I\right) \qquad 4.2c$$

Where γ is the Davies activity coefficient, A is 0.51 for water at 25°C, and I is ionic activity in moles.

$$K_{calc} = K^o \cdot \gamma^2 \qquad 4.2d$$

Comparison of calculated to field measured conductivity based on ionic concentrations should by within 15% of each other to properly relate specific conductivity to chloride concentration when modeling the event runoff. This is the link in the theoretical application of the model to the field measurements developed in the next section. Figure 4.11 displays a typical result when comparing the field measurement of specific conductivity of the collected automated samples and the calculated specific conductivity from the analytic results of the laboratory analysis.

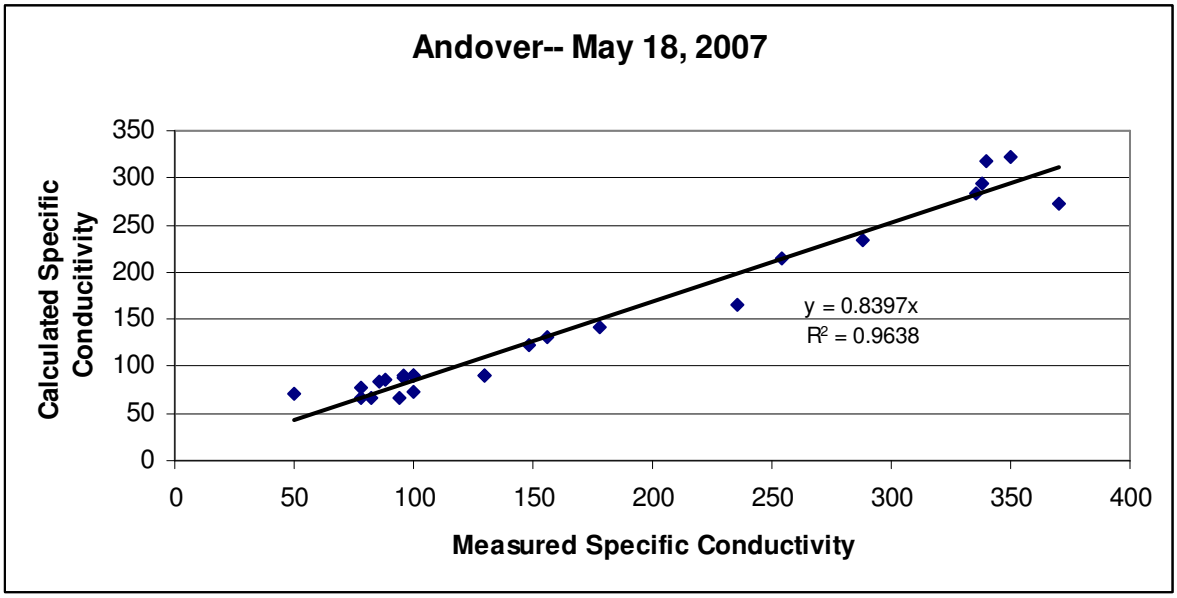

Figure 4.11: Accuracy of Calculated to Measured Specific Conductivity (µS/cm)

CHAPTER 5

5.0 THEORETICAL DEVELOPMENT AND APPLICATION

The development of chloride flux models for the three sites involves starting with the creation of a hyetograph, the development of a hydrograph, and onto the expansion to a pollutograph. This section will detail the chemistry, hydraulics and the development of the flux model with classic linear reservoir theory and two and three lumped parameter models. The hydraulic and chloride flux models explained below have been developed through the work of previous graduate students, researchers and investigators studying the application of the Instantaneous Unit Hydrograph and linear reservoir theory.

5.1 Stochiometry

Electrical conductivity is a measure of water's ability to conduct electricity, and therefore a measure of the water's ionic activity and content. The higher the concentration of ionic (dissolved) constituents contained, the higher the conductivity. Conductivity of the same water changes substantially as its temperature changes. Specific conductivity is the conductivity normalized to a temperature of 25 ºC and is calculated with a typical Arrhenius equation like Equation 5.1.

$$SpecificConductivity = \frac{ActualConductivity}{\left[1 + r(T - 25)\right]} \qquad \textbf{5.1}$$

where r is the temperature coefficient correction from the calibrating fluid, T is temperature in degrees Celsius, and specific and actual conductivity are in micro Siemens per centimeter.

Interactions between solute ions are directly related to the amount of constituent or activity's of the dissolved species. The interaction is largely coulombic and these effects are described by the ionic strength, I of the solution which is defined as in Equation 5.2

$$I = \frac{1}{2}\sum (m_i z_i^2) \qquad \textbf{5.2}$$

Where I is in molar units and z_i is the charge of the ith ion. The sum of all the charged species in the solution is defined as the ionic strength. The most accurate value of ionic strength is obtained from a total water analysis which includes all ionic species. Most common and for the accuracy required of this investigation, partial analysis is appropriate. The molal ionic strength is estimated from the total dissolved substance or specific conductance of the water. Specific conductance and ionic strength are both accurate measurements of the total concentrations of ionic species and vital in the Cl^- ion analysis of highway runoff used in this project.

5.2 Hydraulic Theory

The transport of chloride at all of the sites depends on the pavement runoff which in turn depends on the pavement watershed characteristics. This is all incorporated into hydraulic behavior of each site. Although each site has a different layout, the theory developed here will hold for all of the sites.

5.2.1 Effective Runoff Area

All of the precipitation that falls on the watershed of each site does not contribute to the accumulated runoff measured discharging over the individual weirs. The collection systems designed control the runoff during transport to the sampling points but can not control agents of the hydrological cycle like infiltration, evaporation, and evapo-transpiration, or road spray attributed to passing traffic and accumulation during cold

weather events. As previously described, road spray (Blomqvist and Johansson, 1999) can attribute considerable loss through transport beyond the collection area of the drainage system as well as resulting transport upon vehicles that can also be considered a loss of applied salt not collected in the runoff or residual upon the impervious surface. These losses vary between storms depending on the storm size, precipitation intensity and in which season of the year the storm occurs. Compensating for some of these losses is done by using the "effective rainfall" from a given storm as the contribution in development of the runoff model. Essentially it is the rainfall that reaches the monitoring point. This is the precipitation that is neither retained on the watershed surface, transported through the air nor infiltrated into the soil.

The objective of rainfall-runoff analysis is to develop a runoff hydrograph where the system is a watershed (highway drainage basin or paved salt storage facility), the input is the rainfall hyetograph, and the output is the runoff or a discharge hydrograph and finally as in this research, a flux of specific conductivity over time. This process is known as the unit hydrograph approach (Mays, 2005). In this way, surface runoff from a watershed due to a particular storm will be used to characterize parameters hydraulically describing the watershed.

Developing the effective runoff area is the first step in examining the relationship between rainfall and runoff. The total volume of flow over the respective weirs divided by the total rainfall of a storm at each particular site will result in the effective area of the watershed contributing to the storm runoff as shown in Equation 5.3.

$$A_{eff} = \frac{Q_R}{p_{Total}} \qquad \textbf{5.3}$$

Where p_{Total} is the observed rainfall depth, A_{eff} is the effective area, and Q_R is the total runoff volume measured at the weir. This conceptual area represents an area that would have 100% of the precipitation collected and contributing to the observed total runoff flow over the weir. Each storm had the effective runoff area analyzed to evaluate the accuracy of the runoff data for this research. Linsley *et al.* (1958) predicted that runoff percentage will increase with increasing rainfall quantity. This is directly related to the absence of the influence of the depression storage layer that will be discussed later. The total watershed area for the Plymouth site is 23,275 m^2, for Cohasset it is approximately is 11,560 m^2, and for the Andover facility it is approximately 1100 m^2.

5.2.2 Unit Hydrograph

A hyetograph represents precipitation intensity per unit time throughout the duration of the storm. This is the input into developing a hydrograph. A direct runoff hydrograph is a unit hydrograph resulting from 1 unit of excess rainfall generated uniformly over the watershed area at a constant rate for an effective duration (Chow *et al.*, 1988). The central hypothesis of the unit hydrograph is that it is a simple linear model that can be used to derive a hydrograph from runoff quantification. This means the time intervals are the same between the hyetograph and hydrograph.

Additional assumptions include:

- The precipitation has a constant intensity within the effective duration
- The precipitation is distributed uniformly throughout the entire drainage area
- The time base of the hydrograph remains constant for all inputs of the duration
- For a given watershed, the hydrograph resulting from the storm runoff reflects the unchanging characteristics of the watershed (Mays, 2005).

The unit hydrograph is a hypothetical unit response of a watershed to a unit of precipitation. The resulting runoff can be predicted and a storm hydrograph can be developed for any given storm in the same watershed by utilizing a convolution integral between the precipitation and the unit output hydrograph.

5.2.3 Synthetic Hydrograph

There have been many types of hydrographs developed to characterize watershed runoff**.** The primary purpose of synthetic hydrograph (S-hydrograph) is to estimate watershed runoff behavior based on characteristics of the watershed when input and response for the said watershed is lacking (Dingman, 2002). The prominent approaches at developing S-hydrographs are by Snyder (1938), the Soil Conservation Service (1972), and Gray (1961).

The assumption of linear reservoirs in the development of the unit hydrograph lends itself to the applicability of using the superposition of individual events of finite length to develop a S-hydrograph. This is not a synthetic hydrograph which it is used in order to change a unit hydrograph from one duration to another. An S-hydrograph results theoretically from a continuous rainfall excess at a constant rate for an indefinite period. This type of hydrograph is a direct runoff hydrograph that results from a watershed receiving continuous effective rainfall at a constant rate, for an infinite duration (Jeng *et al*., 2003). The construction of the S-hydrographs involves the summation of a series of unit hydrographs of a duration D and time of separation of the same duration D. The result is a smooth S shaped curve with the peak approaching the rate of rainfall excess at the time of equilibrium.

5.2.4 Instantaneous Unit Hydrograph

Reducing the duration interval between the S-hydrographs to an infinitesimally small increment results in an impulse response or instantaneous unit hydrograph (IUH) (Peeling, 1999). The traditional concepts proposed by Nash (1959) connect watershed response to a cascade of identical linear reservoirs. Classic linear reservoir theory is then applied to each of the identical reservoirs with the instantaneous unit depth of effective rainfall being input into only the farthest from runoff (nth) reservoir in a series. The IUH is the direct runoff hydrograph that would result from a unit volume from an instantaneous effective rainfall hyetograph applied uniformly over the watershed. The outflow of each reservoir serves as the inflow into the next reservoir in the series as the flow moves toward the outlet of the watershed. A linear reservoir is an idealized reservoir in which outflow q_R and storage S have a linear relationship or Equation 5.4,

$$S = A \times h = \frac{1}{\Omega} q_R \qquad \textbf{5.4}$$

where A is the effective area of the watershed, h is depth of effective rainfall, and Ω is the storage coefficient. In the Nash model the outflow of the first reservoir of the series, at the outlet of the watershed, was considered to be the IUH for the watershed and was shown to be a gamma probability density function (Nash, 1959). The two parameter gamma function is a typical fit for a instantaneous unit hydrograph and will be explained further in the hydraulic and flux model development.

5.2.5 Depression Storage Layer

The depression storage layer is a hydrologic control volume (Bedient and Huber, 2002) incorporated in the top of the pavement texture of bituminous aggregate surfaces. For this research the depression storage depth ζ, was optimized for each site as the amount

of precipitation p, required to fill the layer before runoff began. This is defined below in Equation 5.5 with precipitation from the N^{th} storm at time t_{PN} and continuous time t and intensity p. The first precipitation contributing to the runoff when $q_R > 0$ value, or runoff begins, is observed after ζ is filled.

$$n\zeta = \int_{t_{PN}}^{t_N} p dt \qquad (q < 0) \qquad \textbf{5.5}$$

The boundary condition explains the minor delay this layer is responsible for and has been previously characterized in classical hydrology (Black, 1991). Gelhar and Wilson (1974) derive a lumped parameter model for groundwater transport which demonstrated that an instantaneous unit hydrograph routes chloride as well as water though a linear reservoir system. Ng *et al*.(1999) derived a model of nonaqueous phase liquid source decay subject to evaporation and Crittenden *et al.* (1986) derived a model of nonaqueous phase liquid source decay subject to dissolution. Ostendorf *et al.* (2001) developed a model characterizing residual chloride persistence in the depression storage layer from the N^{th} application of deicing agent u_n throughout the year. Figure 5.1 visualizes the lumped parameter model with depression storage layer and the surface storage layer. The subscripts I and N represent conditions at time I and at the start of the N^{th} storm. The chloride dissolution kinetics are determined in this depression storage layer and are discussed further in the chloride flux model derivation section.

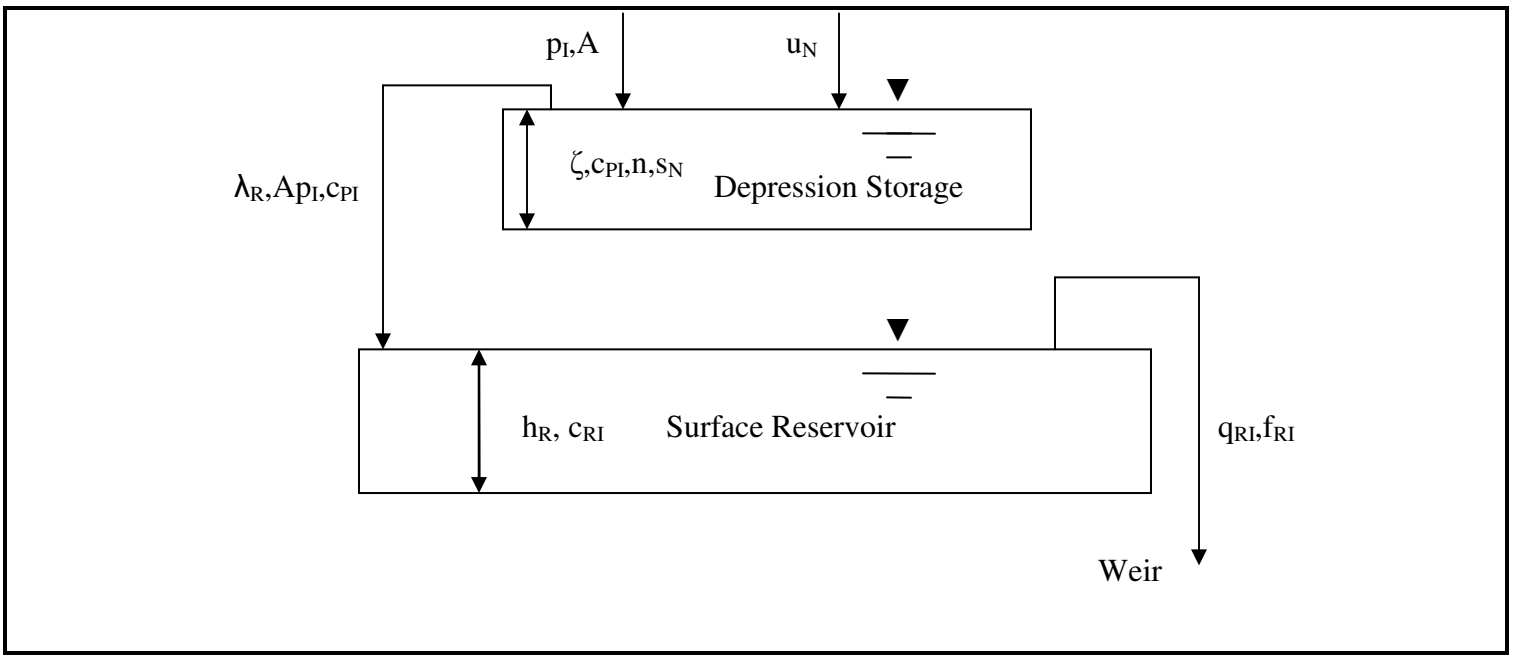

Figure 5.1: **Lumped Parameter Model of Site Drainage System**

5.3 Hydraulic Model

Following the Nash (1959) model, q_R is the discharge from a series of linear reservoirs which is the last reservoir in a series of linear reservoirs representing the watershed. The assumption is that the pavement routes successive precipitation into and out of the depression storage layer and onto the next surface reservoir as the event continues. Our analysis will have these two control volumes composing the system, the depression storage layer and the impervious surface reservoir. Since the surface reservoir will only discharge after the depression storage layer is full, a mass balance will be done here between the two reservoirs. The following set of equations 5.6a-c represents the relationship of the two parameters to be optimized in characterizing the runoff for the three watersheds under consideration in this study. Equation 5.6a is the change of mass in the surface reservoir and Equation 5.6b represents the storage of the system Ah_R, directly

related to the fraction of runoff. The boundary conditions state that runoff doesn't begin until the onset of the N^{th} or simply when the depression storage layer is filled and that τ is the convolution time or the time that it takes for the N^{th} storm unit of precipitation to contribute to the surface runoff at time t.

$$A\frac{dh_R}{dt} + q_R = \lambda_R A p \qquad (t > t_N) \qquad \textbf{5.6a}$$

$$Ah_R\Omega_R = q_R \qquad \textbf{5.6b}$$

$$q_R = 0 \qquad (t = t_N) \qquad \textbf{5.6c}$$

The runoff decay constant $\Omega_{R,}$ relates the depth of water in the reservoir h_R, to the discharge, $q_{R.}$ Solving this set of equations by LaPlace transformation (Rainville and Bedient, 1969) reveals a convolution integral Equation 5.7 (Abramowitz and Stegun, 1972):

$$q_R(t) = \lambda_R A\int_{t_N}^{t} i_R(t-\tau)p(\tau)d\tau \qquad \textbf{5.7a}$$

$$i_R(t) = \Omega_R \exp(-\Omega_R t) \qquad \textbf{5.7b}$$

Where $i_R(t)$ is the instantaneous unit hydrograph, λ_R is the number of linear reservoirs, τ is the convolution time and t is the elapsed time. Combining these equation results in Equation 5.8 (Ostendorf *et al*., 2001) which is the hydraulic model used to analyze all storms for the research sites in this study.

$$q_R(t) = \lambda_R A\Omega_R\int_0^t e^{-\Omega_R(t-\tau)}p(\tau)d\tau \qquad \textbf{5.8}$$

Calibration with a Fibonacci search and Visual Basic programming to optimize the two gamma parameters in this model will be explained in later sections. This model provides an understanding of site behavior and optimization of the depression storage depth and the

runoff decay constant for each individual site. The optimum reservoir quantity was assumed to be one as the area is actually the effective area and the hydrological cycle losses like infiltration, evaporation, and evapo-transpiration were compensated for in this reduction. This shows that the watershed response to each storm increment entering the cascade of linear reservoirs is dictated by the Nash (1957) IUH and the individual runoff response increments can be summed according to the convolution integral (Dooge,1959). That is, the runoff volume is equal to the effective area times the decay constant times the summation of the exponentially declining contribution that the N^{th} precipitation unit at the N^{th} intensity adds to the runoff at time t from time τ the Nth precipitation unit began contributing to the runoff until the end of the event.

5.4 Mass Flux Model

The dispersion transport component is neglected in the corresponding advective model of chloride transport through the depression storage and surface reservoirs. A mass balance will be performed on the depression storage layer and the surface reservoir in the lumped parameter approach illustrated in Figure 5.1. According to the linear reservoir unit hydrograph approach, the chloride inflow to the surface reservoir is the chloride flux, f_P leaving the depression storage layer. Evaluation of the mass balance of the depression storage layer results in Equation 5.9:

$$nR^2\zeta\frac{dc_P}{dt}+R^2pc_P=4\pi r^2\frac{Dn^{\frac{4}{3}}c_{sat}}{R} \qquad \textbf{5.9}$$

Where n is porosity, R is the dissolution volume width where a granule of chloride would reside and dissolve after application, c_P is the concentration of ions leaving the depression

storage layer, p is the precipitation intensity, r is the granule radius, D is the free liquid diffusivity, and c_{sat} is the saturated granule concentration. This expression has the term representing the change in stored mass plus the mass out of the layer equal to the dissolution which is the amount of deicing agent dissolved per time. This expression has been proposed and simplified by Ostendorf et al (2001) with the addition of a source strength term ω (s^{-1}) and the accumulated solid chloride load s (kg/m^2) represented in Equations 5.10:

$$\omega = \frac{6Dn^{\frac{4}{3}}c_{sat}}{\rho_{g_i}\zeta R} \qquad \textbf{5.10a}$$

$$s = \left[\frac{4\pi\rho_g}{3}\frac{\zeta}{2}\frac{1}{R^2}\right]r^2 \qquad \textbf{5.10b}$$

$$\frac{dc_P}{dt} + \frac{pc_P}{n\zeta} = \frac{\omega s}{n\zeta} \qquad (t_N < t < t_N + \Delta t_N) \qquad \textbf{5.10c}$$

where ρ_g is the density of the deicing agent (chloride) solid and ζ is the depression storage depth. Equation 5.10c states that the residual chloride is a source for the dissolved ion concentration subject to transport. Equation 5.10a shows that the strength of the source weakens as the diameter of the granule dissolves and Equation 5.10c revealing that source strength is inversely related to the depth of the depression storage layer thickness. The solution to Equation 5.10 in finite difference form is Equation 5.11 and will be used in the governing equation to define the 'first flush' specific conductivity concentration leaving the depression storage layer.

$$c_{P_I} = \frac{\frac{\omega s_N}{n\zeta} + \frac{c_{P_{I-1}}}{\Delta t}}{\frac{p_I}{n\zeta} + \frac{1}{\Delta t}} \qquad \textbf{5.11a}$$

$$c_{PI} = c_{PN} \qquad (t_I = t_N) \qquad \textbf{5.11b}$$

The above boundary condition and the fact that the solid phase dissolves slowly over time results in the assumption that s is constant over a given storm at its starting value s_N. The quantity ωs_N is the parameter optimized through the lumped parameter search .

As can be seen in Figure 5.1, the specific conductivity leaving the surface reservoir and discharging over the weir is a product of c_R and q_R. The specific conductivity inflow from the depression storage layer into the surface reservoir is the product of the effective area, the precipitation intensity, and the specific conductivity in the depression layer, c_P. These relationships can be seen in Equation 5.12.

$$f_R = q_R c_R \qquad \textbf{5.12a}$$

$$f_P = Apc_P \qquad \textbf{5.12b}$$

With the control volume being the surface reservoir, exercising the conservation of mass on specific conductivity results in an equation for the change of specific conductivity flux in the control volume subject to reservoir optimization and to runoff decay constant optimization resulting in Equation 5.13.

$$A\frac{d(c_R h_R)}{dt} + q_R c_R = \lambda_R f_P \qquad \textbf{5.13a}$$

$$\frac{1}{\Omega_R}\frac{df_R}{dt} + f_R = \lambda_R f_P \qquad \textbf{5.13b}$$

$$f_R = 0 \qquad (t = t_N) \qquad \textbf{5.13c}$$

The boundary condition as seen in Equation 5.13 says that the specific conductivity flux does not begin until the N^{th} unit of precipitation falling at t_N contributes to the surface runoff. The same Laplace transform principle can be applied to Equation 5.13 resulting in a convolution integral representative of the instantaneous unit hydrograph routing water containing specific conductivity through the surface reservoir, Equation 5.14.

$$f_R(t) = \lambda_R \int_{t_N}^{t} i_R(t-\tau) f_P(\tau) d\tau \qquad \textbf{5.14a}$$

$$f_R(t) = \lambda_R A \int_{t_N}^{t} i_R(t-\tau) p(\tau) c_P(\tau) d\tau \qquad \textbf{5.14b}$$

This is the flux model was used at all three research sites to characterize the transport of chloride from application and the dissolution in the depression storage layer, through the surface reservoir and over the weir. The resulting governing equation of the dissolution kinetics throughout the storm event is Equation 5.15.

$$f_R(t) = \lambda_R A \int_{t_N}^{t} \Omega_R \exp\left[-\Omega_R(t-\tau)\right] p(\tau) c_p(\tau) d\tau \qquad \textbf{5.15}$$

The parameters optimized from the measured conductivity flux data to arrive at the modeled flux are specific conductivity source, ωs_N ($\mu S\text{-}m^2/cm\text{-}s$) and the 'first flush' of specific conductivity, c_{pi} ($\mu S/cm\text{-}m^3$). The arrival at an estimated chloride concentration from the modeled specific conductivity prediction will be calibrated using automated sampler results with similar measured specific conductivity and chloride concentrations.

5.5 Specific Conductivity to Chloride Conversion

The linear relationship between chloride concentration and the specific conductivity measurements can be simplified to a constant that varies seasonally throughout the year. The relationship can be seen to clearly remain linear whether the

storm is in November for the Plymouth site as seen in Figure 5.2 or February as seen for the Andover site in Figure 5.3.

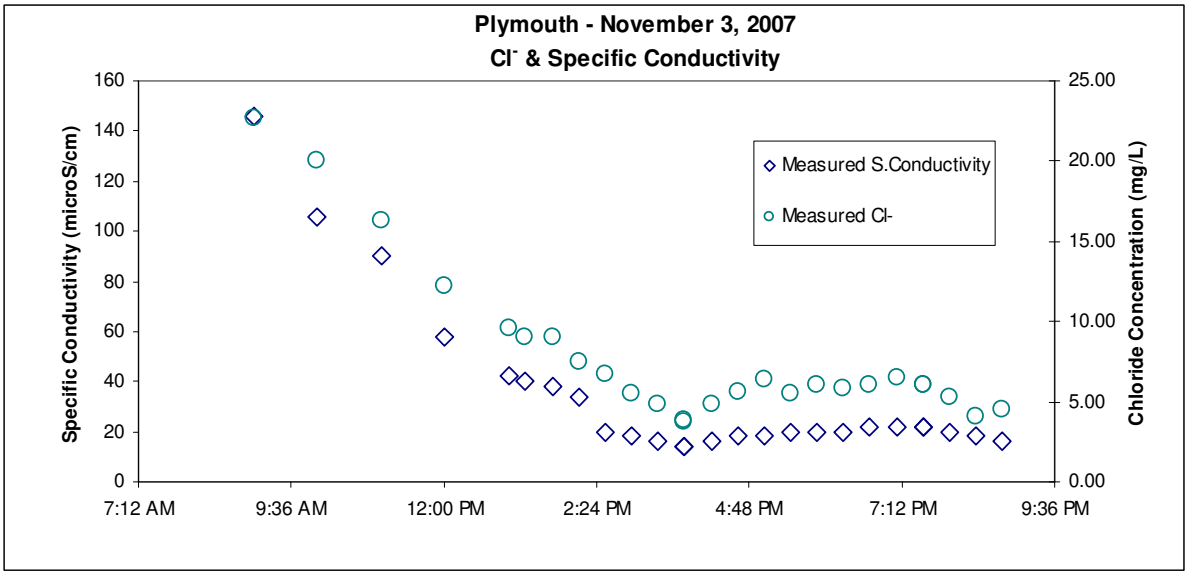

Figure 5.2: Pre-Salting Season Relationship between Conductivity and Chloride

This direct linear relationship is the association utilized to model chloride flux in the impervious surface runoff. As seen in Figures 5.3 & 5.4, chloride multiplied by a constant will reveal approximate values for the specific conductivity. Note the different scales for conductivity and chloride in the figures and the span of only. The initial runoff holds the greatest degree of inaccuracy but as the runoff progresses, the variance between the two water quality parameters is relatively constant. This constant is utilized in converting the specific conductivity flux model optimization of the specific conductivity source term ωs_N in the governing equation into chloride flux.

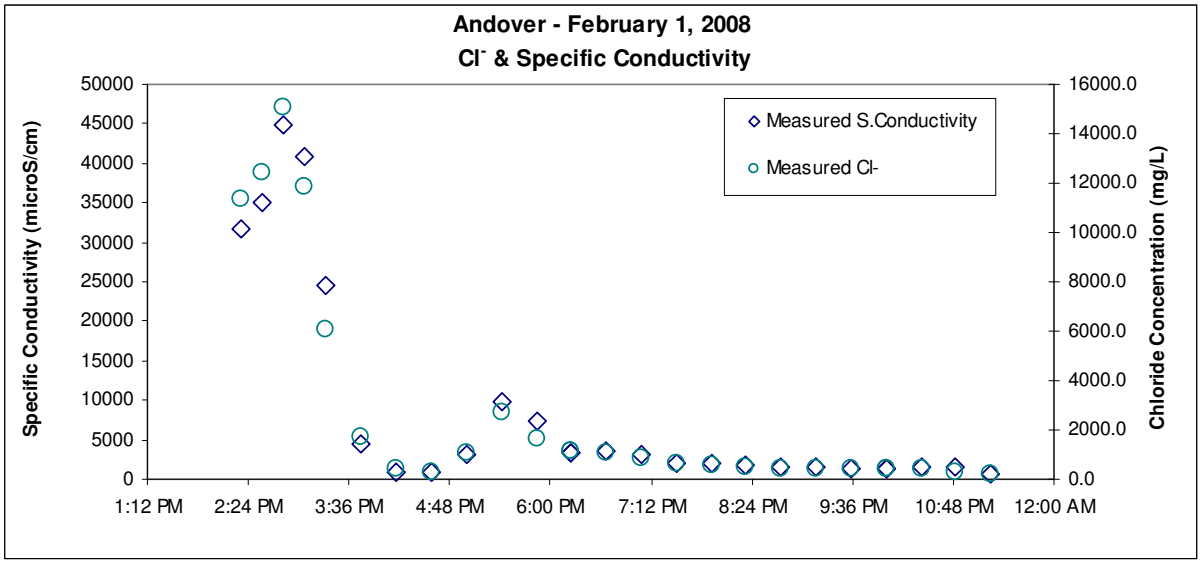

Figure 5.3: Mid-Salting Season Relationship between Conductivity and Chloride

A linear regression analysis as in Figure 5.4 is typical for the sites. This reinforces the linear relationship between the water quality parameters and justifies the surrogate use of specific conductivity for chloride in the flux analysis. Regardless of the season of scale of the concentration, the R^2 of the solid linear regression line indicates the continued relationship between the parameters throughout the year with fairly consistent accuracy in the regression. The small July R^2 factor can be attributed to the unwavering specific conductivity readings with minimal changes in chloride concentration. The slight changes seem more errant given the small scale of change compared to the scale of the parameters. The annual regression relationship is very good and provides support for the direct relationship used in converting the measured specific conductivity to chloride concentration.

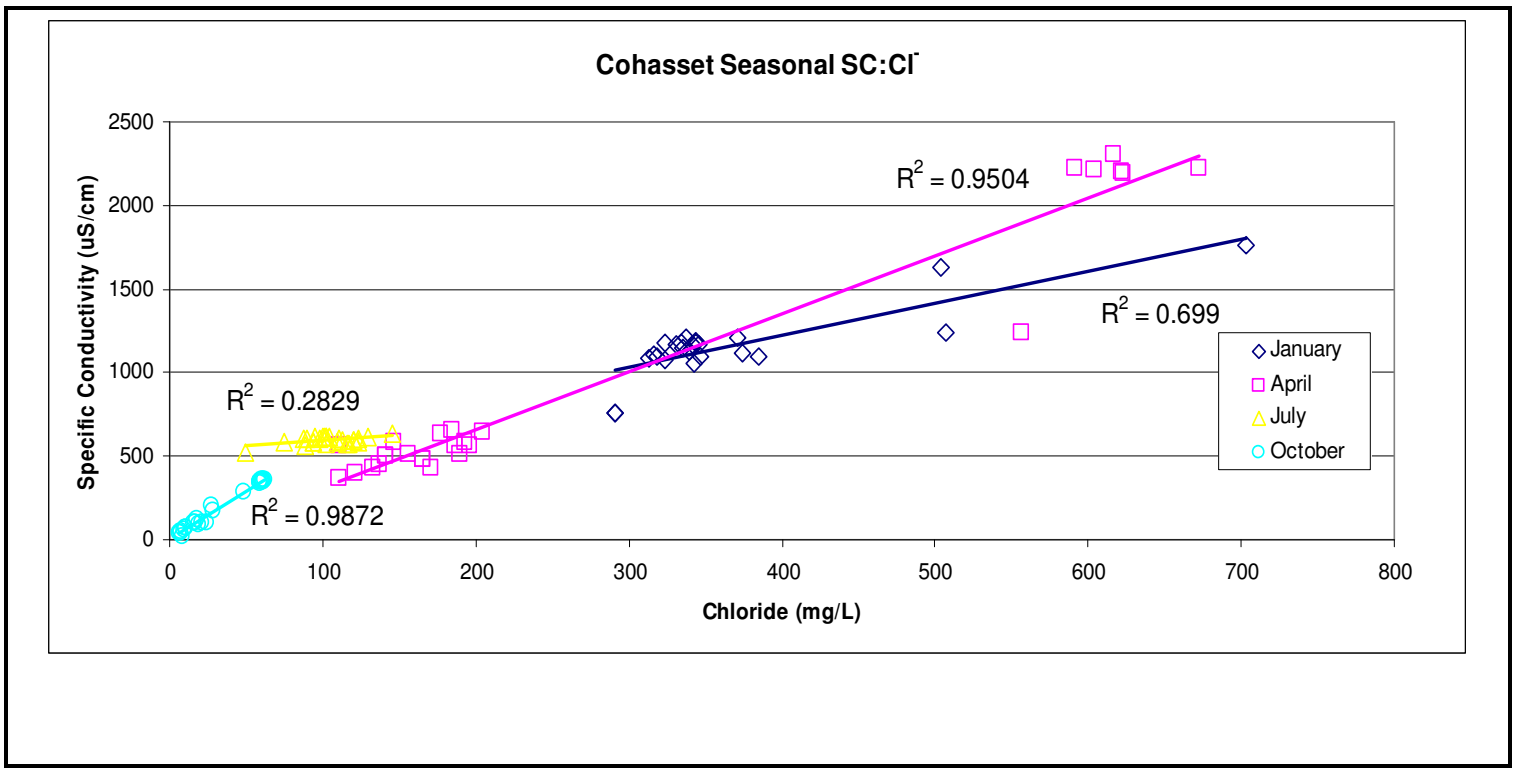

Figure 5.4: Typical Linear Relationship between Specific Conductivity and Chloride

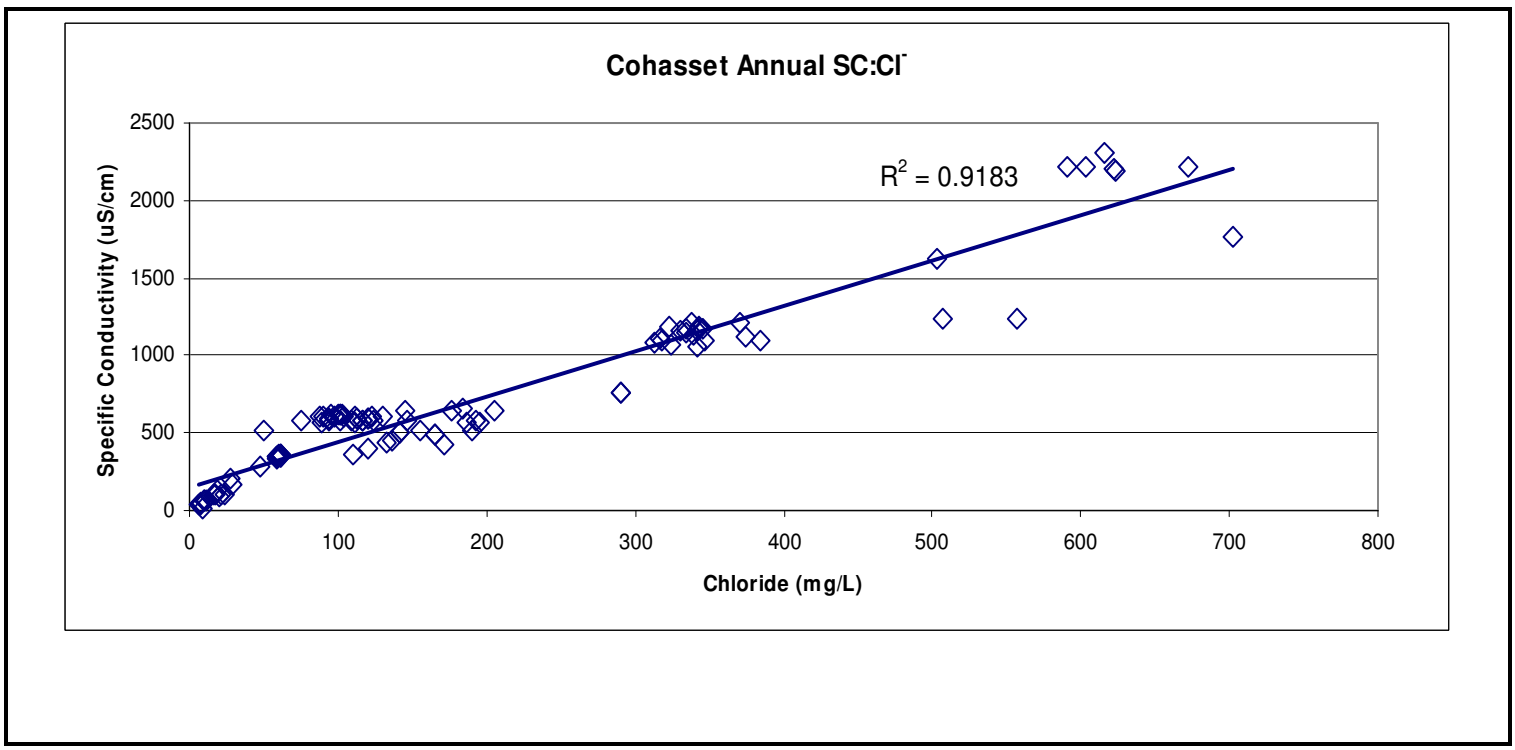

Figure 5.5: Annual Linear Relationship between Specific Conductivity and Chloride

CHAPTER 6

6.0 RESULTS

6.1 Precipitation and Effective Area

The first step in the analysis to identify parameters of each watershed site was establishing reliable precipitation data representative of the entire research area. A similar process was used for all three sites so established results will demonstrate reliability of method. The individual characteristics of each area will be incorporated in to the calibration of the three primary parameters as compared to each other but typical of impervious bituminous surfaces.

6.1.1 Hyetograph

A hyetograph has been constructed as a graphical representation of the distribution of rainfall over the total duration of each storm event analyzed for each research site. Care was taken to select storms with significant peaks in precipitation intensity, with sufficient runoff quantity providing accurate measurements, and with adequate time between other events to prevent interference. These precautions in storm selection minimized error in parameter analysis for depression storage depth, ζ, the optimal runoff coefficient Ω_R, and the optimal number of linear reservoirs, λ. The data accumulated each month from the continuous monitoring equipment is reduced and analyzed to three informative plots as seen in Figure 6.1. During times of the year with colder weather, analysis with these three summarizing graphs avoided choosing storms when significant accumulation or excessive snow and ice melt would have construed data.

The continuous monitoring of specific conductivity represented in Figure 6.1c verifies that at the onset of the flow at the beginning of a storm the ‘first flush’ of residual

ions spikes as indicated with the higher specific conductivity reading. Figure 6.1a is the representation of the precipitation resulting in the flow over the weir in Figure 6.1b. As the ion source dissolves, the chloride granule in this study, and is diluted in the runoff, the specific conductivity also decreases throughout the event. This initial chloride 'source' is a parameter calibrated in the flux model. The reason for the sustained measurement of

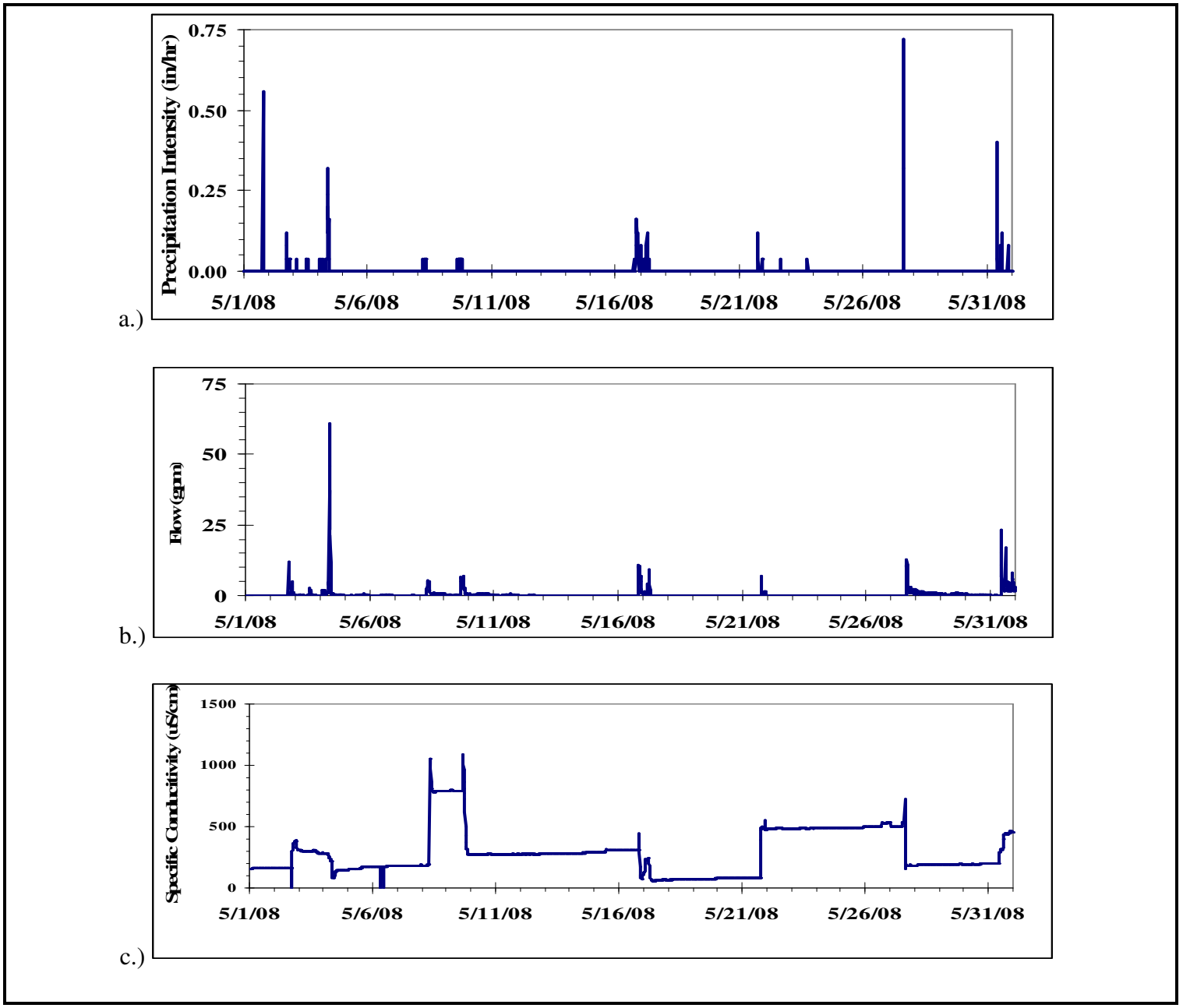

Figure 6.1: Typical Data Representation from Continuous Monitoring Equipment

Specific conductivity as seen between events is because the probe may be in standing water of the weir. Data for each event does not begin to be recorded until a sufficient level of runoff is flowing over the weir to prevent the influence of this standing water on accuracy of the measurements. The automated samplers are set to begin the sampling procedure when flow over the weir increases at 1/10 on an inch per hour or more.

A hyetograph constructed from the data represented above can be seen in Figure 6.2. Ideally the precipitation intensity is constant for each period represented by the fifteen minute increment the monitoring equipment is programmed to record for at Andover and Cohasset and the five minute increment in Plymouth. This is also a requirement of a unit hydrograph which is constructed from the hyetograph with the addition of flow data. Another assumption and requirement of then unit hydrograph approach is that the precipitation is uniform throughout the watershed. Conforming to these requirements is accomplished due to the small area of consolidation.

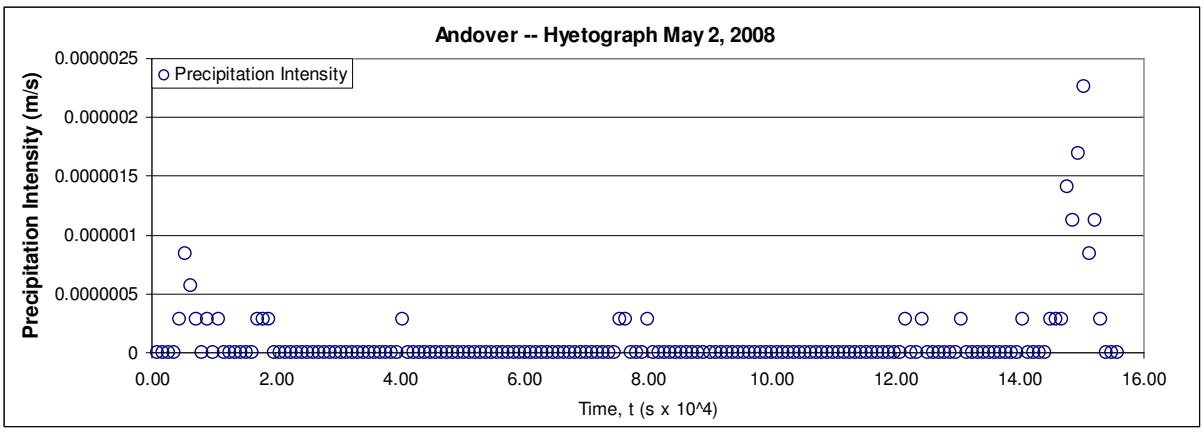

Figure 6.2: Hyetograph of Typical Andover Storm Event

6.1.2 Effective Runoff Area

Initial hydrograph modeling were designed for these three sites using a lumped parameter gamma distribution to calibrate the primary characteristics of each site, ζ, Ω_R, and the optimal number of linear reservoirs, λ_R. It was found that the optimal number of reservoirs varied not only seasonally but from storm to storm within the same month, sometimes even within days. This was more prominent in the winter with snow and ice accumulation and the melting process. During very warm periods evaporation contributed to a large fluctuation in the optimized number of linear reservoir. To limit the influence that variable natural conditions may have in the watershed parameter optimization, the effective runoff area was incorporated into the modeling. This will attain one of the goals of the research in developing a model describing watershed runoff while also being applicable to various types of pavement structures and uses. As described in Chapter 5.2.1, the effective runoff area is the total flow over the weir divided by the total precipitation. Due to the use of heated rain gauges and weirs, this procedure provided more reliable results. The fluctuating values for λ_R for Andover can be found in Table 6.1 and summarized average values for all three sites are in Table 6.2. The individual results for Plymouth and Cohasset are in Appendix A. The fluctuations as seen in the March and August events can be expected but the discrepancies in May and October storms may be attributed to the precipitation intensity and previous atmospheric and local conditions.

As predicted by Linsley et al (1958), smaller storms will have lower effective area as a percentage of total area of watershed than larger events. This is evident when used for this research in Figure 6.3 for the Cohasset facility, slightly apparent for the Plymouth basin, but the Andover facility does not seem to hold the suggested relationship.

Table 6.1: Optimzed λ_R for Andover

Date	λ_R	Date	λ_R	Date	λ_R	Date	λ_R
1/14/2006	0.627	2/3/2006	0.698	3/13/2006	0.784	4/5/2006	0.714
1/23/2006	0.799	2/2/2007	0.603	3/24/2007	0.931	4/22/2006	0.735
1/1/2007	0.784	2/1/2008	0.789	3/7/2008	0.485	4/15/2007	0.694
1/11/2008	0.660	2/6/2008	0.760			4/28/2008	0.786
5/12/2006	0.784	6/1/2006	0.598	7/22/2006	0.768	8/14/2005	0.606
5/18/2007	0.593	6/3/2007	0.632	7/4/2007	0.899	8/4/2006	0.444
5/2/2008	0.874	6/22/2008	0.547	7/23/2008	0.691	8/6/2007	0.490
						8/10/2008	0.614
9/29/2005	0.784	10/7/2005	0.501	11/15/2005	0.805	12/25/2005	0.735
9/8/2007	0.832	10/14/2006	0.469	11/15/2007	0.794	12/22/2006	0.555
9/6/2008	0.869	10/19/2007	0.663			12/2/2007	0.727
						12/27/2007	0.636

Table 6.2: Average Runoff Fraction

Site Runoff Fraction, λ_R	December to April	May to November	Annual Average
Plymouth	0.852	0.847	0.846
Cohasset	0.714	0.729	0.718
Andover	0.711	0.679	0.694

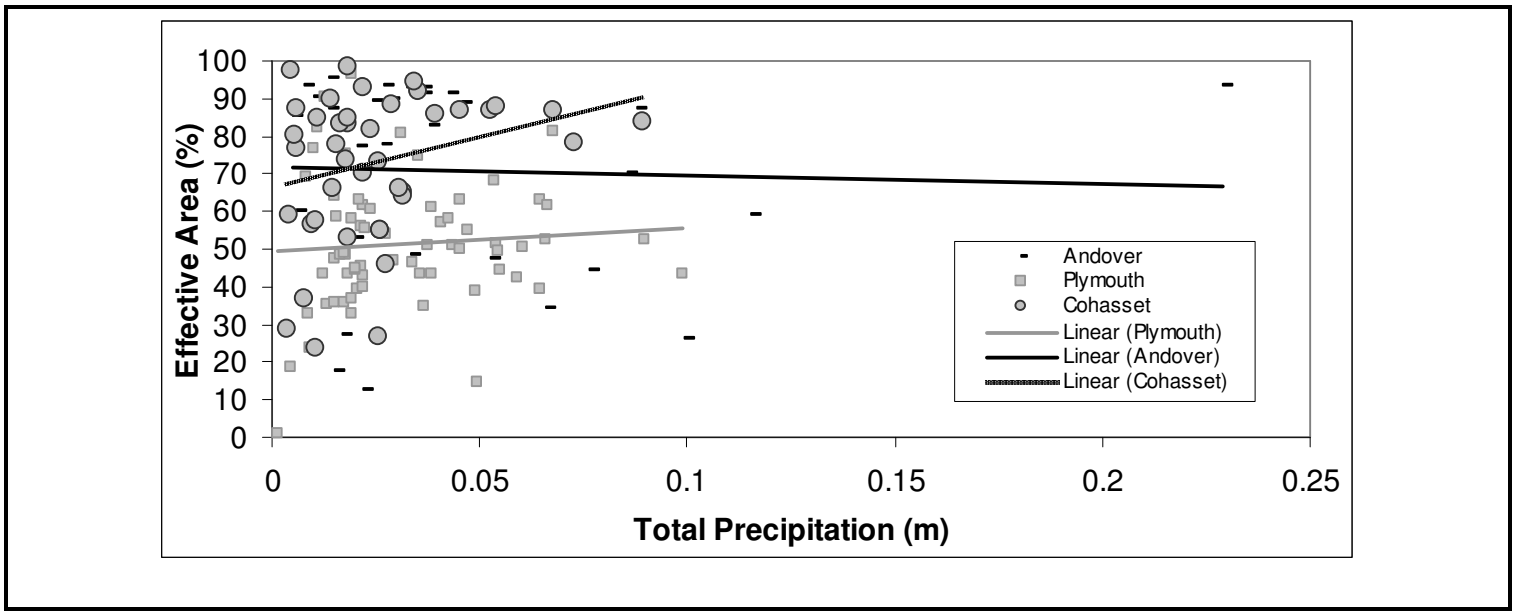

Figure 6.3: Effective Area Relationship with Total Precipitation

The trend lines in the figure represent the interpolated slope of the data points. The ordinate is the effective area to total actual watershed area percentage. The depression storage layer contribution is not individualized in the "effective rainfall" contribution and therefore can be slightly influential in the effective area calculation. The influence was thought to have been constant for each site but when the temperature drops, which is of course seasonally, there may be a decrease in the depth of the layer due to frozen precipitation. Taking this into account, and the fact that the optimized depression storage depth for Andover is approximately 2/3 the depth as optimized for Cohasset and Plymouth, the higher percentage of effective runoff area to quantity of precipitation relationship exemplified in Figure 6.3 is reasonable.

6.2 Hydrograph Model

The hydrographs developed for the three sites utilized one ideal linear reservoir for the reasons stated above and focused on optimizing the two parameters, depression storage depth ζ and surface runoff decay constant Ω_R. This assumption reduced the run time of the Visual Basic program performing the two parameter rather than three parameter optimization utilizing a Fibonacci Golden Section search.

6.2.1 Fibonacci Golden Section Search

The golden section is an area of a number set where the location of points within it is controlled by a Fibonacci progression. Mathematically the position of a point between the two extremes of the section could be predicted. Within this golden section, the added point will fall somewhere between the fractional part of τ_G, the golden ratio as defined by Equation 6.1

$$\tau_G = \frac{1+\sqrt{5}}{2} = 1.61803339887... \qquad \textbf{6.1}$$

The golden ratio is mathematically seen in a multitude of natural settings (Conway and Guy, 1996). The fractional part of each section, starting from the initial boundaries set by the programming for each parameter, will be the section between 38.2% and 61.8% of the interval. So essentially, as the program runs, two parameters will be optimized by reducing the section a solution resides in for each of two parameters in the governing equation. The net result of each iteration eliminates the top and bottom 38% while minimizing the value of the calculated average error in reference to the known solution. The error is calculated by Equation 6.2.

$$\delta = \sqrt{\frac{\sum (Q_{measured} - Q_{predicted})^2}{n_{effective}}} \qquad \textbf{6.2}$$

Where $n_{effective}$ is the number of time increments recorded, δ is the error during optimization, and $Q_{predicted}$ is the flow defined in the governing equation as compared to the flow, $Q_{measured}$ from field data. The result will have lower error than previous iterations. The efficiency of this method is important in handling the large data sets incurred in this investigation. A reduced computing time was imposed with the assumption of $\lambda_R = 1$ and the optimization of only two parameters.

The logic of this search performed with Visual Basic Program uses an inner and outer loop algorithm. The hydrograph parameter optimization code can be found in Appendix B. Appendix C lists the input and output spreadsheets of a typical storm event. The repetitions of the search or length of loop was kept to ten iterations for the depression storage layer, zeta and ten for the runoff decay coefficient, Ω_R. Further calibration was not gained with extension of the repetitions. All three sites used the same code except for

different time increments used depending on each site. The initial range set for the runoff decay constant search interval was 0 to 0.001 m and for the depression storage layer, the range was 0 to 0.01m.

6.2.2 Depression Storage Layer

The importance of the texture of the impervious surface in characterizing individual watershed hydrological parameters cannot be neglected. Figures 6.4 and Figure 6.5 display the difference of optimizing a depression storage layer and without optimization. The precipitation hyetograph is represented in Figure 6.5a and the sensitivity of the hydrograph without ζ optimization can be seen in Figure 6.5b. The delay in the runoff after ζ optimization is displayed in Figure 6.5c. Allowing for the delay in runoff resulting from this volume is not as evident in the Andover site due to the rapid response there. The site is small, contained with curbing, and does not have contributions routed through pipelines as Plymouth and Cohasset do. Compared to Figure 6.4 displaying a

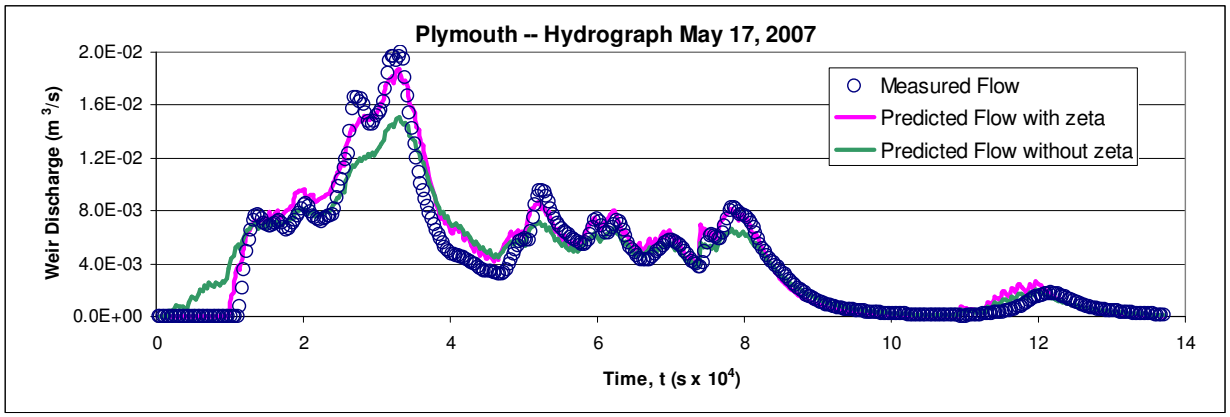

Figure 6.4: Influence of Depression Storage Layer

storm event occurring at the Plymouth site, the importance of including the depression storage layer is much more evident.

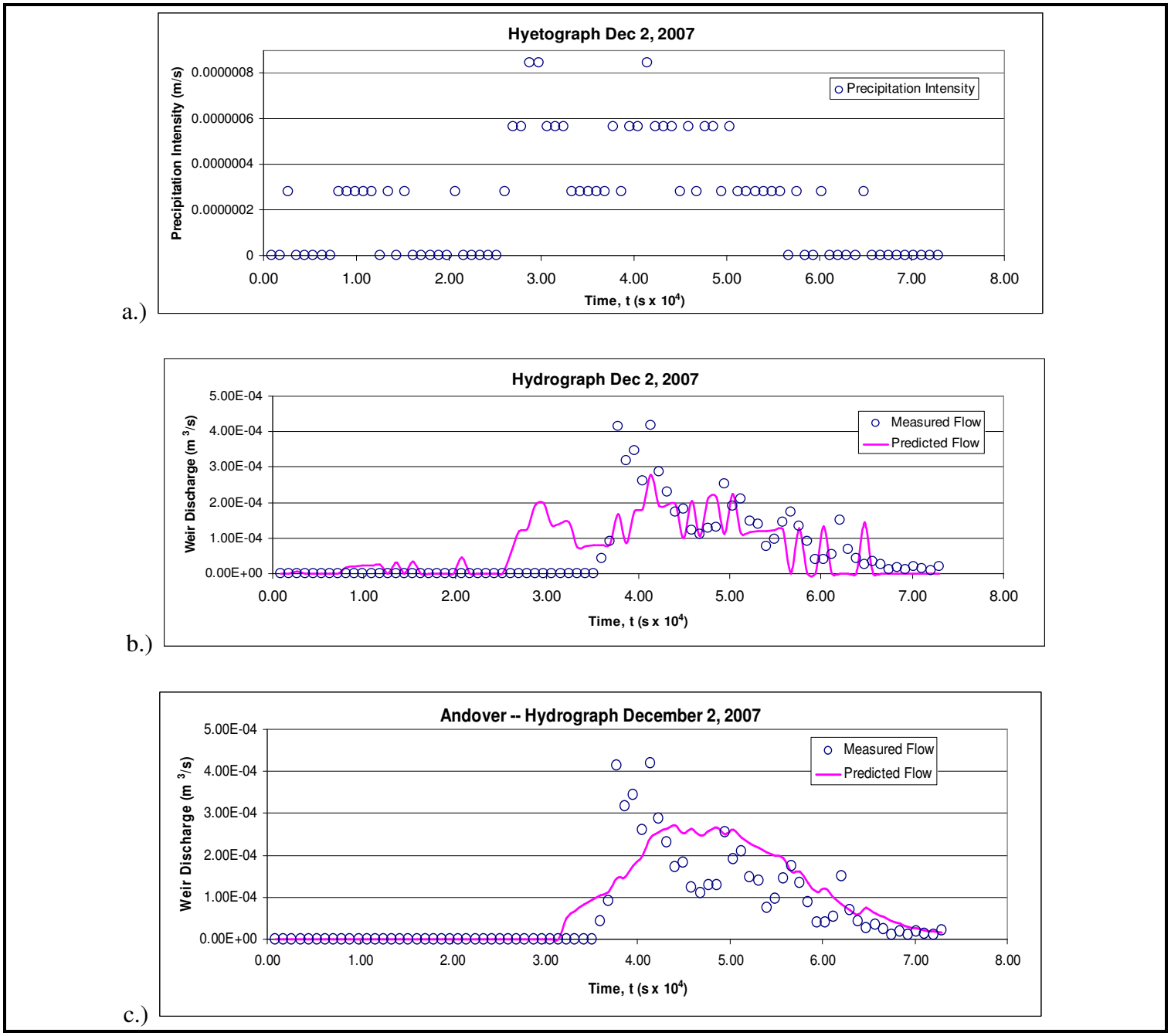

Figure 6.5: Andover Hydrograph with (c) or without (b) the Depression Storage Layer Characterization

6.2.3 Hydraulic Parameter Optimization

The final optimized hydrologic parameters resulting from the Fibonacci elimination method of a lumped parameter search are summarized in Table 6.1 for all

three of the research sites. The complete list of hydraulic and flux parameter optimization results for each individual storm at each site is available in Appendix F.

Table 6.3: Optimized Watershed Parameters

Depression Storage Layer, ζ (mm)			Runoff Decay Constant, Ω_R (s^{-1})			A_{Eff} (% of Total Area)			Error, δ (%)		
Low	Avg	High	Low	Avg	High	Low	Avg	High	Low	Avg	High
Andover Storage Facility											
0.45	0.90	6.29	9.09e-6	3.02e-4	8.93e-4	12	79	205	0.003	0.067	0.212
Cohasset Storage Facility											
0.5	1.3	9.5	1.22e-5	4.21e-4	9.96e-4	24	93	193	0.029	0.383	1.60
Plymouth Infiltration Basin											
0.5	3.0	9.5	4.07e-6	3.60e-4	8.11e-4	0.76	58	308	0.001	0.48	0.752

The accuracy of the parameter search is evident in the proximity of the resulting ranges of parameters and the optimized average values for the depression storage layer and the runoff decay constants between the three sites. Although the 0.90 mm depth of the Andover texture is slightly below the typical range of 1.0 to 4.0 mm cited by Croney and Croney (1998), it is reasonable. The Cohasset texture depth of 1.3 mm is lower than the 3.0 mm established from previous work from Ostendorf *et al.* (2001) investigating the Cohasset site from February 1998 to May 2000. There could be a correlation to pavement texture as the drainage system at the Cohasset site was excavated and repaved after the 2000 salting season. Both Andover and Cohasset have newer bituminous pavement as

compared to Plymouth. The optimized depression storage layer depth listed above of 3.0 mm for Plymouth is similar to the 2.44 mm established in Ostendorf (2006) for the same site with data obtained for three salting seasons from 1999 to 2002.

The runoff decay constants optimized for all three sites reduced to very similar averages of 3.02×10^{-4}, 4.21×10^{-4}, and 3.6×10^{-4} s^{-1} respectively for Andover, Cohasset and Plymouth from ranges of three orders of magnitude for each site between individual events. Coupled with the very low percent errors for the three sites, this is an excellent indication the parameter search is accurate. Stygar (2005) completed similar work at the Plymouth site with data collected from 2001 - 2004 establishing Ω_R of 7.79×10^{-4} s^{-1} with a range of 3.2×10^{-4} to 1.61×10^{-3} s^{-1}, very similar to the result described here of Ω_R of 3.60×10^{-4} s^{-1} with a range of 4.07×10^{-4} to 8.11×10^{-4} s^{-1}.

Typical hydrographs for the three sites resulting from the individual storm parameter searches is displayed in Figure 6.6. An event that occurred on the same day at approximately the same time is displayed in Figure 6.7. The Cohasset is 35 miles south of the Andover site and Plymouth is approximately 33.5 miles south of the Cohasset site. Slightly different precipitation intensities resulted in the differences in the runoff hydrographs for the same event.

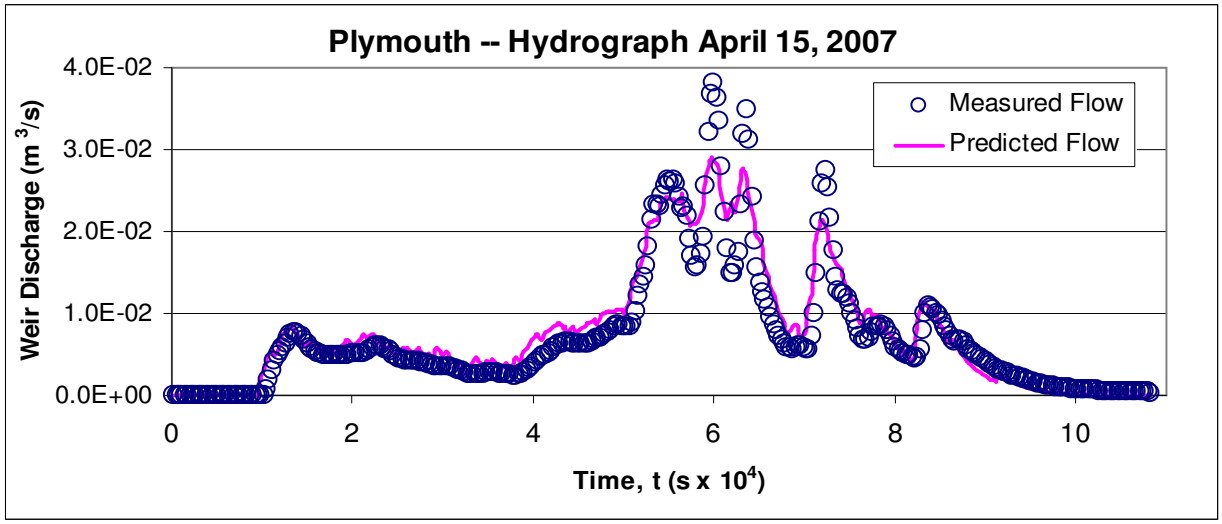

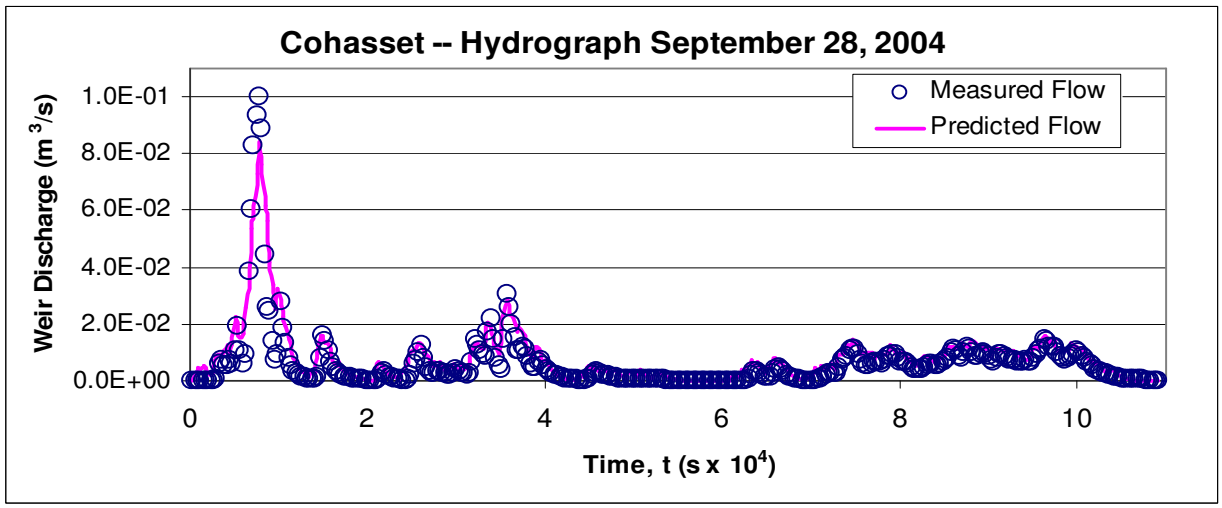

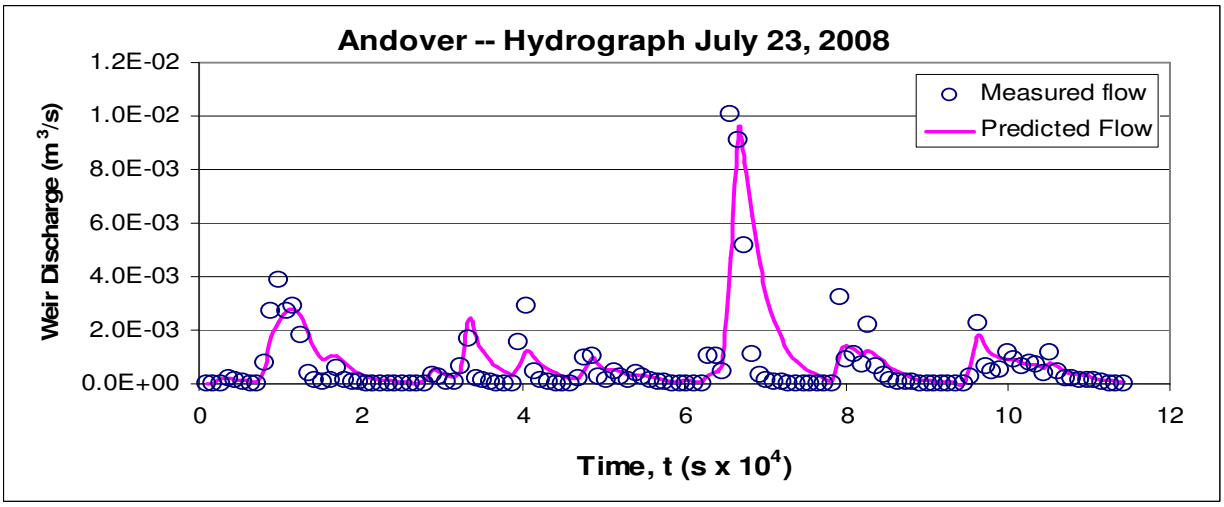

Figure 6.6: Typical Site Hydrographs

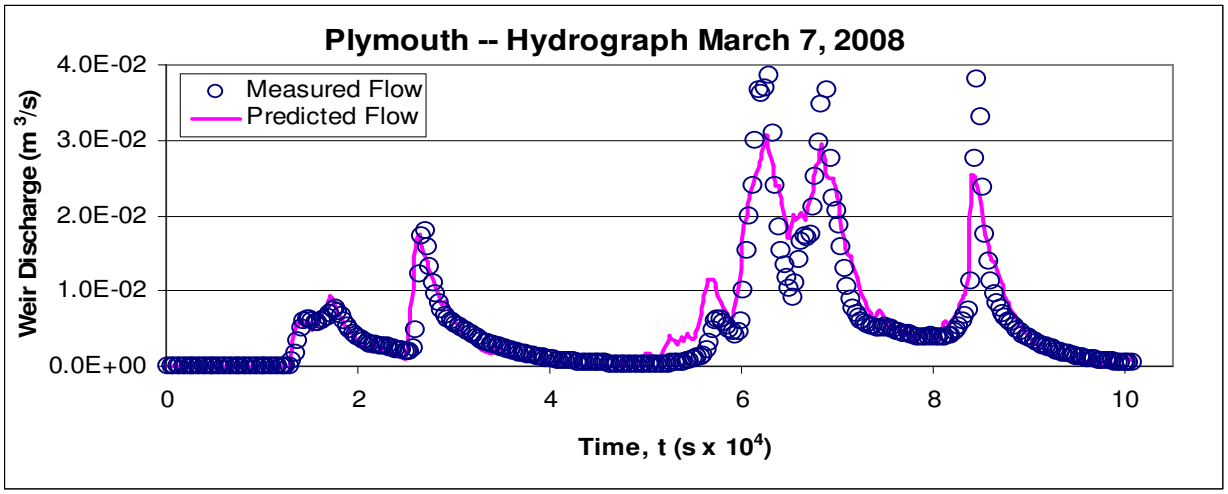

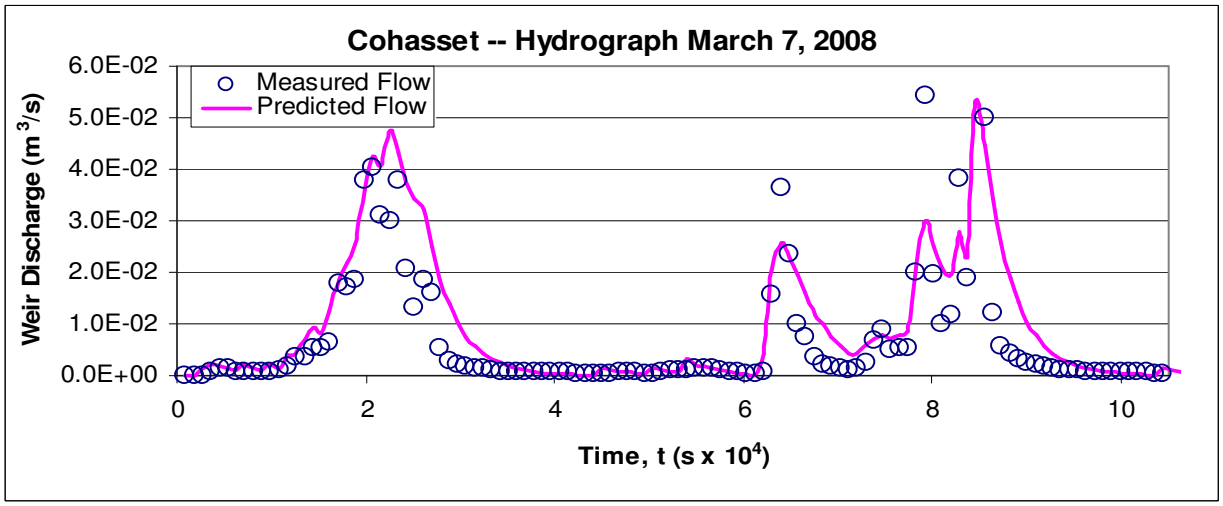

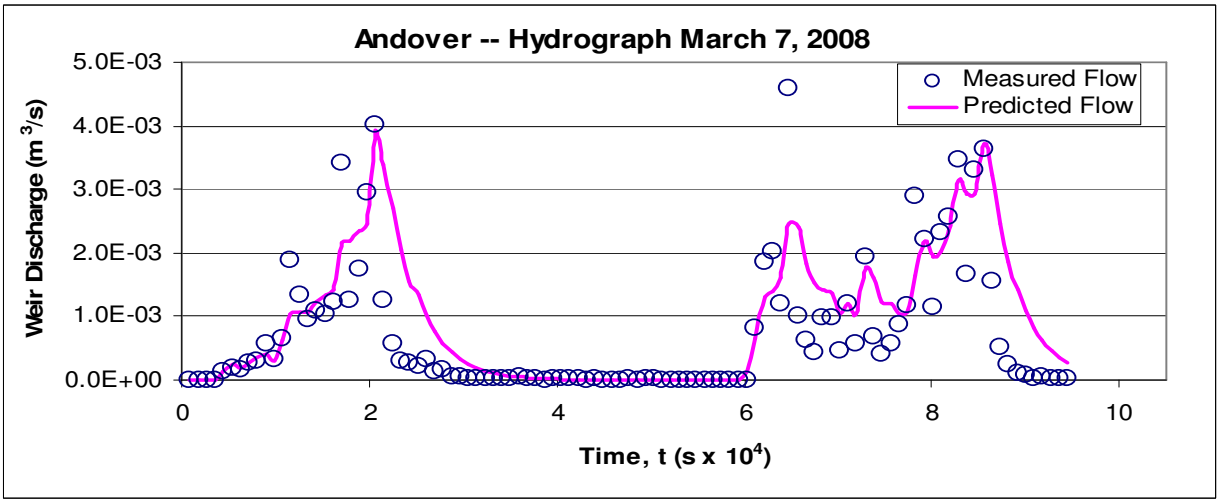

Figure 6.7: Same Event at all Three Sites

6.3 Flux Model Calibration

Model calibration for the specific conductivity flux used the parameters defined and calibrated in the hydraulic response model. The runoff decay coefficient, the depression storage layer, and the runoff fraction (assumed equal to 1.0) were used from the calibrated hydraulic model output as well as the same porosity of 0.4 used for all three research sites. This porosity suggests that the aggregate and bitumen fill most of the depression storage layer. The ranges of the parameter values determined from the flux optimization model for each site are displayed in Table 6.3.

Table 6.4: Optimized Depression Storage Layer Dissolution Parameters

Specific Conductivity Source, ωs_N ($\mu S/cm/m^2$-s)			'First Flush' Specific Conductivity, c_{pi} ($\mu S/cm\text{-}m^3$)			Error, δ ($\mu S/cm\text{-}m^3$)		
Low	Avg	High	Low	Avg	High	Low	Avg	High
Andover Storage Facility								
3.31×10^{-7}	1.67×10^{-3}	1.00×10^{-2}	0.34	102096	1104408	1.43×10^{-4}	4.25	51.4
Cohasset Storage Facility								
3.31×10^{-7}	4.41×10^{-4}	3.31×10^{-3}	16	43942	663210	0.68	4.10	117.0
Plymouth Infiltration Basin								
3.31×10^{-7}	4.66×10^{-4}	1.00×10^{-2}	4	35934	1568637	2.87	4.59	282

The source chloride has an initial amount of residual contained in the texture or depression storage layer of the pavement surface for each precipitation event. The model employed here defines the optimized source term ωs_N, for each storm event.

Concurrently, the model optimizes the 'first flush' concentration, c_{pi} that this source contributes to the storm runoff leaving the depression storage layer. As can be seen in Table 6.3, the source term covers a range of four or five orders of magnitude for each site with the average of the 47 storms for Andover, 71 for Cohasset, and 69 for the Plymouth site reducing to very similar values for the Cohasset and Plymouth sites and a slightly larger value for the Andover site. The factor of ten larger for the SC source at Andover can be attributed to the partial handling of the salt outside of the storage facility structure as opposed to Cohasset where all material is now handled under cover.

Table 6.4 displays the average monthly conversion factors used to characterize the chloride concentrations in the storm runoff from the modeled SC values.

Table 6.5: Conversion Factors of Specific Conductivity to Chloride Concentrations (µS/cm/mg/L)

Month	Andover	Cohasset	Plymouth
January	2.67	3.33	3.65
February	2.57	3.44	3.08
March	3.10	3.07	3.38
April	3.59	3.78	4.14
May	3.72	4.31	4.92
June	4.11	4.92	6.77
July	4.80	5.52	6.71
August	4.79	6.31	6.83
September	5.77	5.52	10.44
October	6.18	4.27	9.31
November	6.02	4.55	6.20
December	2.95	2.93	3.59

Applying these monthly averaged factors to each storm's calibrated parameters and recalculating the site averages results in Table 6.5 displaying the optimized chloride source term, ωs_N and first flush concentration c_{pi}, after conversion.

Table 6.6: Flux Parameters Converted from Specific Conductivity to Chloride

Chloride Source, ωs_N (mg/m^2-s)			'First Flush' Chloride, c_{pi} (mg/m^3)		
Low	Avg	High	Low	Avg	High
Andover Storage Facility					
5.36×10^{-8}	5.64×10^{-4}	3.89×10^{-3}	0.06	33562	319872
Cohasset Storage Facility					
1.08×10^{-7}	1.30×10^{-4}	2.90×10^{-3}	4.0	10374	169014
Plymouth Infiltration Basin					
3.55×10^{-8}	2.16×10^{-4}	3.25×10^{-3}	0.44	11228	509124

The chloride concentrations averaged above are individually listed by storm event in Appendix D. The average source concentration during two April 1998 storm events from Peeling's (1999) pre-remodel of the Cohasset site was 38995 and 89977 mg/m^3 while this study revealed 4330 mg/m^3 average for seven April storm during the 2004 - 2008 study period with a high of 12650 mg/m^3 and a low of 220 mg/m^3. Figure 6.8 displays Peeling's (1999) calibrated source term results from April 1998 to February 1999 as well as the present values in a monthly order. Largest chloride source terms calibrated in this study are from February and March 2007. Clearly the re-pavement, rework of the drainage system, and construction of large sheds allowing indoor handling of material reduced the residual chloride in the depression storage layer and hence salt in storm runoff from the site. This can be seen by the reduction of Peeling's calibrated source terms by

one to three orders of magnitude to the present calibrated values. Figures 6.9, 6.10 and 6.11 show the seasonal trend of chloride dissolution in the depression storage layer for the Cohasset, Andover and Plymouth sites. The peak of chloride concentration in storm runoff is during the winter periods of the study as can be expected and the residual decline throughout the year as salt is no longer applied. Units are converted to kg/m^3 and a solid line is added to highlight trends in chloride storage increases and decreases.

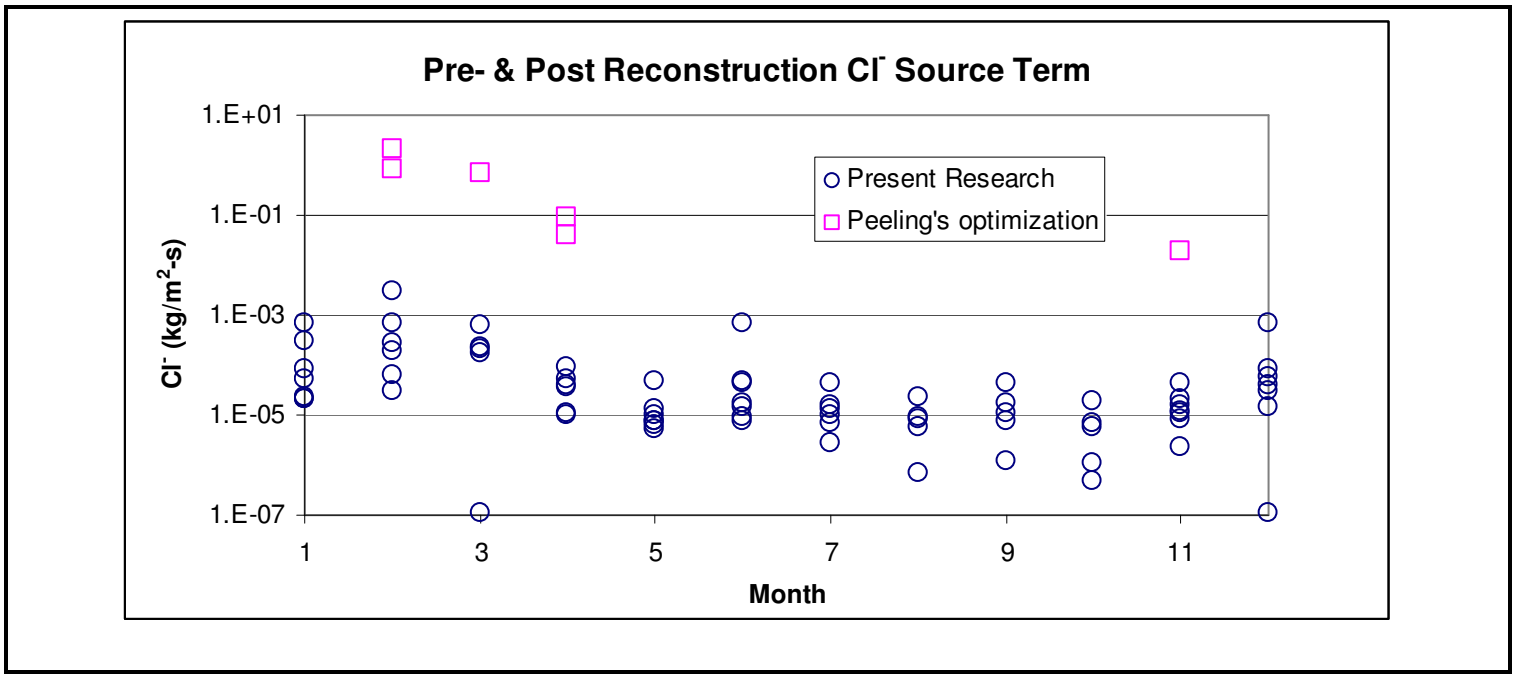

Figure 6.8: Cohasset Calibrated Chloride Source Term pre- and post- Reconstruction

A strong point to make is the evidence of chloride months after the last application of salt. Although all of the Cohasset material expenditures were not available for the entire period of storm evaluation, a clear trend of increased first flush concentration immediately after and during the salting season can be seen. Figure 6.8 shows the optimized source term and first flush concentration parameters for Cohasset for the period the solids distribution data is available for. Gradual weakening in chloride concentration can be seen to exist throughout the warmer months but a reduction to zero does not occur before the

next deicing season begins. Massoudieh *et al*. (2007) examined the different mechanisms governing the detachment of particle-associated and dissolved constituents from the pavement surface besides the hydraulic characteristics examined here. This study of detachment is the dissolution kinetics controlling the residual and runoff water quality leaving and remaining within the impervious surfaces. This handling issue between the two storage facilities is also evident in the average first flush concentrations. The formulation of the governing equation has these two optimized parameters mathematically related. The previous figures relate the relationship between the solids application and the following increased first flush concentration. This can easily be seen in the Andover data representation. The two fairly mild seasons of 2005-2006 and 2006-2007 are followed by the lowest first flush concentrations and chloride source factor. A large distribution in January 2007 renewed the chloride flux source and hence the first flush concentration leaving the depression layer.

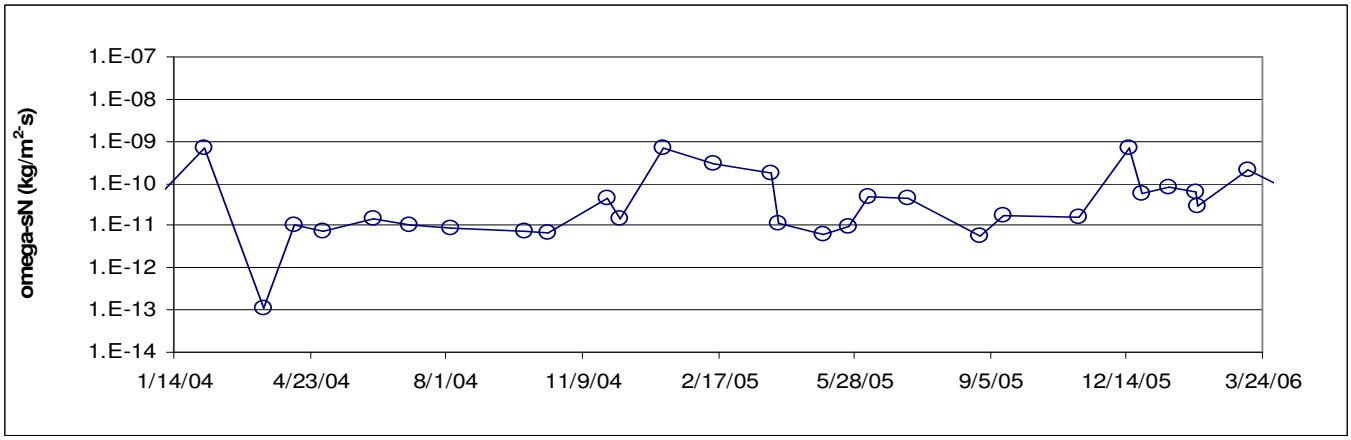

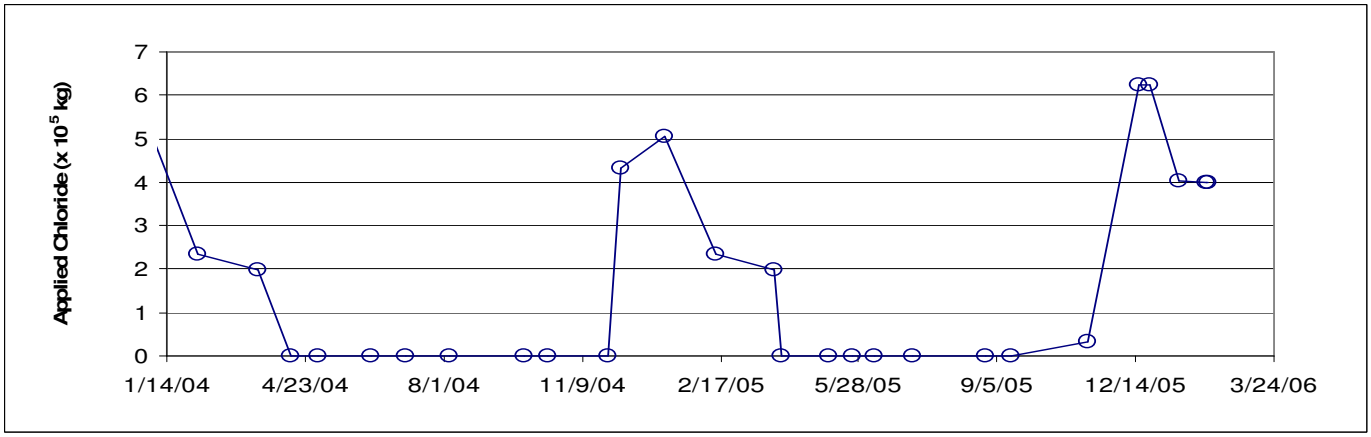

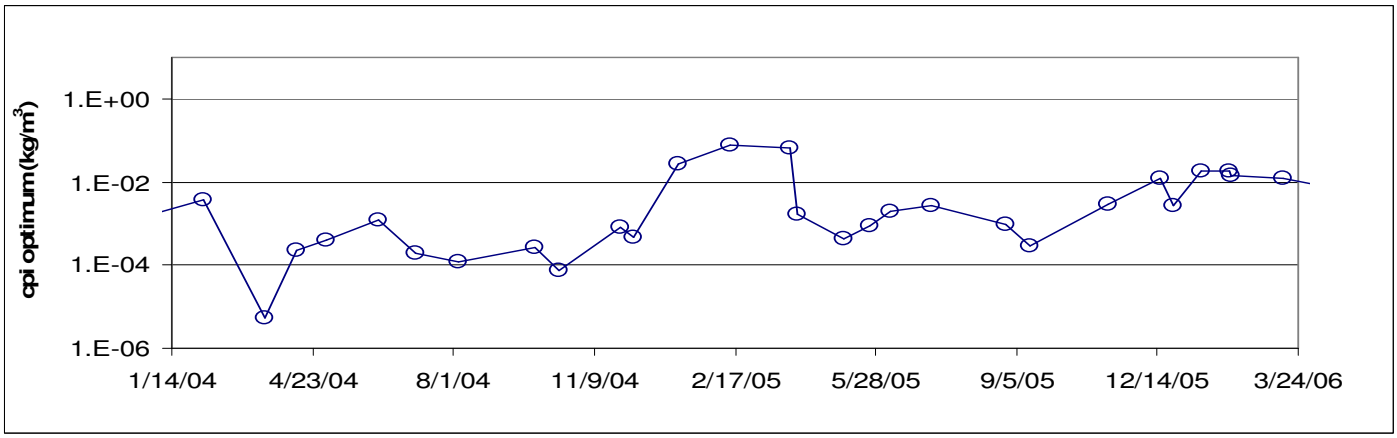

Figure 6.9: Cohasset Cl^- Optimized Source Parameter, Solids Applied, and Optimized First Flush Concentrations

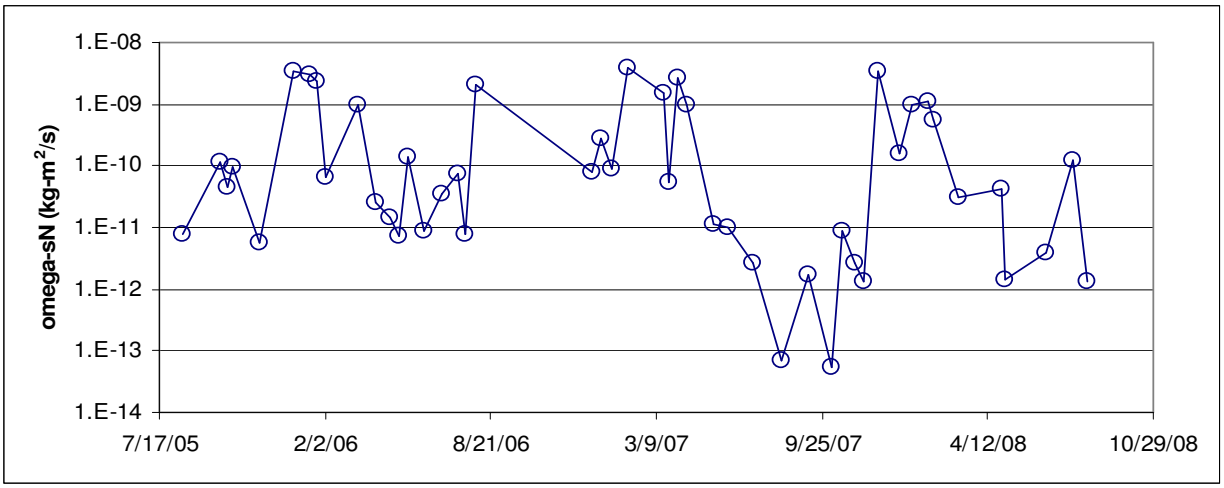

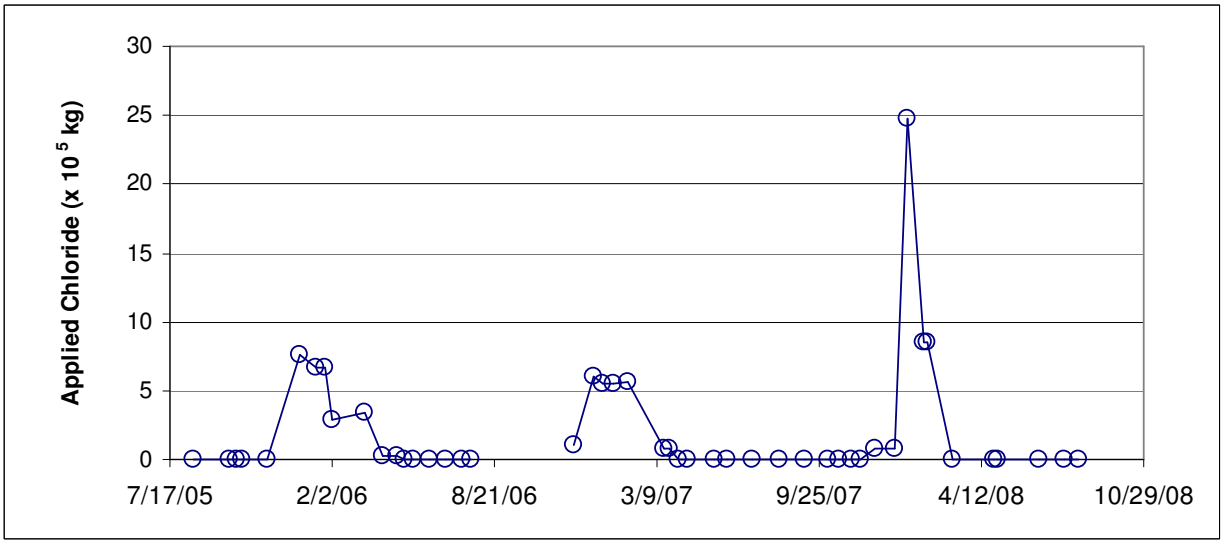

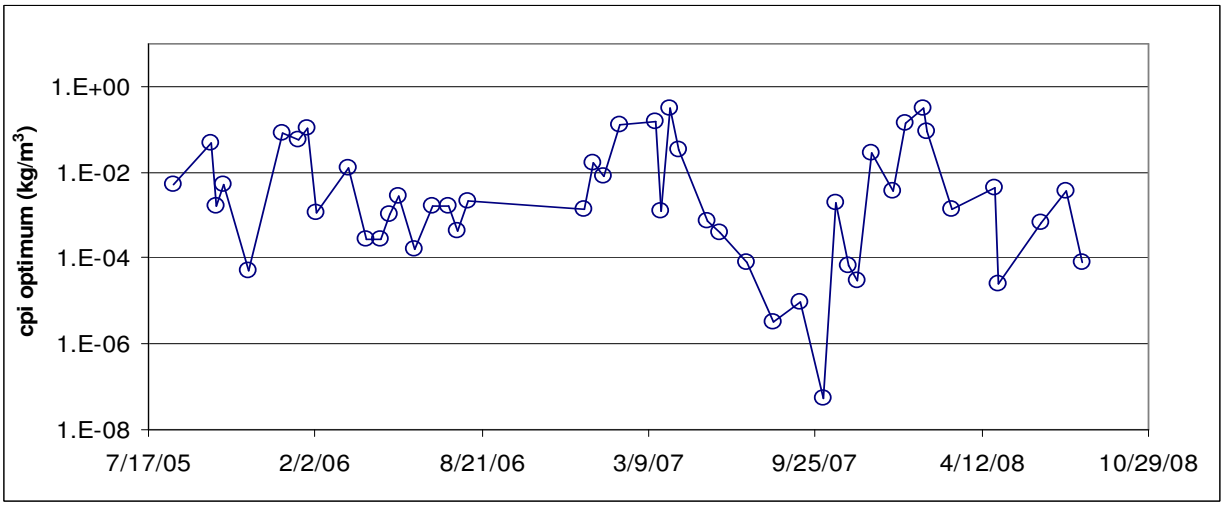

Figure 6.10: Andover Cl^- Optimized Source Parameter, Solids Applied, and Optimized First Flush Concentrations

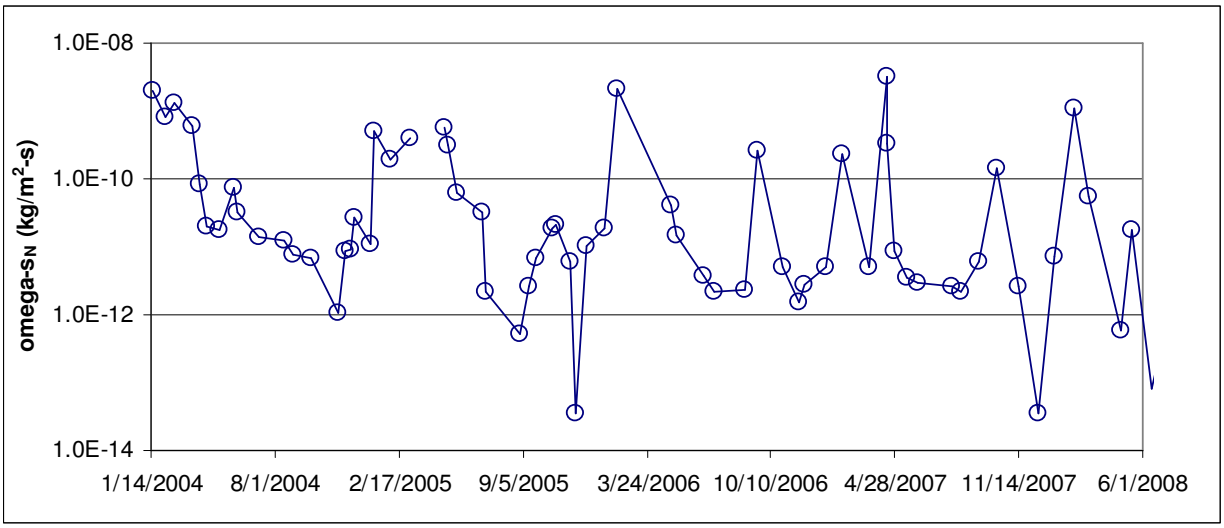

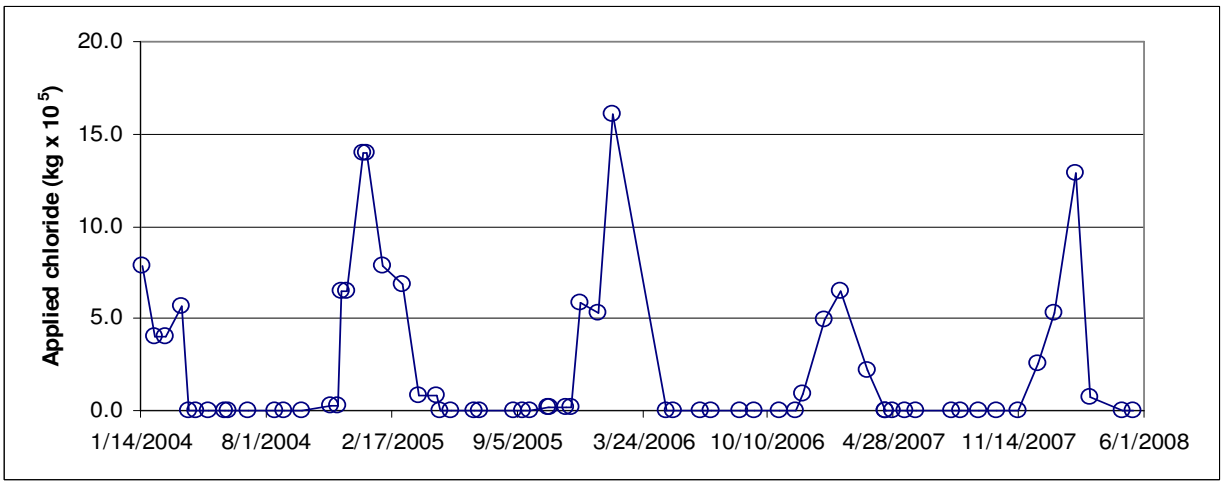

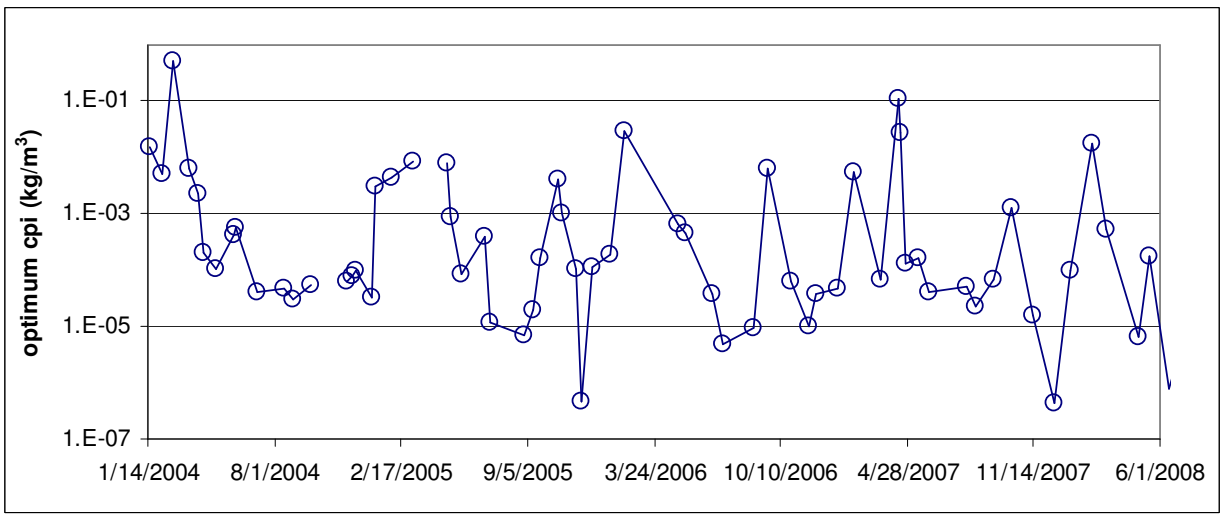

Figure 6.11: Plymouth Cl^- Optimized Source Parameter, Solids Applied, and Optimized First Flush Concentrations

Plymouth should follow these trends as well even though an additional factor of heavier traffic exists here compared to the two salt storage facilities. The October of 2005 and November of 2007 had above normal rainfall which would lead to a higher dilution of the existing chloride source on the pavement surface and hence the first flush concentrations.

The previous presentation was effective in relating salt application to source and flush parameters. The following Figures 6.11, 6.12, and 6.13 present the specific conductivity flux modeled from the calibration of the hydraulic and source parameters of the three watersheds. The trend of a high concentration of ions in the first flush is indicated by the large spike in the specific conductivity towards the beginning of the storm. As the granule of chloride dissolves during dilution throughout the storm event, chloride exits the depression storage layer, travels through the surface reservoir and over the weir to the conductivity probe. This is most notable in the April event at the Plymouth site. Clearly the initial surge of ions exits the water shed in the beginning of the storm and residual trace continues throughout the event.

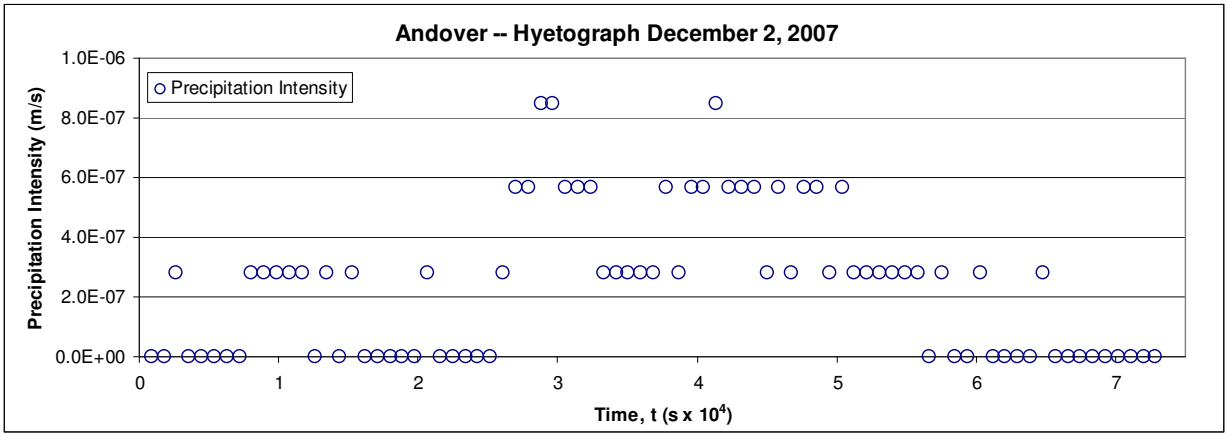

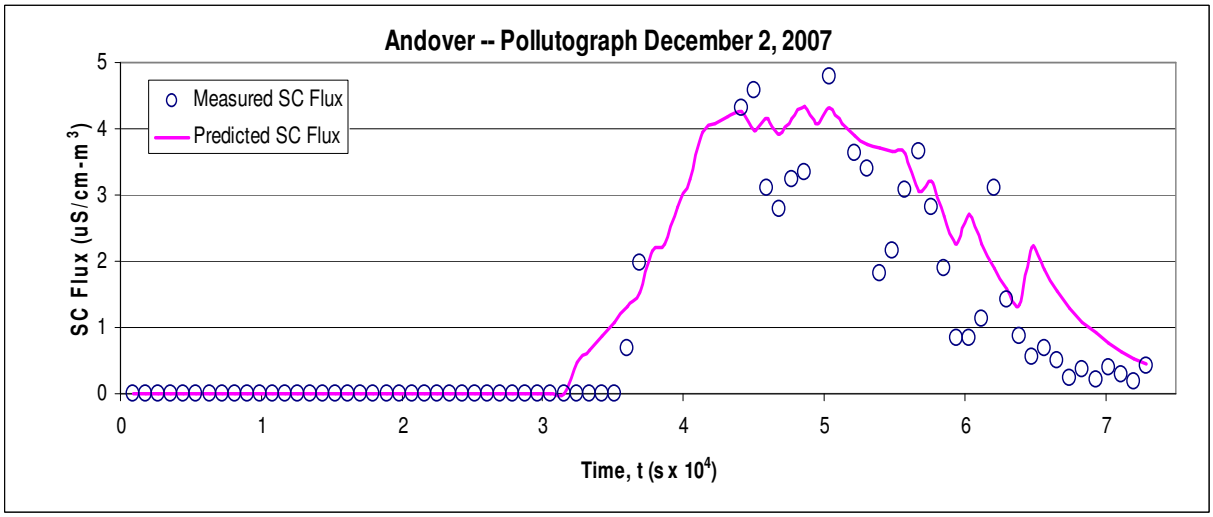

Figure 6.12: Andover Specific Conductivity Flux Model Progression

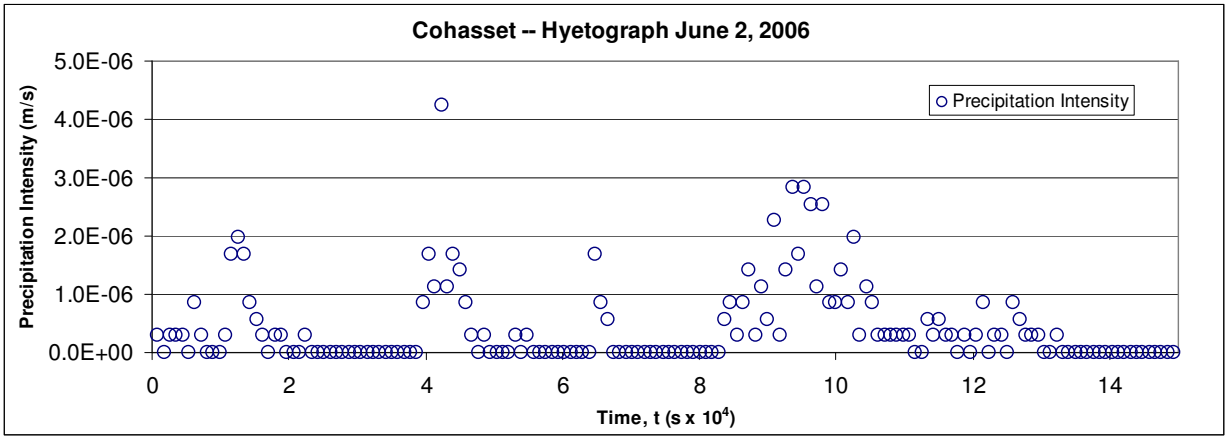

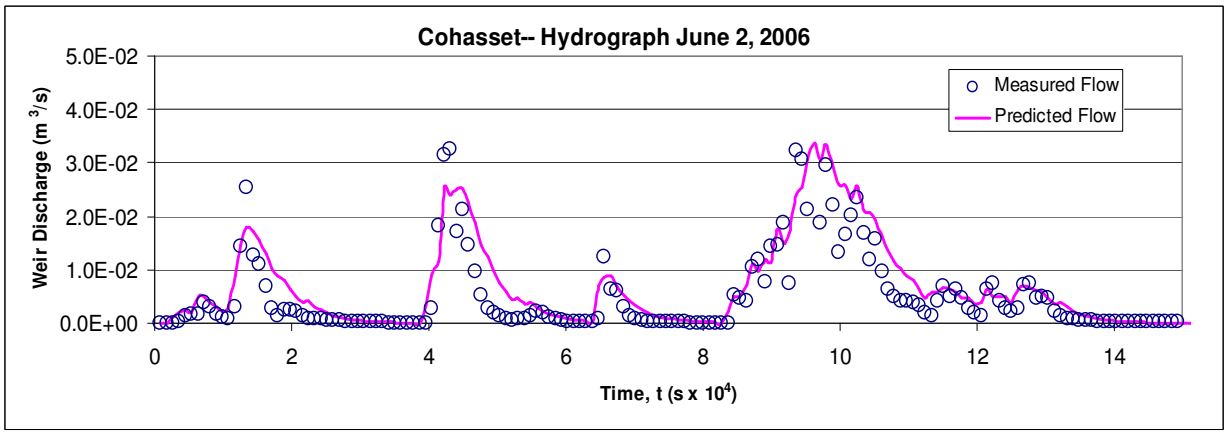

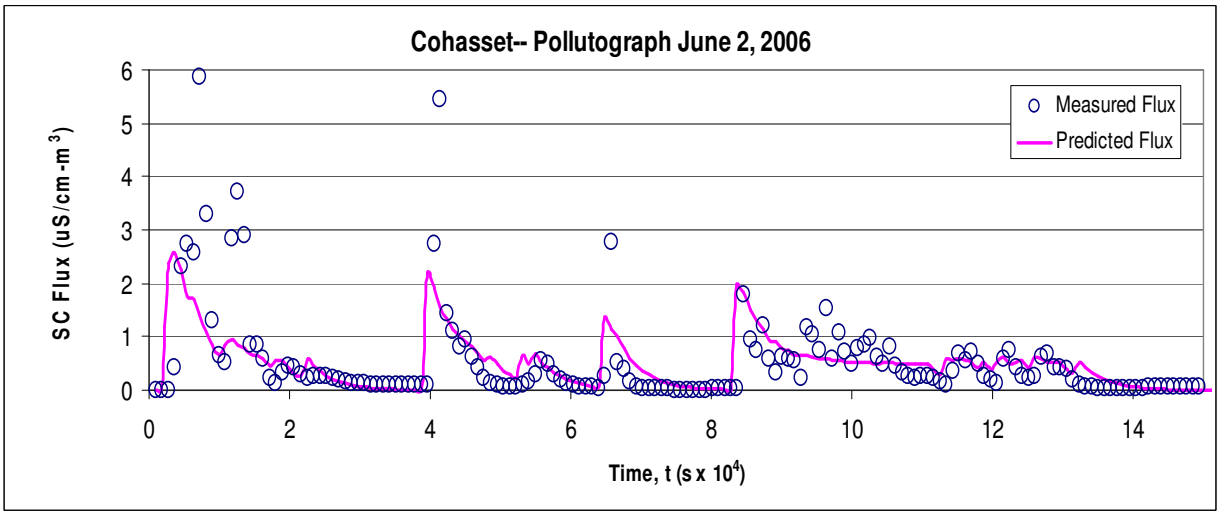

Figure 6.13: Cohasset Specific Conductivity Flux Model Progression

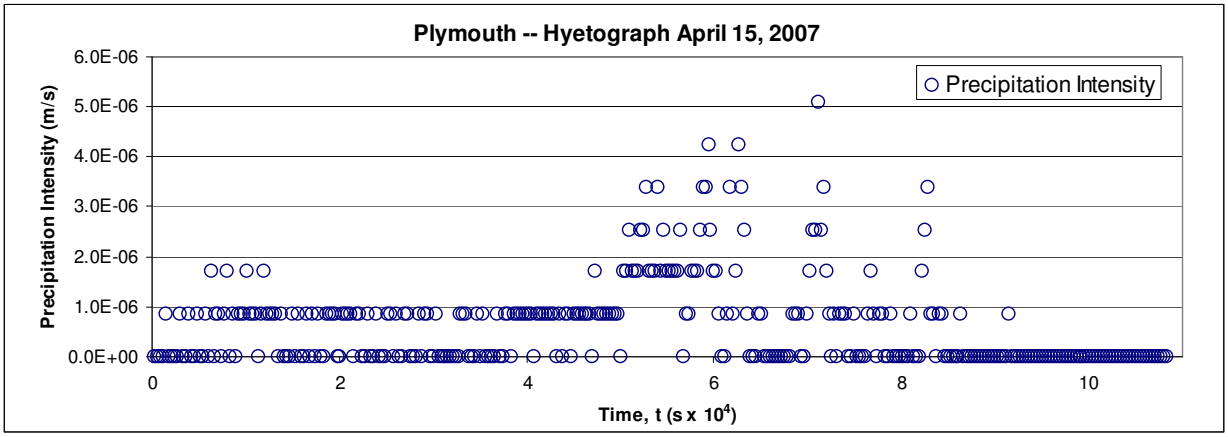

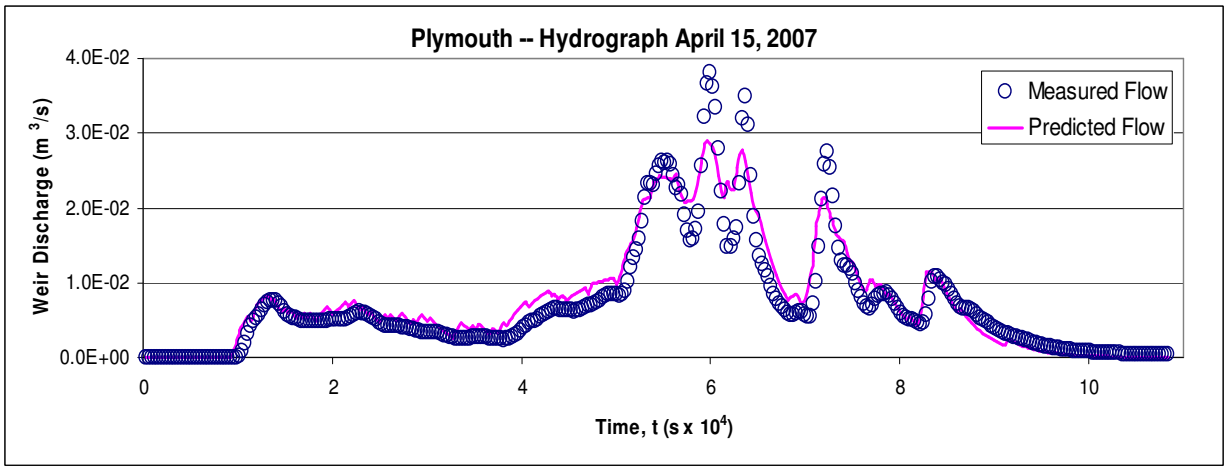

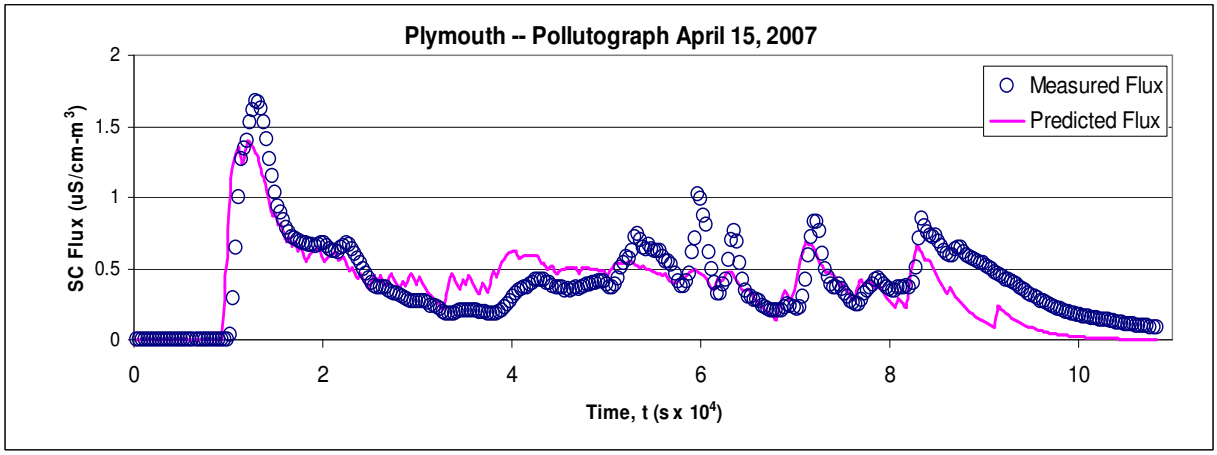

Figure 6.14: Plymouth Specific Conductivity Flux Model Progression

CHAPTER 7

CONCLUSIONS

7.1 Hydraulic Model

The hydraulic model parameters calibrated for each individual storm at each site provide an excellent fit between measured and predicted flow. This is an excellent indication the parameter search is accurate and the most influential watershed parameters are accurately characterized in the hydraulic of the pavement storm runoff. The error within the two parameter search averages less than 1% for all three sites. This is with utilization of an effective area.

The effective areas determined from this research are also comparable to the previous studies done on two of three of these sites. The λ_R of 0.65 optimized by Peeling (1999) resulted in an effective area of 81.6%. The λ_R of 0.72 established within this research resulted in an effective area of 93%. This increase in drainage efficiency can be expected since the system was reworked and curbing installed with the 2001 remodel of the Cohasset site. The effective runoff of 79% for Andover is not what was expected since the majority of the area is contained with curbing. The Plymouth λ_R of 0.85 established with the initial two parameter search neglecting the depression storage layer seemed large for a highway drainage system including grassy swales. Ostendorf (2006) arrived at an average of 0.68 for 50 storms at the same site. These discrepancies were the main reason an effective area was utilized for this study.

The effective area allows savings computation time with minimal difference in accuracy. An averaged linear reservoir value could be appropriate to assume for all storms at a single watershed. The assumption could only be assumed at that particular watershed.

The standard deviations are 0.07 in Plymouth, 0.20 at Andover and in Cohasset is 0.14. This is not a large difference and this approach could definitely be used to obtain an approximate value of runoff volume, but when applying to the detection of a first flush, a small amount of offset can influence the timing of high concentrated runoff. Such is the case with the depression storage depth and the runoff decay constant. A high degree of accuracy was obtained, but when applying an averaged quantity in place of an individually calibrated value, the hydraulics were not as accurate and the timing is very important in a first flush investigation, just as when the depression storage layer was not compensated for at all. In particular is the temperature of the pavement and extraneous conditions such as the drying effects of wind. These variables are difficult to integrate into a model so the constant factors that can provide the best control of the hydraulic characterization is what is focused on.

The pavement texture provides appropriate traction for accelerating and decelerating. The texture is the perfect place for a salt granule to reside and slowly dissolve throughout a storm or throughout a season. This has been shown in the past to be the source so the ability to characterize that influence the texture has on the hydraulic routing of runoff is an important step in developing the model to describe the dissolution kinetics in that textured depression storage layer. It is evident in the hydraulics and therefore must be in the release of previously applied deicing agents. Overall, the generalization of each parameter for each specific watershed is an assumption that can be made without drastic alterations in the site hydraulics.

7.2 Flux Model

The flux model follows the hydraulic model and adequately reflects the first flush increase in the initial specific conductivity high concentration runoff values. The group of Figures 6.9 to 6.11 clearly correlates the application of deicing agents to the increase in first flush concentration and initial source of SC. The annual cyclical nature of this trend can also be seen between all three sites. This is the significance of an accurate sampling procedure. Originally optimized by Stygar (1999), sufficient samples need to be taken in the beginning of a storm to capture the first flush concentration changes yet adequate sampling needs to extend into the storm to characterize the event. The limited quantity of samples available in the automated sampler's capabilities causes the need for optimization of the sampling procedure. Clearly the procedure used for this study characterizes the first flush of a storm and allows adequate length into the storm to develop the accurate flux model used here.

All the sites have the SC source term and SC first flush follow the same trend; although they independently related in the dissolution model, Equation 5.9a. A significant finding is confirmed with the chloride flux and applied chloride correlation in Figure 6.8 for the Andover site. Each application data point is representative of the total deicing chloride distributed in one month. The January 2008 distribution is much higher than previous months. Just about 3 times as much salt was used in this one month than the next highest use month. Yet the residual first flush leaving the depression storage layer and the chloride source term are no higher than the previous two year's 'after season' values. This is because the texture of the bituminous watershed had been thoroughly diluted from the following wetter than usual fall season. This 2007 wetter than average fall season is confirmed with the lowest point of chloride source and first flush terms in Plymouth and

Cohasset being during this fall period and the fall of 2005, another very wet fall period. The depression storage layer was essentially supplying the chloride source from a much lower residual amount. The larger gradient between the excessive application during the winter correlates to the rise of the source term to average warm weather values from a site low residual value.

Further support of a seasonal relationship between the dissolution kinetic of the depression storage layer controlling the flux of chloride off of the watershed can be seen from the peak salt application in the 2005-2006 Plymouth season followed by a lower than average salt season the next 2006-2007 salting year. Yet the summer following this low salt application year provided average source and first flush values. Precipitation was average so this could indicate that residual effects can last more than a year. This reveals possible future work investigating a solids model developed from application data and mass flux predictions from the flux model.

The trend of a larger SC to chloride linear conversion factor during the warmer months gradually growing until the first deicing agent application during the late fall is exemplary of the chloride residual within the depression storage layer dissolving and being removed from the watershed in the storm runoff throughout the year. The rather larger conversion factors for the highway watershed area of Plymouth comparable to the other sites is understandable considering that chloride has been diluted and removed for several months and the addition of substantial highway vacation traffic. Heavy metals, hydrocarbons, and fuel additives from exhaust emissions, tire ware, and braking system ware deposit ions to the watershed pavement area which is removed during storm events and increases the SC measurement recorded in automated and continuous measurement

equipment. Andover and Cohasset are storage facilities that do not have such significant traffic contributing other ions to the SC readings.

The range of chloride source after conversion from SC source is comparably to two to three orders of magnitude lower than Peeling's (1999) findings pre-remodel for the same Cohasset site with approximately the same area but with outdoor salt handling. Figure 6.9 illustrates Peeling's (1999) November to November first flush values and the significant residual value after the summer period. Clearly the containment of salt handling operations under cover has attributed to less chloride stored in the depression storage layer and hence to the watershed runoff.

An indication that the model is accurately characterizing the runoff and dissolution parameters for each site is confirmed with the actual applied quantities being within agreeable ranges of source an first flush values comparing site to site. The two storage facilities have very similar source and first flush factors with the Andover averages an order of magnitude larger which is understandable due to the distribution of twice as much deicing agent per season. The fact that Cohasset is a much larger surface area than Andover could be one explanation as to keeping the values similar.

The magnitude of the flux difference in first flush values is notable for Plymouth. The first flush value is approximately an third of the Andover value yet the distribution being roughly the same. Considering the fact that the runoff fraction is about 0.85 for Plymouth to 0.70 for Andover, lower source terms can be due to loss within the roadside deposition and contribution of other ions to the specific conductivity readings. Recall the conversion factors were slightly higher most of the year at this site without compensation for other ions besides chloride.

Clearly the approach works well for characterizing the dissolution kinetics within the depression storage layer and contributions to impervious surface runoff. Ranging three to four orders of magnitude seasonally from site to site and the averages are within agreement to magnitudes of deicing agents applied. The hydraulic and dissolution parameter calibration of continuously collected data by automated sampler analytical result has great possibilities in evaluating BMP's.

CHAPTER 8

FUTURE WORK

From this hydrologic and dissolution depression storage layer kinetics parameters characterization a few possibilities could be more closely examined.

Related to pavement texture, these results can be confirmed with other methods of measurement such as remote sensing, and actual measurement. The method used here is very efficient and characterizes the hydraulics quite well, but the ranges that some texture thickness cover are quite large and can only be attributed to weather and precipitation intensity so far.

The goal of developing a model applicable to sites of various uses will obviously have more parameters. A general average for each watershed, even though monthly, did not always allow for the depression storage delay or overcompensated for it. Even though the hydraulic models are very accurate, further investigation into the flux throughout an event is needed. The contribution of other ions to the specific conductivity measurements could be further investigated when active highway lanes are studied compared to storage facilities. Clearly the process described here adequately characterizes multiple site hydraulics, the ions flux models need more fine tuning. As can be seen in the figures at the end of Appendix E, the flux model will follow the first flush and perhaps some other spikes, but somewhere within the duration of the storm, the prediction ‘runs out of ‘ contaminant source which usually returns with even the slightest recorded intensity of precipitation.

The introduction of a solids model will confirm and further support the findings reported here. A simple mass accumulation from the flux model calibrated from actual

measurements can characterize the amount of deicing agent that is removed in the watershed runoff compared to the actual solids application records. This additional model will strengthen the present support that the depression storage layer dissolution kinetics controls the individual storm's first flush concentrations and seasonal residual loadings.

CHAPTER 9

REFERENCES

Abramowitz, M., Stegun, I.A. (1972). "Handbook of Mathematical Functions". National Bureau of Standards, Washington, DC.

Alley, W. M., (1981). "Estimation of Impervious-Area Washoff Parameters". *Water Resour. Res.* 17(4):1161-1166.

Amrhein C., Strong, J.E., Mosher, P.A., (1992). "Effect of Deicing Salts on Metal and Organic Matter Mobilization in Roadside Soils". *Environ. Sci. Technol*. 26:703-709.

Barrett, M. E., Irish L. B., Jr., Malina, J. E. Jr., and Charbeneau, R. J., (1998). "Characterization of Highway Runoff in Austin, Texas Area". *J. Environ. Eng.* 124(2):131-137.

Bedient, P. B. and Huber, W. C. (2002). *Hydrology and Flood Plain Analysis.* Prentice-Hall, Upper Saddle River, N.J., pp. 53–54 and 396.

Benjamin, M.M., (2002). *Water Chemistry*. McGraw-Hill, New York, USA. pp. 25-31.

Black, P.E. (1991). *Watershed Hydrology*. Prentice–Hall, Englewood Cliffs, NJ.

Blomqvista, G. and Johansson, E.L. (1999). "Airborne spreading and deposition of de-icing salt -- A Case study"*, Sci. Tot. Environ.* 235:161-168.

Bower, M. C. and Hesterberg, J. H.., (1976). "Environmental implications of highway agents on white pine in Marquette County, Michigan", *Michigan botanist.* 15(2):75–89.

Briggins, D. and Walsh, J., (1989). "The environmental implications of road salting in Nova Scotia". Nova Scotia department of the environment and Nova Scotia department of transportation and communication.

Chen, J., Adams and B.J., (2007). "A derived probability distribution approach to stormwater quality modeling", *Advances in Water Resources* 30:80–100.

Chow, V.T., Maidment, D.R., and Mays, L.W., (1988). *Applied Hydrology*. McGraw-Hill, New York, USA.

Clark, D. L., Asplund, R., Ferguson, J., and Mar, B. W., (1981). "Composite Sampling of Highway Runoff", *J. Environ. Eng.* 107(5):1067-1081.

Conway, J.H. and Guy, R.K., (1996). "The Book of Numbers", *Copernicus, An Imprint of Springer-Verlag,* New York.

Crittenden, J.C., N.J. Hutzler, D.G. Geyer, J.L. Oravitz, and G. Friedman, (1986), "Transport of organic compounds with saturated ground water flow: Model development and parameter sensitivity". *Water Resour. Res.,* 22:271–284.

Croney, P., and Croney, D. (1998). *Design and performance of road pavements*, McGraw-Hill, New York, pp. 465-491.

Crowther, R. A. and Hynes, H. B. N. (1977*). "*The effects of road deicing salt on the drift of stream benthos"*, Environmental Pollution 14:*113–126.

Defourny, C., (2000). "Environmental risk assessment of deicing salts", World Salt Symposium, 8th The Hague, Netherlands 2, pp. 767–770.

Deletic, A., (1998). 'The first flush of urban surface runoff", *Wat. Res*. 32(8):2462-2470.

Diment, W. H., Bubeck, R.C. and Deck, B.L., (1973). "Some effects of deicing salts on Irondequoit Bay and its drainage basin", *Highway Research Record* 425, pp. 23–35.

Dingman,S.L., (2002). *Physical Hydrology, 2nd ed*., Prentice Hall, NJ, pp. 450-453.

Dooge, J. C. I., (1959). "A general theory of the unit hydrograph.", *J. Geophys. Res*., 64(2):241–256.

Fritzsche, C. J.,(1992). "Calcium magnesium acetate deicer"*, Water Environ. and Tech.* 4(1):44–51.

Gelhar, L. W. and Wilson, J. L., (1974). "Ground-Water Quality Modeling", *Ground Water*, 12(6):399-408

Godwin, K. S., Hafner, S. D., and Buff, M. F., (2003). "Long-term trends in sodium and chloride in the Mohawk river New York; The effect of fifty years of road salt application", *Environmental pollution* 124(2):273–281.

Granato, G. E , Church, P.E., and Stone, V.J., (1995). "Mobilization of Major and Trace Constituents of Highway Runoff in Groundwater Potentially Caused by Deicing Chemical Migration", *Transportation Research Record 1483*, Transportation Research Board, National Research Council, Washington, D.C.

Granato, G. E., (1996). "Deicing chemical as Source of Constituents of Highway Runoff", *Transportation Research Record 1533*, Transportation Research Board, National Research Council, Washington, D.C., pp. 50-51.

Granato, G. E. and Smith, K.P., (1999). "Estimating Concentrations of Road-Salt Constituents in Highway-Runoff from Measurements of Specific Conductivity", *Water Resources Investigation Report 99-4077*, US Department of the Interior, US Geological Survey prepared in cooperation with Massachusetts Highway Department, Northborough, Massachusetts, pp. 10-12.

Gray, D. M. (1961). “Synthetic unit hydrographs for small drainage areas”, *J. Hydr.* 87(4):33–54.

Han, Y., Lau S. L., Kayhanian, M., and Stenstrom, M. K., (2006). “Characteristics of Highway Stormwater Runoff”, *Water Environ Res*., 78:2377–2388.

Hinton, M. J. and Schiff, S. L., (1994). “Examining the contributions of glacial till water to storm runoff using two- and three- component hydrograph separations”, *Water Resour. Res.*, 30(4):983-993.

Irish, L. B.., Lesso, W. G., Barrett, M. E., Malina, J. F., Jr., and Charbeneau, R. J. (1995). “An evaluation of the factors affecting the quality of highway runoff in the Austin, Texas area.” *Tech Report No. CRWR 264*, Ctr. for Res. in Water Resour., Univ. of Texas at Austin, Austin, TX.

Jeng, R.I. and Coon, G.C., (2003), “True Form of Instantaneous Unit Hydrograph of Linear Reservoirs”, *J. of Irrig. Drain. Eng.*, 129(1):11-17.

Jones, P.H. and Jeffery, B.A., (1992), “Environmental impact of road salting”, in F.M. D’Itrie (ed), *Chemical Deicers and the Environment*, Boca Raton, Florida, Lewis Publishing, pp. 1-97.

Judd, J. H. (1970), “Lake stratification caused by runoff from street deicing”, *Water Research,* 4:521–532.

Kang, J. H., Kayhanian, M., and Strenstrom, M. K.,(2007), “Predicting the existence of stormwater first flush from the time of concentration”, *Water Research,*(42):220-228.

Kallergis, N. (2007). “Cation Exchange in Glacial Till Subjected to Highway Deicing Agent Infiltration”, Masters Thesis, University of Massachusetts, Amherst, MA.

Kayhanian, M., Suverkropp C., Ruby, A., and Tsay. K., (2007) “Characterization and prediction of highway runoff constituent event mean concentration”. *J. Environ. Management,* 85:279–295.

Kelley, S.P. (2003). “Detection and delineation of deicing materials in an unconfined aquifer via EC measurements.” PhD. Thesis, University of Massachusetts, Amherst, MA.

Khan, S., Lau, S.-L., and Stenstrom, M.K., (2006). “Oil and grease measurement in highway runoff—sampling time and event mean concentrations”, *J. Environ. Eng*., 132 (3):415–422.

Kim, J. Y. and Sansalone, J.J., (2008), “Event-based size distributions of particulate matter transported during urban rainfall-runoff events” *Water Research,* 42:2756–2768.

Kim, L. H. , Ko, S. O., Jeong S., and Yoon J., (2007). “Characteristics of washed-off pollutants and dynamic EMCs in parking lots and bridges during a storm” *Sci. of the Tot. Environ.,* 376:178–184.

Lee, H., Swamikannu, X., Radulescu, D., Kim, S.J., and Stenstrom, M. K., (2007). "Design of stormwater monitoring programs", *Water Research* 41:4186 – 4196.

Linsley, R. K., Kohler, M. A., and Paulhus, J. L. H., (1958). " *Hydrology for Engineers*", McGraw-Hill, New York.

Makepeace, D. K., Smith, D. W., and Stanley, S. J. (1995). "Urban Stormwater quality: Summary of contaminant data." *Critical Rev. in Envi. Sci. and Tech*., 25(2):93-139.

Mason, C. F., Norton, S. A., Fernandez, I. and Katz, L. E., (1999), 'Deconstruction of the Chemical effects on road salt on stream water chemistry', *J. Environ. Quality* 28(1):82–91.

Massoudieh, A., Abrishamchi, A., and Kayhanian, M., (2007). 'Mathematical modeling of first flush in highway storm runoff using genetic algorithm', *Sci. Tot. Environ.*, 398:107-121.

Mays, L. W,(2005) *Water Resour. Eng.*, John Wiley & Sons, Inc., Hoboken, NJ., pp. 251-253.

McBean E. and Al-Nassri S.,(1987). "Migration pattern of de-icing salts from roads", *J Environ Manage*. 25:231-238.

Nash J. E., (1959) "Systematic Determination of Unit Hydrograph Parameters*", J. of Geophysical Research*, 64(1):111–115.

Nash, J.E. (1960). "A unit hydrograph study, with particular reference to British catchments". *Proc. Inst. Civ. Eng*. 17:249–282.

Ng, C.O., C.C. Mei, and D.W. Ostendorf. (1999). "A model for stripping multicomponent vapor from unsaturated soil with free and residual nonaqueous phase liquid". *Water Resour. Res*. 35:385–406.

Ostendorf, D.W, Progress Report No 17(1998), University of Massachusetts on *ISA No. 38721 "Salt Remediation Program*", March 1998.

Ostendorf, D.W., Peeling, D.C., Mitchell, T.J., and Pollock, S.J. (2001). "Chloride Persistence in a Deiced Access Road Drainage System." *J. Enviro. Quality, 30*:1756-1770.

Ostendorf, D.W, *Progress Report No 16* (2006), University of Massachusetts on *ISA No. 38721 "Salt Remediation Program".,* December 2006.

Ostendorf, D.W., Hinlein, E.S., Ahlfeld, D.P., and DeJong, J.T. (2006). "Calibrated models of deicing agent solids, pavement texture, and specific conductivity of highway runoff." *J. Environ. Eng.,* 132(12):1562-1571.

Ostendorf, D. W., DeGroot, D. J., and Hinlein, E. S. (2007). "Unconfined aquifer response to infiltration basins and shallow pump tests." *J. of Hydrology*, 338:132-144.

Pedersen PA and Fostad O., (1996). "Effects of deicing salt on soil, water and vegetation. Part I: Studies of soil and vegetation", *Norges landbrukshøgskole, Institutt for Plantefag*, 65 in Norwegian, English summary.

Peeling, D. C., (1999). "Development of a Chloride Flux Model for the Cohasset Salt/Premix Storage Facility", Masters Thesis, University of Massachusetts, Amherst, MA.

Rainville, E.D. and P.E. Bedient, (1969). *Elementary Differential Equations*. MacMillan, New York.

Ramakrishna, D.M. and Viraraghavan, T., (2005). "Environmental Impact of Chemical Deicers – A Review", *Water, Air, and Soil Pollution*, 166:49–63.

Robinson, J. B., Hazel, W. F. and Garrett, R. G., (1996). " Precipitation, streamflow, and water quality data from selected sites in the city of Charlotte and Mecklenburg county, North Carolina. 1993 -1995." *Open-File Rep*. pp 96 -150, U.S. Geological Survey, Denver, CO.

Rotura, C., (2005). "Tritium/^{3}He Dating of a Clayey Sand Till Aquifer", Masters Thesis, University of Massachusetts, Amherst, MA

Sansalone, J. J., and Cristina, C., (2004). "First Flush Concepts for Suspended and dissolved solids in Small Impervious Watersheds", *J. Environ. Eng.*. 130(11):1301 – 1314.

Scott, W. S., (1980). "Road salt movement into 2 Toronto streams", *J.Environ. Eng. Division* 106(EE3):547–560.

Scott, W. S., (1981). "An analysis of factors influencing deicing salt levels in streams", *J. Environ. Management* 13:269–287.

Shanley, J. B., (1994), "Effects of ion exchange on stream solute fluxes in a basin receiving highway deicing salts", *J. Environ. Quality* 23(5):974–986.

Shi, X., (2005). "The use of road salts for highway winter maintenance: an asset management perspective." *2005 Institute of Transportation Engineers District 6 Annual Meeting.* Kalispell, Montana.

Singh, S. K., (2000). "Transmuting Synthetic Unit Hydrographs into Gamma Distribution"*, J. Hydrologic Eng.* 5(4):380-85.

Snyder, F. F., (1938). "Synthetic Unit Hydrographs", Transactions of the American Geophysical Union, 19:447-454

Standard Methods 19th edition, United Book Press, Inc. 1995.

Stygar, S. C., (2005). "Characterization of Storm Event Sampling Using an Automated Sampler", Masters Thesis, University of Massachusetts, Amherst, MA.

Town of Andover Massachusetts, (2006). *Fish Brook Initiative Final Report, 2006.*

Tollner, E. W., *Natural Resources Engineering,* Blackwell Publishing.

Transportation Research Board, (1991a), "NCHRP Synthesis of Highway Practice 24: Minimizing Deicing Chemical Use", *Special Report No.235,* National Research Council, Washington D.C.

Transportation Research Board,. (1991b). "Highway deicing comparing salt and calcium magnesium acetate." *Special Report No. 235*, National Research Council, Washington, D.C.

United States Geological Survey, (1996). "Effectiveness of highway-drainage systems in preventing contamination of ground water by road salt, Route 25, Southeastern Massachusetts – description of study area, data collection programs, and methodology.", *Open File Report 96-317*, USGS, Denver, CO.

U. S. Environmental Protection Agency (USEPA). (1983). "Results of the nationwide urban runoff program: executive summary." Report No. 832/S83-101, Washington, D.C.

Wisconsin Transportation Center, "Wisconsin Transportation Bulletin No. 6: Using Salt and Sand for Winter Road Maintenance", March 1996.

Wu, J. S., Holman, R. E., and Dorney, J. R., (1996). "Synthetic evaluation of pollutant removal by urban wet detention ponds." *J. Envir. Engrg*. 122(11):983-988.

APPENDICES

APPENDIX A

OPTIMIZED λ_R

PLYMOUTH

Date	λ_R	Date	λ_R	Date	λ_R	Date	λ_R
1/18/2004	0.861	2/6/2004	0.781	3/20/2004	0.931	4/1/2004	0.859
1/3/2005	0.866	2/22/2004	0.853	3/8/2005	0.786	4/12/2004	0.781
1/8/2005	0.760	2/3/2005	0.928	3/2/2006	0.773	4/2/2005	0.786
1/14/2006	0.881	2/4/2006	0.864	3/17/2007	0.920	4/30/2005	0.923
1/8/2007	0.864	2/2/2007	0.789	3/7/2008	0.845	4/23/2006	0.998
1/11/2008	0.879	2/13/2008	0.820			4/15/2007	0.794
						4/16/2007	0.889
						4/27/2007	0.870
						4/28/2008	0.884
5/2/2004	0.928	6/1/2004	0.798	7/5/2004	0.912	8/15/2004	0.886
5/28/2004	0.786	6/30/2005	0.748	7/13/2004	0.918	8/31/2004	0.743
5/6/2005	0.866	6/24/2006	0.732	7/8/2005	0.884	8/30/2005	0.786
5/23/2005	0.861	6/3/2007	0.812	7/11/2006	0.972	8/28/2006	0.872
5/1/2006	0.832	6/16/2008	0.667	7/30/2007	0.843	8/13/2007	0.635
5/12/2006	0.948			7/24/2008	0.891	8/11/2008	0.799
5/17/2007	0.885						
5/16/2008	0.868						
9/28/2004	0.824	10/2/2004	0.998	11/12/2004	0.818	12/1/2004	0.894
9/15/2005	0.926	10/24/2005	0.815	11/24/2004	0.877	12/7/2004	0.918
9/26/2005	0.990	10/29/2005	0.824	11/21/2005	0.853	12/16/2005	0.818
9/19/2006	0.791	10/28/2006	0.894	11/30/2005	0.884	12/4/2006	0.818
9/11/2007	0.909	10/11/2007	0.769	11/23/2006	0.807	12/16/2007	0.787
9/26/2008	0.853			11/3/2007	0.866		

COHASSET

Date	λ_R	Date	λ_R	Date	λ_R	Date	λ_R
1/3/2004	0.714	2/6/2004	0.953	3/20/2004	0.791	4/12/2004	0.840
1/8/2005	0.748	2/14/2005	0.905	3/28/2005	0.851	4/2/2005	0.840
1/14/2006	0.864	2/3/2006	0.539	3/14/2006	0.585	4/4/2006	0.717
1/1/2007	0.694	2/4/2006	0.874	3/2/2007	0.794	4/4/2007	0.649
1/8/2007	0.407	2/14/2007	0.635	3/7/2008	0.511	4/15/2007	0.632
1/1/2008	0.523	2/1/2008	0.495			4/4/2008	0.516
1/11/2008	0.735					4/28/2008	0.632
5/3/2004	0.872	6/9/2004	0.827	7/5/2004	0.751	8/5/2004	0.840
5/6/2005	0.818	6/8/2005	0.830	7/6/2005	0.969	8/28/2005	0.810
5/24/2005	0.881	6/2/2006	0.536	7/12/2006	0.853	8/15/2006	0.698
5/1/2006	0.635	6/3/2007	0.881	7/8/2007	0.751	8/8/2007	0.498
5/9/2006	0.735	6/24/2008	0.753	7/18/2008	0.791	8/6/2008	0.485
5/18/2007	0.838			7/20/2008	0.663		
5/16/2008	0.687						
9/28/2004	0.886	10/15/2004	0.810	11/28/2004	0.778	12/7/2004	0.926
9/15/2005	0.730	10/11/2006	0.534	11/9/2005	0.627	12/16/2005	0.735
9/5/2006	0.686	10/11/2007	0.665	11/7/2006	0.477	12/25/2005	0.467
9/11/2007	0.606			11/24/2006	0.824	12/4/2006	0.998
9/6/2008	0.678			11/3/2007	0.547	12/22/2006	0.781
						12/3/2007	0.788

APPENDIX B

VISUAL BASIC PROGRAM FOR HYDRAULIC MODEL

```
'10/24/08
'Andover
'Declarations
Dim t(1100)      'time during storm
Dim p(1100)      'measured intensity (m/s)
Dim qrim(1100)   'measyred flow (m3/s)
Dim qrip(1100)   'predicted flow (m3/s)
Dim delta(1100)  'error
Dim delt         'RMS error
Dim lambdaopt    'optimum lambda (# of linear reservoirs)
Dim omegar       'optimum runoffdecay constant
Dim ierr         'error counter
Dim nn           '# data points
Dim A            'effective area of runoff
Dim Qave         'Average measured flow
Dim length       'length of storm (s)
Dim dtau         'data collection time increment
Dim sump         'sum of precipitation
Dim sumq         'sum of flow
Dim zeta         'depression storage layer
Sub Main()     'Main calling program
  'For Each sh In ThisWorkbook.Worksheets
      'sh.Activate
      Depression
      OutPut
  'Next sh
End Sub
Sub Depression()   'search for optimum zeta
   zeta = 0
   xmin = 0       'low value of inital section search
   xmax = 0.01    'high value of initial section search
   x1 = xmin + 0.382 * (xmax - xmin)
   zeta = x1
   ReadData
   OutSearch
   del1 = delt
   x2 = xmin + 0.618 * (xmax - xmin)
   zeta = x2
   ReadData
   OutSearch
   del2 = delt
   For iout = 1 To 10
      If del2 > del1 Then
         xmax = x2
         x2 = x1
```

```
            del2 = del1
            x1 = xmin + 0.382 * (xmax - xmin)
            zeta = x1
            ReadData
            OutSearch
            del1 = delt
        Else
            xmin = x1
            x1 = x2
            del1 = del2
            x2 = xmin + 0.618 * (xmax - xmin)
            zeta = x2
            ReadData
            OutSearch
            del2 = delt
        End If
        Cells(7 + iout, 7) = delt
        Next iout
    zeta = (x1 + x2) / 2
    ReadData
    OutSearch
End Sub
Sub ReadData()
    sumq = 0
    sump = 0
    length = 0
    nn = Cells(2, 6)
    dtau = Cells(4, 6)
    For iread = 1 To nn
        p(iread) = Cells(iread + 1, 2)
        sump = sump + p(iread) * dtau
        If sump < zeta Then
            p(iread) = 0
            Else
        End If
        qrim(iread) = Cells(iread + 1, 3)
        sumq = sumq + qrim(iread) * dtau
        t(iread) = Cells(iread + 1, 4)
    Next iread
    A = sumq / (sump - zeta)
    Qave = sumq / (nn * dtau)
    Cells(19, "F") = A
End Sub
Sub OutSearch()  'search for optimum omega
    xmin = 0
    xmax = 0.001
    x1 = xmin + 0.382 * (xmax - xmin)
    omegar = x1
    Errc
    del1 = delt
    x2 = xmin + 0.618 * (xmax - xmin)
    omegar = x2
    Errc
```

```
    del2 = delt
    For iout = 1 To 10
        If del2 > del1 Then
            xmax = x2
            x2 = x1
            del2 = del1
            x1 = xmin + 0.382 * (xmax - xmin)
            omegar = x1
            Errc
            del1 = delt
        Else
            xmin = x1
            x1 = x2
            del1 = del2
            x2 = xmin + 0.618 * (xmax - xmin)
            omegar = x2
            Errc
            del2 = delt
        End If
        Cells(7 + iout, 7) = delt
        Next iout
    omegar = (x1 + x2) / 2
    Errc
End Sub
Sub Errc()
    delt = 0
    For ierr = 1 To nn
        Prediction
        delta(ierr) = qrim(ierr) - qrip(ierr)
        delt = delt + (delta(ierr)) ^ 2
    Next ierr
    delt = (delt / nn) ^ 0.5
End Sub
Sub Prediction()
    Sum = 0
    For ipred = 1 To ierr
        tau = ipred * dtau
        For jpred = 1 To 10
            ttau = tau + dtau * jpred / 10
            inc = p(ipred) * omegar * Exp(-omegar * (t(ierr) - ttau)) * dtau / 10
            Sum = inc + Sum
        Next jpred
    Next ipred
    qrip(ierr) = (Sum * A * 1)
    length = dtau * nn
End Sub
Sub OutPut()
    Cells(2, 6) = nn
    Cells(15, "F") = omegar
    Cells(16, "F") = Qave
    Cells(17, "F") = length / 3600
    Cells(18, "F") = delt
    Cells(20, "F") = delt / Qave
```

```
    Cells(21, "F") = zeta
    For iout = 1 To nn
        Cells(iout + 1, "H") = p(iout)
        Cells(iout + 1, "I") = qrim(iout)
        Cells(iout + 1, "L") = qrip(iout)
        Cells(iout + 1, "K") = delta(iout)
    Next iout
End Sub
```

APPENDIX C

SPREADSHEET for HYDRAULIC MODEL with GRAPHS

	Intensity (m/s)	Flow (m^3/s)	t(s)				delt	p(m/s)	qrim (m^3/s)	t(x10^-4s)
1	2.822E-07	0.00E+00	900		nn =	127	1.004E-03	0.00E+00	0.00E+00	0.09
2	0	0.00E+00	1800	Effective runoff area (m^2) =		1500	8.142E-04	0.00E+00	0.00E+00	0.18
3	5.644E-07	0.00E+00	2700	dtau		900	7.179E-04	5.64E-07	0.00E+00	0.27
4	2.822E-07	1.91E-04	3600				6.704E-04	2.82E-07	1.91E-04	0.36
5	0	1.04E-04	4500				6.468E-04	0.00E+00	1.04E-04	0.45
6	0	3.36E-05	5400				6.346E-04	0.00E+00	3.36E-05	0.54
7	0	2.33E-05	6300				1.096E-03	0.00E+00	2.33E-05	0.63
8	0	1.25E-05	7200				1.072E-03	0.00E+00	1.25E-05	0.72
9	1.6932E-06	7.45E-04	8100				1.031E-03	1.69E-06	7.45E-04	0.81
10	4.5152E-06	2.72E-03	9000				1.032E-03	4.52E-06	2.72E-03	0.90
11	3.3864E-06	3.85E-03	9900				1.023E-03	3.39E-06	3.85E-03	0.99
12	3.3864E-06	2.72E-03	10800				1.024E-03	3.39E-06	2.72E-03	1.08
13	2.822E-06	2.90E-03	11700				1.022E-03	2.82E-06	2.90E-03	1.17
14	1.6932E-06	1.83E-03	12600	**Omegar (s^{-1}) =**		0.00037	1.022E-03	1.69E-06	1.83E-03	1.26
15	0	3.57E-04	13500	**Average Flow (m3/s) =**		0.00062	1.022E-03	0.00E+00	3.57E-04	1.35
16	0	1.04E-04	14400	**length of strm(hrs) =**		31.75	1.022E-03	0.00E+00	1.04E-04	1.44
17	0	4.76E-05	15300	**Delt (m^3/s) =**		0.001022	1.964E-04	0.00E+00	4.76E-05	1.53
18	1.1288E-06	1.04E-04	16200	**Effective Runoff Area (m2) =**		757.3513	3.883E-05	1.13E-06	1.04E-04	1.62
19	1.1288E-06	5.88E-04	17100	**Normalized Error =**		1.649546	1.065E-04	1.13E-06	5.88E-04	1.71
20	0	1.43E-04	18000	**zeta(m) =**		0.000451	5.974E-05	0.00E+00	1.43E-04	1.80
21	0	8.66E-05	18900				6.778E-05	0.00E+00	8.66E-05	1.89
22	0	4.90E-05	19800				7.324E-05	0.00E+00	4.90E-05	1.98
23	0	2.52E-05	20700				7.131E-05	0.00E+00	2.52E-05	2.07
24	0	1.13E-05	21600				7.299E-05	0.00E+00	1.13E-05	2.16
25	0	1.02E-05	22500				6.566E-05	0.00E+00	1.02E-05	2.25
26	0	5.48E-06	23400				6.465E-05	0.00E+00	5.48E-06	2.34
27	0	2.90E-06	24300					0.00E+00	2.90E-06	2.43
28	0	2.39E-06	25200					0.00E+00	2.39E-06	2.52
29	0	1.58E-06	26100					0.00E+00	1.58E-06	2.61
30	0	6.30E-07	27000					0.00E+00	6.30E-07	2.70
31	2.822E-07	9.45E-07	27900					2.82E-07	9.45E-07	2.79
32	1.411E-06	3.30E-04	28800					1.41E-06	3.30E-04	2.88
33	2.822E-07	2.87E-04	29700					2.82E-07	2.87E-04	2.97
34	0	8.73E-05	30600					0.00E+00	8.73E-05	3.06
35	0	3.50E-05	31500					0.00E+00	3.50E-05	3.15
36	8.466E-07	6.29E-04	32400					8.47E-07	6.29E-04	3.24
37	6.7728E-06	1.70E-03	33300					6.77E-06	1.70E-03	3.33
38	0	2.15E-04	34200					0.00E+00	2.15E-04	3.42
39	0	1.04E-04	35100					0.00E+00	1.04E-04	3.51
40	0	5.09E-05	36000					0.00E+00	5.09E-05	3.60
41	0	2.02E-05	36900					0.00E+00	2.02E-05	3.69
42	0	1.93E-05	37800					0.00E+00	1.93E-05	3.78
43	0	1.04E-05	38700					0.00E+00	1.04E-05	3.87
44	1.411E-06	1.56E-03	39600					1.41E-06	1.56E-03	3.96

45	2.5398E-06	2.92E-03	40500	2.54E-06	2.92E-03	4.05
46	2.822E-07	4.27E-04	41400	2.82E-07	4.27E-04	4.14
47	0	1.44E-04	42300	0.00E+00	1.44E-04	4.23
48	0	4.66E-05	43200	0.00E+00	4.66E-05	4.32
49	0	2.74E-05	44100	0.00E+00	2.74E-05	4.41
50	0	1.54E-05	45000	0.00E+00	1.54E-05	4.50
51	0	1.22E-05	45900	0.00E+00	1.22E-05	4.59
52	2.822E-07	1.79E-04	46800	2.82E-07	1.79E-04	4.68
53	1.1288E-06	9.78E-04	47700	1.13E-06	9.78E-04	4.77
54	1.9754E-06	1.05E-03	48600	1.98E-06	1.05E-03	4.86
55	0	2.78E-04	49500	0.00E+00	2.78E-04	4.95
56	0	1.13E-04	50400	0.00E+00	1.13E-04	5.04
57	5.644E-07	4.42E-04	51300	5.64E-07	4.42E-04	5.13
58	2.822E-07	2.90E-04	52200	2.82E-07	2.90E-04	5.22
59	0	1.01E-04	53100	0.00E+00	1.01E-04	5.31
60	2.822E-07	3.57E-04	54000	2.82E-07	3.57E-04	5.40
61	2.822E-07	2.62E-04	54900	2.82E-07	2.62E-04	5.49
62	0	1.28E-04	55800	0.00E+00	1.28E-04	5.58
63	0	5.64E-05	56700	0.00E+00	5.64E-05	5.67
64	0	3.36E-05	57600	0.00E+00	3.36E-05	5.76
65	0	1.98E-05	58500	0.00E+00	1.98E-05	5.85
66	0	1.39E-05	59400	0.00E+00	1.39E-05	5.94
67	2.822E-07	1.19E-05	60300	2.82E-07	1.19E-05	6.03
68	0	7.62E-06	61200	0.00E+00	7.62E-06	6.12
69	0	5.48E-06	62100	0.00E+00	5.48E-06	6.21
70	8.466E-07	1.03E-03	63000	8.47E-07	1.03E-03	6.30
71	8.466E-07	1.03E-03	63900	8.47E-07	1.03E-03	6.39
72	1.1288E-06	4.37E-04	64800	1.13E-06	4.37E-04	6.48
73	1.38278E-05	1.01E-02	65700	1.38E-05	1.01E-02	6.57
74	2.00362E-05	9.11E-03	66600	2.00E-05	9.11E-03	6.66
75	4.7974E-06	5.18E-03	67500	4.80E-06	5.18E-03	6.75
76	1.1288E-06	1.07E-03	68400	1.13E-06	1.07E-03	6.84
77	0	3.20E-04	69300	0.00E+00	3.20E-04	6.93
78	0	9.92E-05	70200	0.00E+00	9.92E-05	7.02
79	0	6.79E-05	71100	0.00E+00	6.79E-05	7.11
80	0	3.36E-05	72000	0.00E+00	3.36E-05	7.20
81	0	1.67E-05	72900	0.00E+00	1.67E-05	7.29
82	0	8.13E-06	73800	0.00E+00	8.13E-06	7.38
83	0	9.14E-06	74700	0.00E+00	9.14E-06	7.47
84	0	2.90E-06	75600	0.00E+00	2.90E-06	7.56
85	0	2.84E-06	76500	0.00E+00	2.84E-06	7.65
86	0	3.09E-06	77400	0.00E+00	3.09E-06	7.74
87	0	2.84E-06	78300	0.00E+00	2.84E-06	7.83
88	3.3864E-06	3.23E-03	79200	3.39E-06	3.23E-03	7.92
89	1.9754E-06	9.05E-04	80100	1.98E-06	9.05E-04	8.01
90	8.466E-07	1.11E-03	81000	8.47E-07	1.11E-03	8.10
91	5.644E-07	6.92E-04	81900	5.64E-07	6.92E-04	8.19
92	1.411E-06	2.21E-03	82800	1.41E-06	2.21E-03	8.28
93	5.644E-07	6.64E-04	83700	5.64E-07	6.64E-04	8.37
94	2.822E-07	3.05E-04	84600	2.82E-07	3.05E-04	8.46
95	0	9.84E-05	85500	0.00E+00	9.84E-05	8.55
96	0	4.57E-05	86400	0.00E+00	4.57E-05	8.64
97	0	5.13E-05	87300	0.00E+00	5.13E-05	8.73

98	0	4.30E-05	88200	0.00E+00	4.30E-05	8.82
99	0	2.78E-05	89100	0.00E+00	2.78E-05	8.91
100	0	1.95E-05	90000	0.00E+00	1.95E-05	9.00
101	0	7.43E-06	90900	0.00E+00	7.43E-06	9.09
102	0	7.94E-06	91800	0.00E+00	7.94E-06	9.18
103	0	1.89E-06	92700	0.00E+00	1.89E-06	9.27
104	0	2.33E-06	93600	0.00E+00	2.33E-06	9.36
105	0	1.51E-06	94500	0.00E+00	1.51E-06	9.45
106	1.9754E-06	2.27E-04	95400	1.98E-06	2.27E-04	9.54
107	4.5152E-06	2.23E-03	96300	4.52E-06	2.23E-03	9.63
108	2.822E-07	6.71E-04	97200	2.82E-07	6.71E-04	9.72
109	2.822E-07	4.35E-04	98100	2.82E-07	4.35E-04	9.81
110	5.644E-07	5.42E-04	99000	5.64E-07	5.42E-04	9.90
111	8.466E-07	1.17E-03	99900	8.47E-07	1.17E-03	9.99
112	8.466E-07	8.72E-04	100800	8.47E-07	8.72E-04	10.08
113	2.822E-07	6.51E-04	101700	2.82E-07	6.51E-04	10.17
114	5.644E-07	7.49E-04	102600	5.64E-07	7.49E-04	10.26
115	5.644E-07	7.06E-04	103500	5.64E-07	7.06E-04	10.35
116	2.822E-07	3.69E-04	104400	2.82E-07	3.69E-04	10.44
117	1.1288E-06	1.14E-03	105300	1.13E-06	1.14E-03	10.53
118	2.822E-07	4.78E-04	106200	2.82E-07	4.78E-04	10.62
119	0	1.90E-04	107100	0.00E+00	1.90E-04	10.71
120	2.822E-07	2.17E-04	108000	2.82E-07	2.17E-04	10.80
121	0	1.22E-04	108900	0.00E+00	1.22E-04	10.89
122	2.822E-07	1.46E-04	109800	2.82E-07	1.46E-04	10.98
123	0	1.18E-04	110700	0.00E+00	1.18E-04	11.07
124	0	6.12E-05	111600	0.00E+00	6.12E-05	11.16
125	0	2.52E-05	112500	0.00E+00	2.52E-05	11.25
126	0	2.72E-05	113400	0.00E+00	2.72E-05	11.34
127	0	1.25E-05	114300	0.00E+00	1.25E-05	11.43

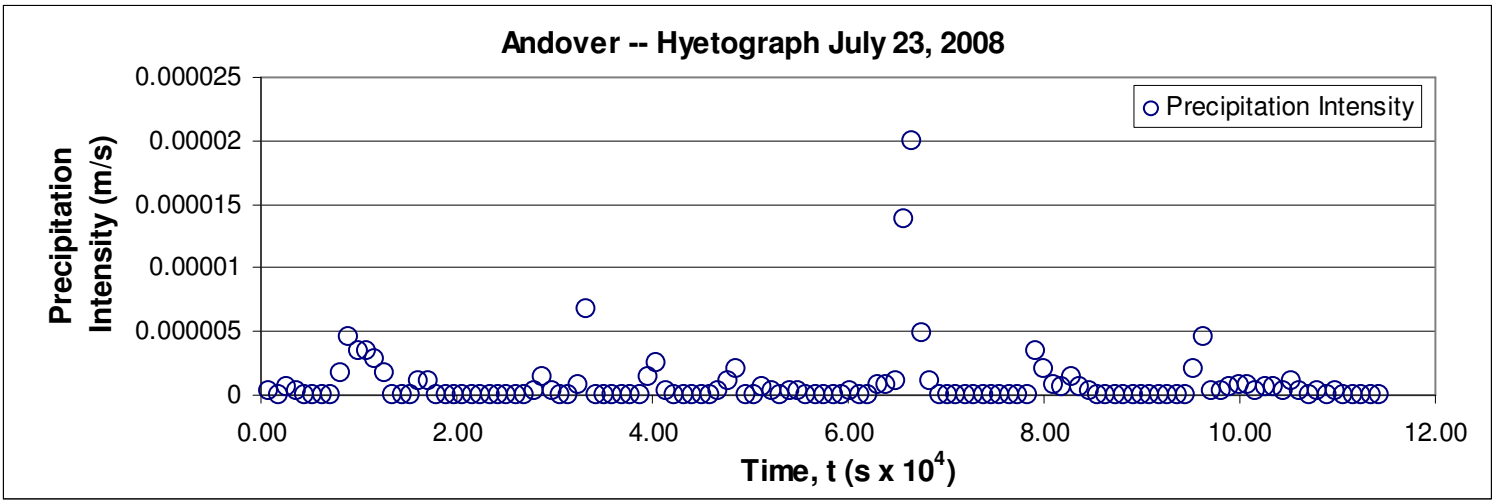
Andover -- Hyetograph July 23, 2008
Precipitation Intensity (m/s)
0.000025
0.00002
0.000015
0.00001
0.000005
0
0.00
2.00
4.00
6.00
8.00
10.00
12.00
Time, t (s x 10^4)
Precipitation Intensity

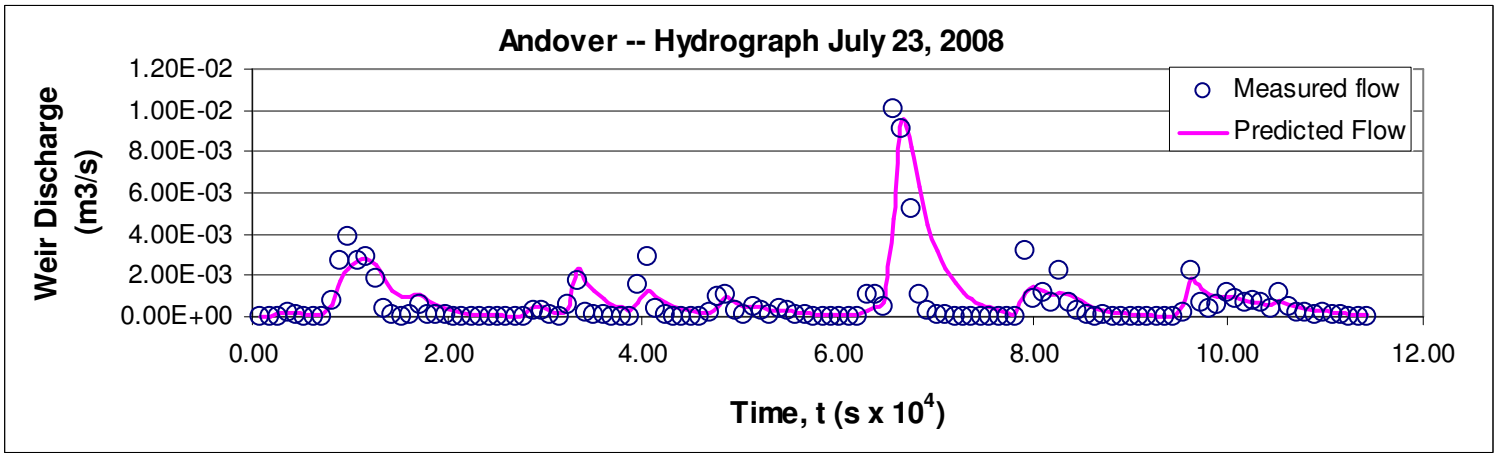
Andover -- Hydrograph July 23, 2008
Weir Discharge (m3/s)
1.20E-02
1.00E-02
8.00E-03
6.00E-03
4.00E-03
2.00E-03
0.00E+00
0.00
2.00
4.00
6.00
8.00
10.00
12.00
Time, t (s x 10^4)
Measured flow
Predicted Flow

APPENDIX D

VISUAL BASIC PROGRAM FOR FLUX MODEL

```
'2/1/09
'Plymouth Specific Conductivity Flux 2007-2008
'Declarations
Dim t(1100)
Dim p(1100)      'measured intensity p (m/s)
Dim qrim(1100)   'measured flow (m^3/s)
Dim delta(1100)  'error
Dim mflux(1100)  'measured Cl- flux (mg/m^2-s)
Dim pflux(1100)  'predicted Cl- flux (mg/m^2-s)
Dim fldSC(1100)  'specific conductivty remote sensing measurement of field(micro
seimens/cm)
Dim cpi         'concentration leaving depression storage, mg/L
Dim actual       'actual start time of runoff
Dim cpsource     'flux term (omegar*source strength*Cl- load)
Dim delt        'RMS error
Dim lambdaopt    'lambda optimum  (s^-1)
Dim omegar       'omega optimum for dmean (s^-1)
Dim ierr        'error counter
Dim nn          '# data points
Dim A           'effective area of runoff
Dim n           'porosity
Dim Qave         'Average measured flow
Dim length       'length of storm (s)
Dim dtau         'Sampling Increment, ttau -- slice of increment to capture sensitivity
Dim sump         'Sum of precipitation
Dim sumq         'Sum of measured flow
Dim zeta         'Depression storage depth
Dim cpist        'first cpi value
Sub Main()     'Main calling program
   For Each sh In ThisWorkbook.Worksheets
      sh.Activate

      ReadData
      OutSearch
      OutPut
   Next sh
End Sub
Sub ReadData()
   sumq = 0
   sump = 0
   length = 0
   ierr = 0
   actual = 0
   zeta = Cells(5, 9)
   n = Cells(7, 9)
   nn = Cells(2, 9)
   dtau = Cells(4, 9)
```

```
    lambdaopt = Cells(6, 9)
    omegar = Cells(8, 9)
    SCtoCl = Cells(9, 9)
    For iread = 1 To nn
        fldSC(iread) = Cells(iread + 1, 6)
        p(iread) = Cells(iread + 1, 3)
        sump = sump + p(iread) * dtau
        If sump < zeta Then
            p(iread) = 0
            actual = iread + 1
            Else
        End If

        qrim(iread) = Cells(iread + 1, 4)
        sumq = sumq + qrim(iread) * dtau
        t(iread) = Cells(iread + 1, 5)
        mflux(iread) = (fldSC(iread) * qrim(iread))
    Next iread
    A = sumq / (sump - zeta)
    Qave = sumq / (nn * dtau)
    Cells(19, "i") = A
End Sub
Sub OutSearch()  'search for optimum cpi
    xmin = 0
    xmax = 10000
    x1 = xmin + 0.382 * (xmax - xmin)
    cpist = x1
    InSearch
    del1 = delt
    x2 = xmin + 0.618 * (xmax - xmin)
    cpist = x2
    InSearch
    del2 = delt
    For iout = 1 To 10
        If del2 > del1 Then
            xmax = x2
            x2 = x1
            del2 = del1
            x1 = xmin + 0.382 * (xmax - xmin)
            cpist = x1
            InSearch
            del1 = delt
        Else
            xmin = x1
            x1 = x2
            del1 = del2
            x2 = xmin + 0.618 * (xmax - xmin)
            cpist = x2
            InSearch
            del2 = delt
        End If
        Cells(7 + iout, 10) = delt
        Next iout
```

```
    cpist = (x1 + x2) / 2
    InSearch
End Sub
Sub InSearch()       'search for optimal source (smallomega*sN)
    xmin = 0
    xmax = 0.01
    x1 = xmin + 0.382 * (xmax - xmin)
    cpsource = x1
    Errc
    del1 = delt
    x2 = xmin + 0.618 * (xmax - xmin)
    cpsource = x2
    Errc
    del2 = delt
    For iin = 1 To 20
        If del2 > del1 Then
            xmax = x2
            x2 = x1
            del2 = del1
            x1 = xmin + 0.382 * (xmax - xmin)
            cpsource = x1
            Errc
            del1 = delt
        Else
            xmin = x1
            x1 = x2
            del1 = del2
            x2 = xmin + 0.618 * (xmax - xmin)
            cpsource = x2
            Errc
            del2 = delt
            End If
        Cells(1 + iin, 10) = delt
        Next iin
        cpsource = (x1 + x2) / 2
    Errc
End Sub

Sub Errc()
    delt = 0
    For ierr = 1 To nn
        Prediction
        delta(ierr) = mflux(ierr) - pflux(ierr)
        delt = delt + delta(ierr) ^ 2
    Next ierr
    delt = (delt / (nn - actual)) ^ 0.5
End Sub


Sub Prediction()
    Sum = 0
    cpi = cpist
    For ipred = actual To ierr
```

```
      tau = (ipred - 1) * dtau
      For jpred = 1 To 10
         ttau = tau + dtau * jpred / 10
         cpinew = (cpsource / (n * zeta) + cpi * 10 / dtau) / (p(ipred) / (n * zeta) + 10 / dtau)
         inc = cpinew * p(ipred) * Exp(-omegar * (t(ierr) - ttau)) * dtau / 10
         Sum = inc + Sum
         cpi = cpinew
      Next jpred
   Next ipred
   pflux(ierr) = (Sum * A * omegar) * lambdaopt
   length = dtau * nn
End Sub
Sub OutPut()
   Cells(2, 9) = nn
   Cells(15, "i") = omegar
   Cells(16, "i") = lambdaopt
   Cells(17, "i") = length / 3600
   Cells(18, "i") = delt
   Cells(20, "i") = delt / Qave
   Cells(21, "i") = zeta
   Cells(22, "i") = cpsource
   Cells(23, "i") = cpi
   For iout = 1 To nn
      Cells(iout + 1, "k") = p(iout)
      Cells(iout + 1, "l") = qrim(iout)
      Cells(iout + 1, "n") = delta(iout)
      Cells(iout + 1, "o") = pflux(iout)
      Cells(iout + 1, "g") = mflux(iout)
   Next iout
End Sub
```

APPENDIX E

SPREADSHEET for HYDRAULIC MODEL with GRAPHS

(NOTE: only first 60000 seconds)

Intensity (m/s)	Flow (m^3/s)	t(s)	Field Spec Cond (weir)	Measured Flux (kg/s)			delt	t ($x10^4 s$)	delta	Predicted Flux (kg/s)
0	0.00E+00	300	12	0	nn =	361	2.48E+01	0.03	0	0
0	0.00E+00	600	6	0	Effective runoff area (m^2) =	13670	1.52E+01	0.06	0	0
0	0.00E+00	900	4	0	dtau (seconds)	300	9.23E+00	0.09	0	0
0	0.00E+00	1200	4	0	zeta (m)	0.003713	5.57E+00	0.12	0	0
8.466E-07	0.00E+00	1500	4	0	Lambda optimum	1	3.30E+00	0.15	0	0
0	0.00E+00	1800	2	0	porosity	0.4	1.91E+00	0.18	0	0
0	0.00E+00	2100	2	0	omegar	2.96E-04	1.05E+00	0.21	0	0
0	0.00E+00	2400	2	0	S. Cond / Cl- constant	4.14	5.38E-01	0.24	0	0
0	0.00E+00	2700	2	0			2.66E-01	0.27	0	0
8.466E-07	0.00E+00	3000	2	0			2.12E-01	0.30	0	0
0	0.00E+00	3300	2	0			2.66E-01	0.33	0	0
0	0.00E+00	3600	2	0			2.12E-01	0.36	0	0
8.466E-07	0.00E+00	3900	2	0			2.26E-01	0.39	0	0
0	0.00E+00	4200	2	0	**Omegar (s^{-1}) =**	2.96E-04	2.09E-01	0.42	0	0
0	0.00E+00	4500	2	0	**lamba optimum =**	1	2.09E-01	0.45	0	0
8.466E-07	0.00E+00	4800	2	0	**length of strm(hrs) =**	30.1	2.10E-01	0.48	0	0
0	0.00E+00	5100	2	0	**Delt (m^3/s) =**	0.209	2.09E-01	0.51	0	0
0	0.00E+00	5400	2	0	**Calculated area, A (m^2) =**	12216.45	2.09E-01	0.54	0	0
8.466E-07	0.00E+00	5700	2	0	**Normalized A =**	29.8	2.09E-01	0.57	0	0
0	0.00E+00	6000	2	0	**zeta(m) =**	0.0037	2.09E-01	0.60	0	0
1.6932E-06	0.00E+00	6300	2	0	**cpsource(uS/cm-m^2-s) =**	3.49E-05	2.42E-04	0.63	0	0
0	0.00E+00	6600	0	0	**cpi (uS/m^3)**	562	1.20E-04	0.66	0	0
8.466E-07	0.00E+00	6900	0	0			2.10E-04	0.69	0	0
8.466E-07	0.00E+00	7200	0	0			2.55E-04	0.72	0	0
0	0.00E+00	7500	0	0			2.98E-04	0.75	0	0
8.466E-07	0.00E+00	7800	0	0			9.69E-05	0.78	0	0
1.6932E-06	0.00E+00	8100	0	0				0.81	0	0
0	0.00E+00	8400	0	0				0.84	0	0

8.466E-07	0.00E+00	8700	0	0	0.87	0	0
0	1.00E-30	9000	0	0	0.90	0	0
8.466E-07	1.00E-30	9300	30	3E-29	0.93	3E-29	0
8.466E-07	1.00E-30	9600	128	1E-28	0.96	-0.37818	0.37818
8.466E-07	1.00E-30	9900	200	2E-28	0.99	-0.67093	0.670928
1.6932E-06	1.09E-04	10200	248	0.027	1.02	-1.09894	1.125945
8.466E-07	7.70E-04	10500	380	0.2926	1.05	-0.94334	1.23591
8.466E-07	1.85E-03	10800	346	0.6409	1.08	-0.66923	1.310139
8.466E-07	3.12E-03	11100	322	1.0044	1.11	-0.35141	1.355782
0	4.19E-03	11400	302	1.2657	1.14	0.02512	1.240624
8.466E-07	4.91E-03	11700	274	1.3443	1.17	0.06522	1.279026
1.6932E-06	5.31E-03	12000	264	1.4012	1.20	-0.00162	1.402848
8.466E-07	5.77E-03	12300	264	1.5227	1.23	0.14257	1.380092
8.466E-07	6.29E-03	12600	256	1.6108	1.26	0.26086	1.349903
8.466E-07	6.89E-03	12900	244	1.6806	1.29	0.36623	1.314372
8.466E-07	7.33E-03	13200	228	1.6719	1.32	0.39676	1.275186
0	7.56E-03	13500	214	1.6183	1.35	0.45141	1.166874
8.466E-07	7.65E-03	13800	200	1.531	1.38	0.39073	1.140243
0	7.52E-03	14100	188	1.413	1.41	0.36961	1.043393
0	7.15E-03	14400	178	1.2732	1.44	0.31845	0.954768
0	6.71E-03	14700	172	1.1548	1.47	0.28117	0.873672
8.466E-07	6.17E-03	15000	168	1.0363	1.50	0.15304	0.883288
0	5.81E-03	15300	162	0.9407	1.53	0.13247	0.808263
8.466E-07	5.57E-03	15600	160	0.8917	1.56	0.07002	0.82169
0	5.38E-03	15900	156	0.8397	1.59	0.08781	0.751897
0	5.20E-03	16200	152	0.7898	1.62	0.1018	0.688032
8.466E-07	5.01E-03	16500	150	0.7521	1.65	0.0362	0.715857
0	4.87E-03	16800	148	0.7208	1.68	0.06577	0.655053
8.466E-07	4.80E-03	17100	148	0.7104	1.71	0.02681	0.683553
0	4.80E-03	17400	146	0.7008	1.74	0.07527	0.625493
8.466E-07	4.80E-03	17700	144	0.6912	1.77	0.03646	0.654709
0	4.80E-03	18000	142	0.6816	1.80	0.08247	0.599099
0	4.80E-03	18300	142	0.6816	1.83	0.13335	0.548212
8.466E-07	4.80E-03	18600	140	0.672	1.86	0.08383	0.588137
8.466E-07	4.80E-03	18900	138	0.6624	1.89	0.04552	0.61685

8.466E-07	4.80E-03	19200	136	0.6528	1.92	0.01624	0.636522
8.466E-07	4.91E-03	19500	136	0.6672	1.95	0.01827	0.648952
0	5.05E-03	19800	134	0.6767	1.98	0.08285	0.593831
0	5.12E-03	20100	132	0.6762	2.01	0.13281	0.543392
8.466E-07	5.12E-03	20400	128	0.6557	2.04	0.08536	0.570348
8.466E-07	5.05E-03	20700	126	0.6363	2.07	0.04701	0.58928
8.466E-07	5.01E-03	21000	124	0.6217	2.10	0.01993	0.601764
8.466E-07	5.09E-03	21300	122	0.6205	2.13	0.01142	0.609101
0	5.23E-03	21600	118	0.6175	2.16	0.06016	0.557365
8.466E-07	5.50E-03	21900	118	0.6486	2.19	0.07791	0.570685
8.466E-07	5.77E-03	22200	114	0.6575	2.22	0.07843	0.57908
0	6.01E-03	22500	112	0.6727	2.25	0.14281	0.529894
0	6.09E-03	22800	110	0.6696	2.28	0.1847	0.484886
8.466E-07	6.01E-03	23100	106	0.6367	2.31	0.12798	0.508687
0	5.93E-03	23400	102	0.6045	2.34	0.13898	0.46548
0	5.69E-03	23700	100	0.5689	2.37	0.143	0.425943
8.466E-07	5.50E-03	24000	98	0.5387	2.40	0.07706	0.461602
0	5.27E-03	24300	94	0.4954	2.43	0.07302	0.422394
0	4.98E-03	24600	92	0.4579	2.46	0.07143	0.386517
0	4.69E-03	24900	92	0.4319	2.49	0.07824	0.353687
8.47E-07	4.46E-03	25200	90	0.401	2.52	-0.00593	0.406927
8.466E-07	4.32E-03	25500	88	0.3804	2.55	-0.06797	0.448324
0	4.29E-03	25800	86	0.3689	2.58	-0.04137	0.410244
8.466E-07	4.29E-03	26100	86	0.3689	2.61	-0.08197	0.45084
0	4.29E-03	26400	86	0.3689	2.64	-0.04367	0.412546
0	4.26E-03	26700	86	0.366	2.67	-0.01146	0.377505
8.466E-07	4.16E-03	27000	84	0.3493	2.70	-0.07676	0.426103
8.466E-07	4.09E-03	27300	82	0.3358	2.73	-0.12791	0.463661
0	4.00E-03	27600	80	0.3199	2.76	-0.10434	0.424278
0	3.97E-03	27900	80	0.3174	2.79	-0.07082	0.388241
0	3.87E-03	28200	80	0.3099	2.82	-0.04532	0.355264
8.466E-07	3.75E-03	28500	80	0.3001	2.85	-0.10985	0.409984
0	3.66E-03	28800	78	0.2856	2.88	-0.08958	0.375161
8.466E-07	3.54E-03	29100	78	0.2763	2.91	-0.14994	0.426278

8.466E-07	3.48E-03	29400	78	0.2718	2.94	-0.19399	0.465779
0	3.48E-03	29700	78	0.2718	2.97	-0.15443	0.426216
0	3.48E-03	30000	78	0.2718	3.00	-0.11823	0.390014
8.466E-07	3.48E-03	30300	78	0.2718	3.03	-0.16599	0.437775
0	3.46E-03	30600	78	0.2695	3.06	-0.13106	0.400591
0	3.43E-03	30900	78	0.2673	3.09	-0.09928	0.366566
0	3.31E-03	31200	78	0.2584	3.12	-0.07703	0.33543
0	3.17E-03	31500	76	0.2412	3.15	-0.06573	0.306939
0	3.07E-03	31800	76	0.2329	3.18	-0.04792	0.280868
0	2.93E-03	32100	76	0.2229	3.21	-0.03415	0.257012
0	2.78E-03	32400	76	0.2111	3.24	-0.02406	0.235182
0	2.65E-03	32700	74	0.1963	3.27	-0.01889	0.215206
8.466E-07	2.53E-03	33000	74	0.1873	3.30	-0.12883	0.316146
8.466E-07	2.48E-03	33300	74	0.1838	3.33	-0.2118	0.395587
8.466E-07	2.46E-03	33600	74	0.182	3.36	-0.27533	0.457371
0	2.51E-03	33900	74	0.1855	3.39	-0.23298	0.418522
0	2.58E-03	34200	74	0.1909	3.42	-0.19209	0.382974
0	2.63E-03	34500	76	0.1997	3.45	-0.1507	0.350445
8.466E-07	2.68E-03	34800	76	0.2035	3.48	-0.22034	0.423834
0	2.68E-03	35100	76	0.2035	3.51	-0.18434	0.387834
8.466E-07	2.68E-03	35400	76	0.2035	3.54	-0.24979	0.453287
0	2.68E-03	35700	76	0.2035	3.57	-0.21129	0.414786
0	2.68E-03	36000	76	0.2035	3.60	-0.17606	0.379554
0	2.65E-03	36300	76	0.2016	3.63	-0.1457	0.347316
0	2.60E-03	36600	76	0.1979	3.66	-0.11992	0.317815
8.466E-07	2.56E-03	36900	76	0.1942	3.69	-0.20797	0.402177
0	2.51E-03	37200	76	0.1906	3.72	-0.17745	0.368017
0	2.46E-03	37500	76	0.187	3.75	-0.1498	0.336758
8.466E-07	2.44E-03	37800	76	0.1852	3.78	-0.23396	0.419132
8.466E-07	2.41E-03	38100	74	0.1786	3.81	-0.3043	0.482868
0	2.48E-03	38400	74	0.1838	3.84	-0.25807	0.441854

8.466E-07	2.58E-03	38700	76	0.196	3.87	-0.30345	0.499496
8.466E-07	2.73E-03	39000	76	0.2073	3.90	-0.33578	0.543066
8.466E-07	2.93E-03	39300	76	0.2229	3.93	-0.35233	0.575192
8.466E-07	3.23E-03	39600	76	0.2454	3.96	-0.35265	0.598052
8.466E-07	3.57E-03	39900	76	0.2715	3.99	-0.34196	0.613453
8.466E-07	3.94E-03	40200	76	0.2992	4.02	-0.32372	0.622889
8.466E-07	4.29E-03	40500	76	0.326	4.05	-0.30161	0.627593
0	4.59E-03	40800	76	0.3489	4.08	-0.22534	0.574286
8.466E-07	4.80E-03	41100	74	0.3552	4.11	-0.23028	0.58546
8.466E-07	4.91E-03	41400	74	0.363	4.14	-0.22896	0.592003
8.466E-07	5.12E-03	41700	72	0.3688	4.17	-0.22604	0.594881
8.466E-07	5.42E-03	42000	72	0.3903	4.20	-0.20461	0.594891
8.466E-07	5.73E-03	42300	70	0.401	4.23	-0.1917	0.592686
8.466E-07	5.97E-03	42600	70	0.4176	4.26	-0.17117	0.588798
8.466E-07	6.17E-03	42900	68	0.4195	4.29	-0.1642	0.583663
0	6.33E-03	43200	66	0.418	4.32	-0.11607	0.534088
8.466E-07	6.50E-03	43500	64	0.4161	4.35	-0.12186	0.537928
0	6.50E-03	43800	62	0.4031	4.38	-0.08917	0.492238
8.466E-07	6.42E-03	44100	62	0.3979	4.41	-0.10543	0.503286
8.466E-07	6.33E-03	44400	60	0.38	4.44	-0.13081	0.510819
0	6.29E-03	44700	58	0.3649	4.47	-0.10249	0.467431
8.466E-07	6.25E-03	45000	58	0.3625	4.50	-0.11895	0.481495
8.466E-07	6.25E-03	45300	58	0.3625	4.53	-0.1291	0.491647
8.466E-07	6.21E-03	45600	56	0.3477	4.56	-0.1509	0.498642
8.466E-07	6.25E-03	45900	56	0.35	4.59	-0.15306	0.503106
8.466E-07	6.33E-03	46200	54	0.342	4.62	-0.16355	0.505557
8.466E-07	6.54E-03	46500	54	0.3533	4.65	-0.15308	0.50642
8.466E-07	6.71E-03	46800	54	0.3626	4.68	-0.14348	0.506045
0	6.89E-03	47100	52	0.3582	4.71	-0.1049	0.463063
1.6932E-06	7.06E-03	47400	52	0.3673	4.74	-0.1431	0.510417

8.466E-07	7.15E-03	47700	52	0.372	4.77	-0.13457	0.506518
8.466E-07	7.42E-03	48000	52	0.3861	4.80	-0.11641	0.502465
8.466E-07	7.65E-03	48300	50	0.3827	4.83	-0.1156	0.498345
8.466E-07	7.94E-03	48600	50	0.3969	4.86	-0.09736	0.494229
8.466E-07	8.32E-03	48900	48	0.3995	4.89	-0.09064	0.49017
8.466E-07	8.52E-03	49200	48	0.409	4.92	-0.07721	0.486209
8.466E-07	8.52E-03	49500	48	0.409	4.95	-0.07338	0.482376
8.466E-07	8.47E-03	49800	48	0.4066	4.98	-0.07208	0.478693
0	8.42E-03	50100	46	0.3874	5.01	-0.05063	0.438034
1.6932E-06	8.32E-03	50400	44	0.3662	5.04	-0.11302	0.479254
1.6932E-06	8.37E-03	50700	44	0.3684	5.07	-0.13656	0.504955
2.5398E-06	8.82E-03	51000	44	0.3882	5.10	-0.15371	0.54187
1.6932E-06	1.03E-02	51300	42	0.4307	5.13	-0.11052	0.541237
1.6932E-06	1.21E-02	51600	42	0.5066	5.16	-0.03143	0.538073
1.6932E-06	1.34E-02	51900	40	0.5356	5.19	0.00222	0.533329
2.5398E-06	1.45E-02	52200	40	0.5782	5.22	0.0354	0.542804
2.5398E-06	1.58E-02	52500	36	0.5683	5.25	0.02407	0.544216
3.3864E-06	1.82E-02	52800	34	0.6184	5.28	0.06719	0.551184
1.6932E-06	2.13E-02	53100	34	0.7245	5.31	0.19379	0.530715
1.6932E-06	2.33E-02	53400	32	0.747	5.34	0.23216	0.514838
1.6932E-06	2.33E-02	53700	30	0.7003	5.37	0.19797	0.502347
3.3864E-06	2.31E-02	54000	28	0.646	5.40	0.13057	0.515445
1.6932E-06	2.44E-02	54300	26	0.6357	5.43	0.1369	0.498798
2.5398E-06	2.57E-02	54600	26	0.6678	5.46	0.17016	0.497606
1.6932E-06	2.63E-02	54900	24	0.6304	5.49	0.14663	0.483719
1.6932E-06	2.61E-02	55200	24	0.6257	5.52	0.15239	0.473284
1.6932E-06	2.62E-02	55500	24	0.628	5.55	0.16265	0.465359
1.6932E-06	2.59E-02	55800	24	0.621	5.58	0.16176	0.459268
1.6932E-06	2.43E-02	56100	24	0.5823	5.61	0.1278	0.454522

2.5398E-06	2.27E-02	56400	24	0.5451	5.64	0.081	0.464105
0	2.30E-02	56700	24	0.5516	5.67	0.12688	0.424685
8.466E-07	2.18E-02	57000	24	0.5239	5.70	0.1125	0.411397
8.466E-07	1.91E-02	57300	24	0.4594	5.73	0.05804	0.401352
1.6932E-06	1.70E-02	57600	24	0.4071	5.76	-0.00914	0.416209
1.6932E-06	1.56E-02	57900	24	0.3754	5.79	-0.05079	0.426204
1.6932E-06	1.59E-02	58200	24	0.3806	5.82	-0.05219	0.432777
2.5398E-06	1.72E-02	58500	24	0.4125	5.85	-0.04008	0.452577
3.3864E-06	1.94E-02	58800	24	0.4652	5.88	-0.00884	0.474062
3.3864E-06	2.57E-02	59100	24	0.6164	5.91	0.13409	0.482306
4.233E-06	3.21E-02	59400	22	0.7056	5.94	0.21478	0.490846
2.5398E-06	3.67E-02	59700	28	1.0264	5.97	0.54791	0.478466
1.6932E-06	3.81E-02	60000	26	0.9907	6.00	0.5297	0.460979

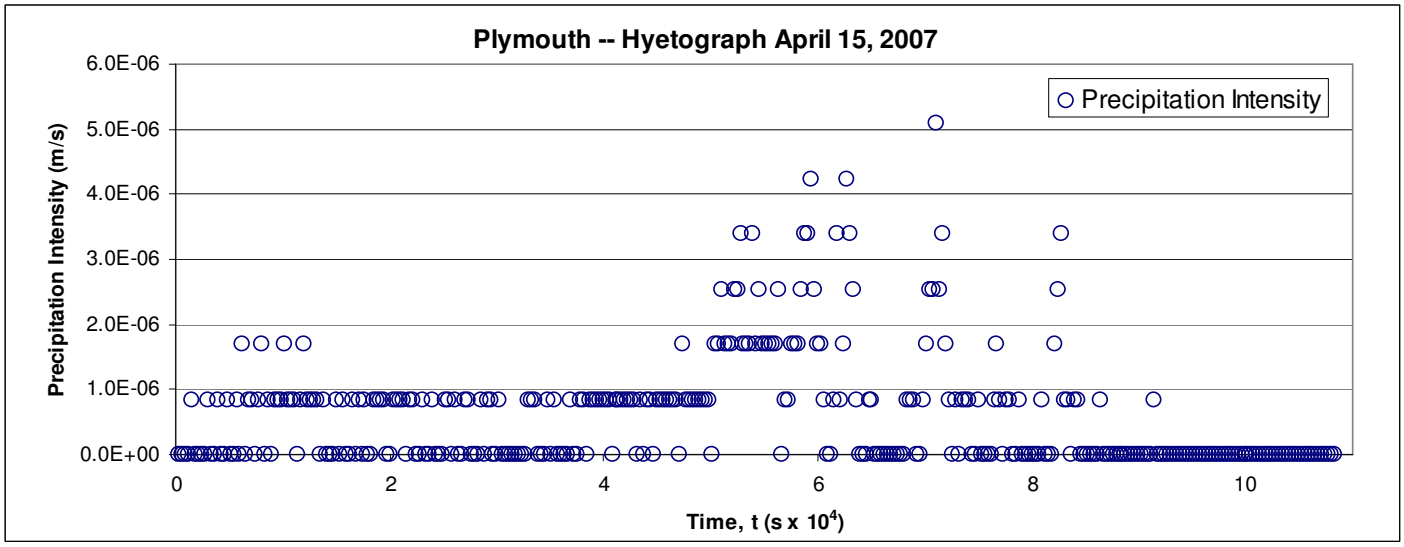
Plymouth -- Hyetograph April 15, 2007
Precipitation Intensity
Precipitation Intensity (m/s)
6.0E-06
5.0E-06
4.0E-06
3.0E-06
2.0E-06
1.0E-06
0.0E+00
0
2
4
6
8
10
Time, t (s x 10^4)

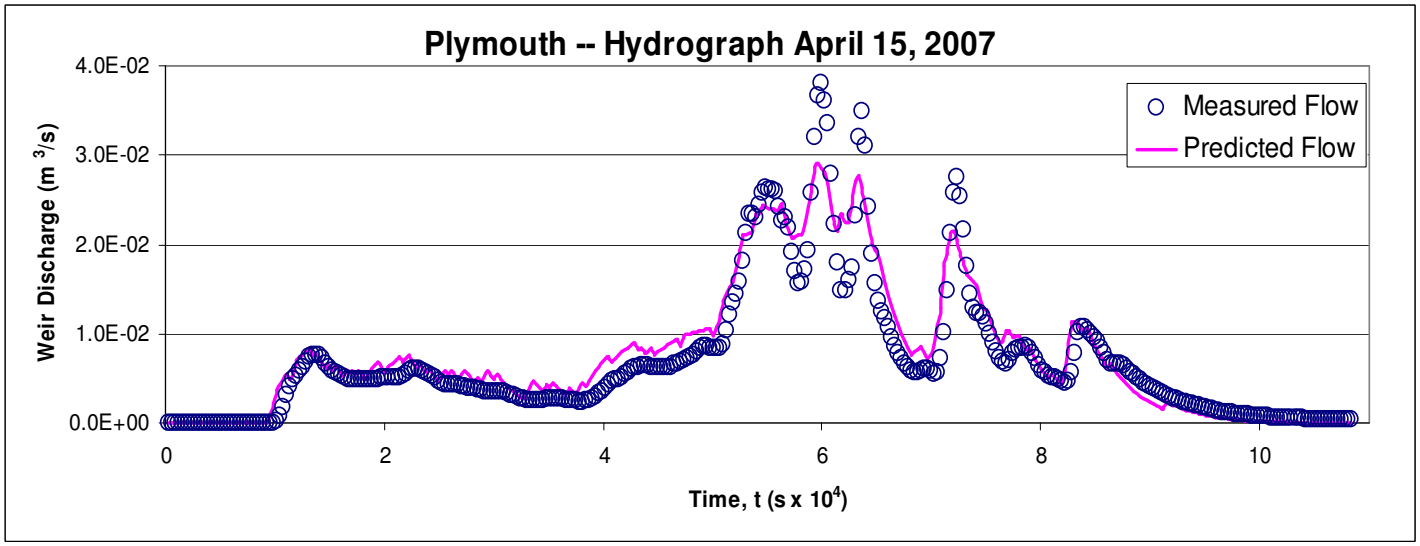
Plymouth -- Hydrograph April 15, 2007
Measured Flow
Predicted Flow
Weir Discharge (m^3/s)
4.0E-02
3.0E-02
2.0E-02
1.0E-02
0.0E+00
0
2
4
6
8
10
Time, t (s x 10^4)

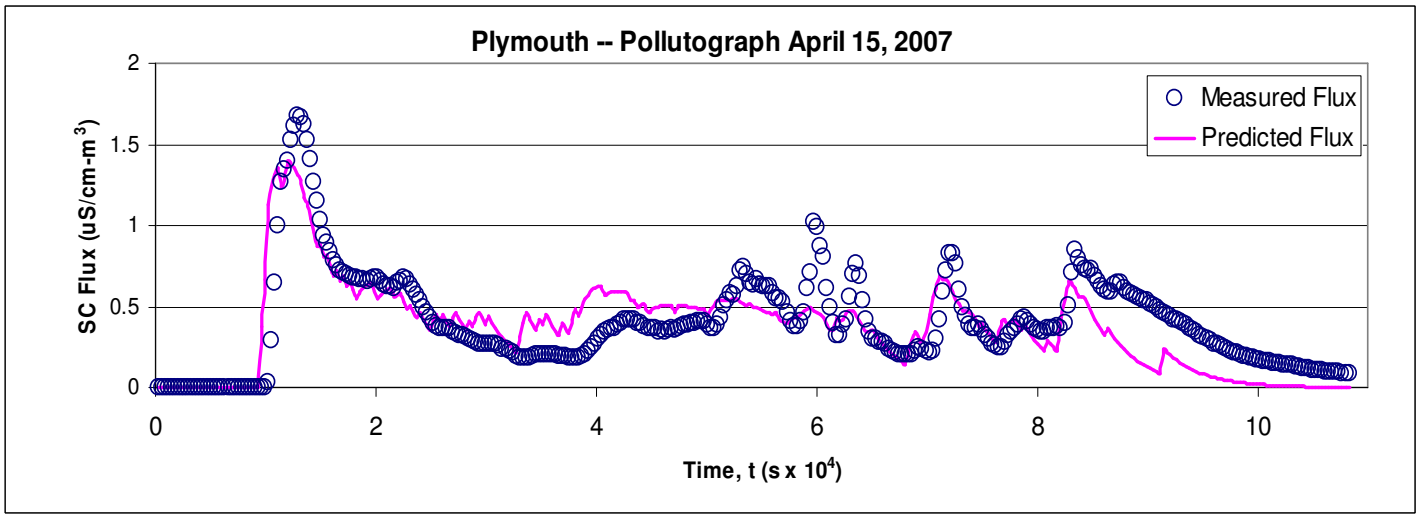
Plymouth -- Pollutograph April 15, 2007
Measured Flux
Predicted Flux
SC Flux (uS/cm-m^3)
2
1.5
1
0.5
0
0
2
4
6
8
10
Time, t (s x 10^4)

APPENDIX F

CALIBRATED PARAMETERS

Andover

Chronological DATE	Runoff Decay Constant Ω_R	Length of Storm t (hrs)	delt (kg/m^2-s)	A (m^2)	Normalized Error (%)(m^2)	zeta (m)	cpsource (uS/cm-m^2-s)	cpi uS/cm-m^3
8/14/2005	3.38E-04	51.3	4.90E-02	1627	427	0.00045	3.77E-05	26008
9/29/2005	6.48E-04	25.0	5.84E-01	4007	1769	0.00045	6.67E-04	285176
10/7/2005	3.35E-04	104.3	4.30E+00	2117	5137	0.00045	2.82E-04	10360
10/14/2006a	2.11E-04	48.3	1.63E+00	2610	1373	0.0009	5.94E-04	32778
11/15/2005	2.11E-04	42.3	8.85E-02	2586	66	0.00045	3.42E-05	316
12/25/2005	2.96E-04	31.3	3.80E+01	1340	85344	0.00045	1.00E-02	235003
1/14/2006	2.80E-04	28.3	2.40E+01	1526	57127	0.00045	8.01E-03	149799
1/23/2006a	7.30E-05	55.3	5.14E+01	3687	121017	0.00045	6.26E-03	291381
2/3/2006	3.14E-04	50.3	1.04E+01	1557	33742	0.00045	1.70E-04	3009
3/13/2006	3.60E-04	21.3	5.55E+00	297	96733	0.00045	3.12E-03	40383
4/5/2006	2.32E-04	7.3	2.59E-01	1449	1007	0.00045	9.33E-05	999
4/22/2006a	3.43E-04	35.3	1.94E-01	1209	850	0.00045	5.17E-05	1015
5/2/2006a	3.02E-04	57.8	5.30E-02	1375	266	0.0009	2.79E-05	3893
5/12/2006	2.35E-04	94.3	1.74E+00	1522	1698	0.00045	5.25E-04	10162
6/1/2006	5.16E-04	54.3	3.93E-01	1482	590	0.00045	3.59E-05	659
7/12/06a	3.02E-04	14.0	1.15E-01	881	225	0.0009	1.46E-04	6454
6/23/2006a	3.02E-04	20.8	7.35E-01	975	868	0.0009	3.56E-04	7886
7/22/2006	4.81E-04	25.3	2.09E-01	1008	331	0.00045	3.83E-05	1996
12/22/2006a	1.34E-04	16.3	5.59E-01	1030	1466	0.00045	2.39E-04	4160
1/1/2007	1.34E-04	20.3	1.38E+00	1101	4435	0.00045	7.42E-04	43003
1/14/2007a	3.02E-04	19.5	1.01E+00	12161	2433	0.0009	2.34E-04	21880
2/2/2007	1.22E-05	27.3	8.29E+00	15820	82960	0.00573	1.00E-02	324566
3/17/07a	3.02E-04	20.5	6.90E+00	2624	43764	0.0009	4.80E-03	494503
3/24/2007	2.45E-04	48.3	2.30E+00	1533	27619	0.00045	1.71E-04	3804
4/4/2007a	3.02E-04	32.0	4.88E+00	325	56019	0.0009	9.88E-03	1104408
4/15/2007	5.67E-05	86.3	2.54E+00	446	17846	0.00045	3.57E-03	118406
5/18/2007	2.88E-04	72.0	1.43E-04	806	351	0.00045	4.15E-05	2721
6/3/2007a	5.06E-04	31.3	7.66E-02	821	320	0.00045	4.19E-05	1586
7/4/2007a	5.53E-04	31.3	9.30E-02	1760	167	0.00045	1.29E-05	392
8/6/2007a	1.22E-05	10.0	7.48E-02	5753	699	0.00517	3.31E-07	15
9/8/2007a	4.76E-04	70.3	5.20E-02	580	355	0.00191	1.01E-05	53
10/6/07a	3.02E-04	11.5	7.03E-02	51	3357	0.0009	3.31E-07	0.342
10/19/2007	3.94E-04	24.3	1.20E-01	1326	304	0.00045	5.51E-05	11684

11/3/2007a	3.02E-04	11.5	1.69E-02	1116	24	0.0009	1.65E-05	401
11/15/2007	3.35E-04	24.3	2.45E-02	1315	81	0.00045	8.33E-06	182
12/2/2007a	1.98E-04	20.3	2.73E+00	462	40138	0.00629	1.00E-02	83111
12/27/2007	7.30E-05	58.3	4.01E+00	3154	23749	0.00045	4.80E-04	11134
1/11/2008	3.04E-04	20.3	1.01E+01	1581	14577	0.00045	2.58E-03	375987
2/1/2008a	3.09E-04	25.3	5.91E+00	1586	12665	0.00045	2.93E-03	821491
2/6/2008	2.58E-04	37.3	7.25E+00	1557	14801	0.00045	1.44E-03	224889
3/7/2008	3.04E-04	26.3	3.44E-01	1509	476	0.00045	9.63E-05	4437
4/28/2008	2.32E-04	24.5	3.82E-01	1581	821	0.00045	1.53E-04	16283
5/2/2008	3.49E-04	16.8	2.96E-02	1224	512	0.00045	9.40E-06	1355
6/22/2008	9.09E-06	47.3	7.00E-03	212	260	0.00045	1.57E-05	2733
7/23/2008	3.70E-04	37.3	7.86E-01	755	1489	0.00045	6.05E-04	18229
8/10/2008	5.53E-04	54.3	2.74E-02	899	320	0.00101	6.60E-06	392
9/6/2008	8.93E-04	8.3	1.42E-01	1191	125	0.00045	5.10E-05	677
Average:	3.04E-04	36.1	4.25E+00	2033	16185	0.00092	1.67E-03	102123

Cohasset

Chronological DATE	Runoff Decay Constant Ω_R	Length of Storm t (hrs)	delt (m^3/s)	A (m^2)	Normalized Error	zeta (m)	cpsource (uS/cm-m^2-s)	C_{SC} uS/cm-m^3
1/3/2004	4.81E-04	8.17	2.96E-04	3315	0.859	0.0010	1.703E-04	5808.52569
2/6/2004	2.14E-04	24.08	8.67E-04	5304	0.612	0.0043	2.366E-03	13275.04459
3/20/2004	1.63E-04	14.08	4.70E-04	2720	0.858	0.0005	3.30829E-07	16.09844168
4/12/2004	7.73E-04	57.58	2.74E-03	11752	1.151	0.0005	3.80735E-05	829.0222225
5/3/2004	6.91E-04	17.58	2.70E-03	13717	0.803	0.0005	3.24716E-05	1663.61239
6/9/2004	6.91E-04	7.08	8.22E-03	16962	1.210	0.0005	7.15343E-05	6046.923295
7/5/2004	9.96E-04	7.92	8.81E-03	17055	1.191	0.0014	5.55438E-05	1047.526145
8/5/2004	5.03E-04	10.58	8.33E-04	8897	0.804	0.0019	5.40644E-05	734.391277
9/28/2004	9.96E-04	30.42	4.64E-03	9046	0.772	0.0005	4.11295E-05	1428.103903
10/15/2004	9.96E-04	13.42	5.45E-03	8440	1.315	0.0019	2.860E-05	3.094E+02
11/28/2004	7.42E-04	8.58	3.71E-03	9429	0.547	0.0014	1.962E-04	3.796E+03
12/7/2004	7.97E-04	29.00	1.91E-03	7559	0.863	0.0010	4.368E-05	1.337E+03
1/8/2005	2.75E-04	6.17	1.48E-03	7650	0.291	0.0005	2.395E-03	9.421E+04
2/14/2005	8.61E-05	22.42	1.20E-03	22267	0.371	0.0005	9.813E-04	2.676E+05
3/28/2005	4.84E-04	32.08	4.68E-03	18509	0.569	0.0005	5.571E-04	2.070E+05
4/2/2005	4.98E-04	33.08	2.80E-03	16744	0.576	0.0005	4.113E-05	6.422E+03
5/6/2005	3.22E-04	49.17	1.26E-03	15937	0.508	0.0005	2.728E-05	1.912E+03
5/24/2005	7.42E-04	66.00	2.82E-03	15230	0.832	0.0005	4.261E-05	3.847E+03
6/8/2005	8.45E-04	7.17	7.07E-03	11951	1.129	0.0005	2.376E-04	9.922E+03
7/6/2005	8.02E-04	16.33	7.76E-03	12628	0.740	0.0005	2.471E-04	1.455E+04
8/28/2005	4.60E-04	53.00	5.24E-03	12288	1.531	0.0005	3.741E-05	6.205E+03
9/15/2005	5.24E-04	15.17	1.17E-02	14158	1.564	0.0043	9.806E-05	1.611E+03
11/9/2005	3.22E-04	22.83	2.42E-03	13971	0.916	0.0005	7.541E-05	1.279E+04
12/16/2005	1.98E-04	20.75	3.33E-03	21170	0.769	0.0063	1.959E-03	3.650E+04
12/25/2005	2.96E-04	33.00	1.18E-03	8968	1.068	0.0014	1.627E-04	7.889E+03
1/14/2006	3.83E-04	36.00	4.29E-03	11734	1.171	0.0005	2.680E-04	6.100E+04
2/3/2006	2.88E-04	21.50	1.82E-03	11649	0.817	0.0005	2.212E-04	6.147E+04

2/4/2006	3.94E-04	40.50	2.75E-03	11370	1.952	0.0005	1.019E-04	5.058E+04
3/14/2006	3.70E-04	16.75	1.47E-03	10072	1.679	0.0014	6.649E-04	3.888E+04
4/4/2006	3.22E-04	17.25	1.35E-03	9790	0.801	0.0005	3.574E-04	3.268E+04
5/1/2006	2.40E-04	53.75	1.34E-03	9953	0.663	0.0005	2.395E-03	9.421E+04
5/9/2006	2.45E-04	55.50	2.48E-03	11910	0.774	0.0005	3.247E-05	5.150E+03
6/2/2006	2.83E-04	73.75	3.08E-03	13267	1.023	0.0005	3.873E-05	2.884E+04
7/12/2006	5.06E-04	10.25	1.39E-02	11714	2.421	0.0005	8.595E-05	3.046E+02
8/15/2006	3.17E-04	8.00	2.69E-03	6105	0.691	0.0005	1.445E-04	1.960E+03
9/5/2006	5.98E-05	6.00	2.87E-03	4283	1.951	0.0005	6.181E-05	2.830E+03
10/11/2006	4.84E-04	17.50	4.32E-03	7407	1.174	0.0005	2.407E-05	9.720E+02
11/7/2006	2.80E-04	36.25	1.02E-03	6336	0.897	0.0028	5.101E-05	1.246E+03
11/23/2006	2.61E-04	23.75	4.92E-03	9688	0.488	0.0005	9.394E-05	7.820E+03
12/22/2006	1.89E-04	16.75	1.01E-03	9618	0.369	0.0014	2.458E-04	5.809E+03
1/1/2007	2.32E-04	22.75	8.69E-04	9609	0.478	0.0010	6.741E-05	2.248E+03
1/8/2007	3.01E-04	17.75	1.74E-03	8517	0.741	0.0005	7.606E-05	6.240E+03
2/14/2007	2.06E-04	14.25	6.04E-03	10065	0.627	0.0037	1.000E-02	2.274E+05
3/2/2007	2.27E-04	23.25	3.44E-03	12097	0.553	0.0005	1.971E-03	5.190E+05
4/4/2007	2.75E-04	48.75	2.36E-03	11949	1.063	0.0005	1.930E-04	1.348E+04
4/15/2007	2.48E-04	44.00	3.81E-03	12449	0.614	0.0005	1.323E-04	4.775E+04
5/18/2007	3.94E-04	78.50	2.35E-03	10042	0.977	0.0005	2.193E-05	3.541E+03
6/3/2007	3.57E-04	37.75	2.62E-03	10222	1.220	0.0005	2.115E-04	7.509E+04
7/8/2007	4.42E-04	22.50	1.27E-03	6553	1.637	0.0014	6.980E-05	2.175E+03
8/8/2007	3.57E-04	13.75	1.10E-03	6853	2.988	0.0019	4.203E-06	1.208E+02
9/11/2007	3.78E-04	12.00	1.05E-02	10611	1.519	0.0075	2.413E-04	1.789E+03
10/11/2007	6.91E-04	38.00	1.15E-02	10070	3.466	0.0005	4.612E-06	3.335E+02
11/3/2007	3.09E-04	16.25	1.39E-03	10417	0.664	0.0025	3.833E-05	7.178E+02
12/3/2007	1.12E-04	13.50	2.21E-03	19790	0.686	0.0081	3.308E-07	4.735E+02
1/1/2008	2.88E-04	16.50	1.00E-03	11267	1.141	0.0005	6.766E-05	1.050E+04
1/11/2008	8.92E-05	23.25	7.03E-04	3097	0.746	0.0005	6.785E-04	5.361E+04
2/1/2008	1.84E-04	26.00	1.05E-03	6353	0.587	0.0005	6.865E-04	2.109E+05
3/7/2008	3.30E-04	31.50	6.33E-03	13303	0.943	0.0005	1.501E-04	1.180E+04
4/4/2008	2.24E-04	20.25	1.32E-03	9834	0.534	0.0005	2.119E-04	3.065E+04
4/28/2008	4.04E-04	33.50	3.10E-03	10908	1.033	0.0014	8.381E-05	3.595E+03
5/16/2008	2.83E-04	27.75	1.77E-03	10767	0.750	0.0005	3.939E-05	1.317E+04
6/24/2008	5.16E-04	10.50	7.66E-03	8112	2.295	0.0063	5.860E-05	6.153E+02
7/18/2008	8.93E-04	5.00	1.09E-02	6655	2.821	0.0005	6.344E-06	2.243E+01
7/20/2008	1.22E-05	15.75	1.60E-02	7662	3.846	0.0005	8.447E-05	3.811E+03
8/6/2008	3.86E-04	13.75	1.51E-03	9285	3.264	0.0034	1.088E-05	1.477E+02
9/6/2008	4.63E-04	28.75	7.39E-03	10130	1.432	0.0014	1.170E-04	3.659E+03

average	4.13E-04	1	23.2	4.23E+00	10571	1246	0.00131	4.41E-04

Plymouth	Runoff Decay Constant	Length of Storm	delt	A	Normalized Error	zeta	cpsource	cpi opt
DATE	$\Omega_{R\,(s^{-1})}$	t (hrs)	(kg/m^2-s)	(m^2)	(%)(m^2)	(m)	(uS/cm-m^2-s)	uS/cm-m^3
1/18/2004	4.55E-04	14.1	1.03E+02	13093	38940	0.0019	7.44E-03	57005
2/6/2004	3.04E-05	22.1	2.82E+02	724177	1201	0.0095	2.55E-03	15288
2/22/2004	2.48E-04	21.1	2.64E+01	37740	9847	0.0005	4.00E-03	1568637
3/20/2004	3.83E-04	12.1	2.97E+01	14616	6492	0.0014	2.00E-03	22099

4/1/2004	4.76E-04	25.1	6.50E+00	14695	892	0.0005	3.54E-04	9573
4/12/2004	4.76E-04	47.1	5.38E+00	13371	1798	0.0005	8.06E-05	820
5/2/2004	3.09E-04	36.1	1.59E+00	11306	1326	0.0043	8.49E-05	499
5/28/2004	5.96E-04	10.1	3.17E+00	14400	415	0.0028	3.56E-04	2031
6/1/2004	4.71E-04	10.2	1.75E+00	14101	362	0.0025	2.20E-04	3712
7/5/2004	2.80E-04	6.1	4.20E+00	22351	699	0.0043	9.53E-05	280
8/15/2004	8.76E-04	12.6	1.77E+00	29659	61	0.0081	8.23E-05	316
8/31/2004	4.12E-04	9.1	9.60E-01	11010	228	0.0025	5.23E-05	203
9/28/2004	4.81E-04	14.0	7.33E-01	12515	176	0.0028	6.94E-05	578
11/12/2004	4.25E-04	25.8	3.99E-01	13263	74	0.0028	5.23E-05	405
11/24/2004	8.11E-04	26.1	9.00E-01	10975	422	0.0031	5.79E-05	492
12/1/2004	5.32E-04	8.1	7.49E-01	13506	96	0.0025	9.53E-05	358
12/7/2004	5.03E-04	23.1	2.21E-01	12949	76	0.0037	3.91E-05	114
1/3/2005	4.68E-04	13.6	2.16E+01	14675	3655	0.0014	1.84E-03	11169
1/8/2005	4.34E-04	7.1	9.05E+00	9180	1233	0.0005	7.15E-04	16026
2/3/2005	3.04E-04	19.6	1.75E+01	16066	12999	0.0025	1.23E-03	25566
2/16/2005	3.60E-04	4.1	2.32E-03	-4464	1	0.0031	3.31E-10	0
3/8/2005	4.29E-04	13.1	1.26E+01	17440	1018	0.0019	1.91E-03	27337
4/2/2005	1.84E-04	10.1	1.31E+01	9956	3800	0.0095	1.26E-03	3712
4/30/2005	6.14E-04	12.6	4.64E+00	15864	256	0.0019	2.51E-04	348
5/6/2005	4.15E-04	19.4	9.50E-01	13704	206	0.0034	1.57E-04	1884
5/23/2005	5.03E-04	81.1	6.46E-01	24741	118	0.0066	1.05E-05	59
6/30/2005	7.25E-04	12.1	3.27E-01	19215	88	0.0025	3.54E-06	48
7/8/2005	4.89E-04	14.1	1.24E+00	22506	161	0.0019	1.78E-05	131
8/30/2005	8.71E-04	18.1	3.12E+00	18919	162	0.0014	4.57E-05	1124
9/15/2005	8.92E-05	16.6	4.20E+00	71782	35	0.0005	1.98E-04	43769
9/26/2005	5.80E-04	25.5	6.31E-01	13526	109	0.0037	2.21E-04	10638
10/24/2005	2.32E-04	30.8	3.27E-01	12039	59	0.0034	5.66E-05	980
10/29/2005	4.07E-06	24.3	9.65E+00	21039	6243	0.0063	3.31E-07	4
11/21/2005	3.57E-04	23.3	7.13E-01	9896	109	0.0037	6.57E-05	712
11/30/2005	3.52E-04	18.6	2.47E+00	9005	411	0.0043	1.19E-04	1150
12/16/2005	2.32E-04	12.1	5.38E+01	10081	14765	0.0028	7.69E-03	103514
1/14/2006	3.35E-04	27.1	4.94E+00	9128	847	0.0025	1.49E-04	2439
2/4/2006	1.42E-04	17.1	2.51E-01	8316	136	0.0014	4.47E-05	1370
5/1/2006	2.27E-04	46.1	1.08E+00	10112	546	0.0034	1.82E-05	186
5/12/2006	2.48E-04	89.1	3.07E-01	10100	100	0.0019	1.09E-05	24
6/24/2006	3.17E-04	20.1	3.27E-01	10336	44	0.0028	1.61E-05	61
7/11/2006	5.67E-05	6.1	9.93E-02	4406	185	0.0019	1.74E-03	43803
8/28/2006	4.89E-04	7.3	3.83E-01	12579	34	0.0037	3.49E-05	432
9/19/2006	8.02E-04	10.1	6.13E-01	11919	50	0.0063	1.61E-05	108
10/28/2006	3.22E-04	20.1	6.65E-02	10140	14	0.0037	2.62E-05	340
11/23/2006	3.78E-04	27.7	1.99E-01	12174	19	0.0037	3.03E-05	299
12/4/2006	8.61E-05	13.1	1.16E+01	8379	3816	0.0005	8.51E-04	19872
1/8/2007	2.03E-04	14.1	7.99E-02	11252	27	0.0028	1.89E-05	249
2/2/2007	3.35E-05	8.1	6.77E+01	5539	40932	0.0005	1.00E-02	348765
3/17/2007	1.16E-04	13.1	1.67E+01	8103	2693	0.0005	1.13E-03	91125
4/15/2007	2.96E-04	30.1	2.09E-01	12216	30	0.0037	3.49E-05	562
4/17/2007	1.47E-04	52.6	1.42E-01	10904	86	0.0005	1.46E-05	693
4/27/2007	3.73E-04	21.0	4.46E-01	10846	105	0.0043	1.22E-05	172
5/17/2007	2.35E-04	38.1	1.89E-01	11494	44	0.0037	1.26E-05	258
6/3/2007	1.50E-04	22.6	1.71E-01	7645	108	0.0025	1.46E-05	154
7/30/2007	3.83E-04	8.1	5.75E-01	10352	91	0.0025	4.11E-05	458
8/13/2007	3.86E-04	4.1	3.90E-01	10118	64	0.0034	1.01E-03	8558

9/11/2007	2.24E-04	10.1	4.10E-01	8593	121	0.0043	2.79E-05	159
10/11/2007	5.58E-04	6.1	8.81E-01	17518	90	0.0057	3.31E-07	4
11/3/2007	3.04E-04	19.5	1.53E-01	11787	16	0.0037	4.39E-05	597
12/16/2007a	2.53E-04	12.1	4.52E+01	14072	6929	0.0037	4.04E-03	65391
1/11/2008	3.09E-04	11.6	1.83E+00	10425	464	0.0043	2.06E-04	1981
2/13/2008	3.60E-04	23.0	7.89E-02	18858	13	0.0037	1.81E-06	20
3/7/2008	3.49E-04	28.0	1.05E+00	12804	191	0.0037	6.01E-05	575
4/28/2008	3.35E-04	26.6	2.87E-02	11627	6	0.0037	3.31E-07	3
5/16/2008	2.03E-04	16.1	1.08E-01	11405	40	0.0037	1.26E-05	142
6/16/2008	3.04E-04	6.1	2.67E-01	13563	66	0.0034	1.85E-05	172
7/24/2008	7.12E-04	16.1	5.67E-01	14302	37	0.0048	2.02E-05	85
8/11/2008	2.83E-04	25.1	1.89E-01	8641	99	0.0025	8.74E-06	262
9/26/2008	2.23E-05	18.8	3.50E-01	3456	139	0.0005	6.60E-06	682
averages	3.62E-04	19.9	1.14E+01	13761	1352	0.00313	4.66E-04	35934